PASKIN Function in Testis, Pancreas and Energy Homeostasis

Dissertation

zur

Erlangung der naturwissenschaftlichen Doktorwürde
(Dr. sc. nat.)

vorgelegt der

Mathematisch-naturwissenschaftlichen Fakultät

der

Universität Zürich

von

Emanuela Borter

von Interlaken BE

Promotionskomitee

Prof. Dr. Roland H. Wenger (Vorsitz & Leitung der Dissertation)
Dr. Gieri Camenisch
PD Dr. Uwe Paasch

Zürich, 2007

This work has been performed under supervision of

Prof. Dr. Roland H. Wenger and
Dr. Gieri Camenisch

at the Institute of Physiology, University of Zürich-Irchel.

To my parents

Carmen and Urs Borter-Ichim

TABLE OF CONTENTS

1 ABBREVIATIONS

AhR	aryl hydrocarbon-receptor
AKT	RAC serine/threonine-protein kinase, Protein kinase B (PKB)
AMPK	AMP-activated kinase
ARNT	aryl hydrocarbon receptor nuclear translocator
bHLH	basic helix– loop–helix DNA-binding domain
C3G	Rho-family guanine nucleotide exchange factor
CAF20	Cap-associated factor 20
CCAMK	calcium / calmodulin-dependent protein kinase
CBP	CREB-binding protein
CREB	cAMP response element binding protein
ChoRE	carbohydrate response element
ChREBP	ChoRE binding protein
DAG	diacylglycerol
DD	cytoplasmic death domains
DED	death effector domains
DISC	death inducing signaling complex
DFX	desferrioxamine
eEF	eukaryotic translation elongation factor
eIF	eukaryotic translation initiation factor
EGF	epidermal-growth-factor
EPO	erythropoietin
ERK1/2	extracellular response kinase-1/2
FADD	Fas associated death domain protein
FOXO	forkhead transcription factor
Glc	glucose
GLUT-1/4	glucose transporter 1/4
Gsy2	glycogen synthase 2
GDP	guanosine diphosphate
GSK3β	glycogen synthase kinase 3 β
GTP	guanosine trisphosphate
H2AX	histone H2A variant X
HERG	human *eag*-related gene

HIF	hypoxia-inducible factor
HNF	hepatocyte nuclear factor
Hsp70	heat-shock protein 70
IGF1R	insulin-like growth factor 1 receptor
IP_3	inositol-trisphosphate
IPF1	insulin promoter factor-1 (human), ortholog of PDX-1
IR	insulin receptor
IRS1/IRS2	insulin receptor substrate ½
IRR	insulin receptor-related receptor
LZ	leucine zipper DNA-binding domains
MEK	mitogen-activated, ERK-activating kinase
MIN6	mouse insulinoma cell line
Mlx	max-like protein X
MODY	maturity-onset diabetes of youth
MAPK	mitogen-activated protein kinase
NPAS	neuronal PAS protein
NMR	nuclear magnetic resonance
p300	300 kDa protein, histone acetyl transferase
PA	phosphatidic acid
PARP	Poly (ADP-ribose) polymerase
PAS	PER/ARNT/SIM
PDX-1	pancreatic duodenal homeobox-1 (mouse), ortholog of IPF-1
PDK-1	phosphatidylinositol phosphate-dependent kinase-1
PER	*Drosophila* Periodic
PGM	phosphoglucomutase
PI3K	phosphatidylinositol 3-kinase
PKA	protein kinase A
PTB	phosphotyrosine-binding domains
pVHL	von Hippel-Lindau tumor suppressor protein
PYP	photoactive yellow protein
p53	53 kDa tumor suppressor protein
RTK	receptor tyrosine kinases
RyRs	Ryanodine receptors
SIM	*Drosophila* single-minded gene

Sds22	protein phosphatase, regulatory subunit 7
Snf1	sucrose non-fermenting 1 protein kinase
SOS	son-of-sevenless
SREBP-1c	sterol response element binding protein 1c
Tif11	translation initiation factor 1A
Ugp1	UDP-glucose pyrophosphorylase
VEGF	vascular endothelial growth factor

2 ZUSAMMENFASSUNG

PASKIN ist eine Serin/Threonin Kinase, welche nah verwandt ist mit der AMP-aktivierten Kinase. Wie der Name vermuten lässt, ist PASKIN zugleich ein PAS Protein, welches wahrscheinlich befähigt ist, Veränderungen in der Umgebung wahrzunehmen. PASKIN wird eine metabolische Funktion in der Hefe zugeschrieben, wobei es die Protein Synthese kontrolliert und den glykolytischen Fluss anregt, indem es der Synthese von Glykogen entgegenwirkt. Auch in Säugetieren ist diese Funktion insofern bestätigt, als dass PASKIN die Glycogen Synthase phosphoryliert. Dementsprechend konnten wir mögliche PASKIN Zielenzyme identifizieren, die eine wichtige Rolle sowohl im glykolytischen Signalweg wie auch im Glykogenmetabolismus spielen (Tröger J., Eckhardt K., Wenger R. H; unveröffentlichte Beobachtungen). Um die Funktion von PASKIN zu untersuchen, haben wir das *PASKIN* Gen durch homologe Rekombination in embryonalen Stammzellen ausgeschaltet. PASKIN knock-out Mäuse verhalten sich normal bezüglich Entwicklung, Wachstum, Lebenserwartung und Fertilität. Erstaunlicherweise konnte eine fast ausschliessliche mRNA Expression von PASKIN im Hoden nachgewiesen werden, speziell in postmeiotischen Keimzellen während der Spermatogenese. Trotz der niedrigen Expression von PASKIN mRNA in allen anderen Geweben kann eine Funktion von PASKIN ausserhalb der Testikel natürlich nicht ausgeschlossen werden. In Anbetracht seiner strukturellen Architektur stellt wohl die Kinasetätigkeit von PASKIN den Effektor dar, der auf Veränderungen des Metabolismus reagiert.

Wir können ausschliessen, dass in den β-Zellen des Pankreas Glukose die PASKIN Genexpression anregt. Zudem ist die Glukose-induzierte Insulinexpression unabhängig von PASKIN. Demzufolge kommt Glukose als direkter Aktivator von PASKIN nicht in Frage. Es scheint jedoch sehr wahrscheinlich, dass ein bis anhin unidentifizierter metabolischer Ligand die Akitvität von PASKIN sowie die darauffolgende Phosphorylierung von Zielproteinen aktiviert. Das Fehlen eines offensichtlichen Phänotyps in den *Paskin* knock-out Mäusen lässt sich demnach durch das Modell erklären, dass ein Aktivator unabdingbar ist. Wie man es von der Hefe her kennt, wird wohl die PASKIN Funktion nur unter veränderten Umgebungsbedingungen sichtbar. Folgedessen müssen PASKIN-aktivierende Bedingungen untersucht werden.

Ein Phänotyp wurde durch das Füttern der *Paskin*$^{-/-}$ Mäuse mit einer hochfett-Diät sichtbar. Die relativ geringe Gewichtszunahme der *Paskin*$^{-/-}$ Mäuse, sowie der verminderte Triglycerid Spiegel im Blutplasma und die erhöhte Glukose Toleranz der männlichen *Paskin*$^{-/-}$ Mäuse,

denen 45% Fett als Futter gegeben wurde, bestätigt eine Funktion von PASKIN im Energiemetabolismus. Eine Ursache könnte die AMPK sein, die als Sensor des zellulären Energiestatus in primären embryonalen Mausfibroblasten von *Paskin*$^{-/-}$ Mäusen aktiver ist als in *Paskin*$^{+/+}$ Fibroblasten. Dies führt zu der Annahme, dass PASKIN mindestens partiell als Antagonist von AMPK fungieren könnte. Überraschenderweise ist jedoch die Spontanaktivität in *Paskin*$^{-/-}$ Mäusen vermindert, was weitere Analysen notwendig macht, um die genaue Wechselwirkung von PASKIN mit AMPK zu verstehen.

3 SUMMARY

The PAS domain serine/threonine kinase PASKIN clearly has a metabolic function in yeast, and the regulation of glycogen synthase supports the idea of a similar function in mammals. Accordingly, potential PASKIN targets are enzymes involved in the glycolytic pathway and the glycogen metabolism (Tröger J., Eckhardt K., Wenger R.H.; unpublished observations). Through the generation of Paskin knock-out mice we acquired the ideal tool for investigating mammalian PASKIN function. By homologous recombination in embryonic stem cells we replaced exon 10 to 14, the part which corresponds to the kinase domain, by a *lacZ* reporter gene. PASKIN knock-out mice show normal growth, development, life expectancy and fertility before and after backcrossing into C57BL/6. Surprisingly, PASKIN mRNA expression in mice was detectable almost exclusively in the testis, specifically in post-meiotic germ cells during spermatogenesis.

Thus, even when the PASKIN mRNA expression levels are rather low in all tissues except testis, a PASKIN function outside of the testis certainly cannot be excluded. However, considering its structural architecture, PASKIN kinase activity probably represents the metabolically regulated effector rather than PASKIN mRNA and/or protein induction. We could show that *Paskin* gene expression is not induced by glucose in pancreatic β-cells [7]. Furthermore glucose stimulated insulin production is independent of PASKIN. We can exclude glucose from being a direct activator of PASKIN *in vitro*, however it appears to be likely that another, yet unidentified metabolic ligand induces PASKIN kinase activity and target protein phosphorylation. Such an activator also explains the lack of an obvious phenotype in *Paskin* knock-out mice. Like in yeast, PASKIN function might become apparent only under altered environmental conditions such as nutrient stress. Emphasis hence must be put on the identification of PASKIN-activating conditions.

High fat diet feeding of mice represents a possible PASKIN-activating condition. The partial resistance to the increase in body weight gain, decreased triglycerides in the blood plasma and the increased glucose tolerance of HFD-fed *Paskin*$^{-/-}$ male mice indicate a role of PASKIN in energy metabolism. AMPK, the sensor of cellular energy status was shown to be more active in *Paskin*$^{-/-}$ mouse embryonic fibroblasts. This leads to the assumption that PASKIN might at least partially counteract the AMPK pathway. Surprisingly, the spontaneous activity of *Paskin*$^{-/-}$ mice is decreased and careful analysis towards a correlation with AMPK needs to be performed.

4 INTRODUCTION

Adaptations to environmental stimuli are crucial for the survival of any organism. Therefore a sophisticated biological sensor is indispensable to allow for sensing and rapid adaptation to changing conditions of the cell. Over the past ten years, PAS domains have been discovered as important signaling modules that monitor changes in light, redox potential, oxygen partial pressure, voltage and small ligands. PAS proteins are found throughout all three kingdoms of life to control various physiological and developmental events thereby spanning phylogeny from bacteria to man.

The aim of the presented thesis is to provide further insights into the physiological context of the mammalian PAS protein PASKIN. This integrative work focuses on PASKIN function in its main expression organ, the testis, in the overall energy metabolism with a main emphasis on the pancreatic β cells. PASKIN knock-out animals are a precious tool for revealing PASKIN action.

4.1 PASKIN – a member of the PAS domain superfamily

The PAS superfamily of proteins is functionally specialized in the cellular response to environmental conditions and developmental signals. The acronym PAS originates from the first three proteins discovered in eukaryotes to bear such a domain: the *Drosophila* period clock protein (PER), the vertebrate aryl hydrocarbon receptor nuclear translocator (ARNT), and *Drosophila* single-minded protein (SIM) [8]. PASKIN belongs to the PAS superfamily of proteins which is involved in inducing and regulating some of the basic adaptive mechanisms of the cell [9, 10]. Besides the few sensor PAS proteins reported in mammals, such as the HERG voltage-dependent potassium channel [11], most other PAS proteins are heterodimerizing to form transcription factors responding to xenobiotics [12], hypoxia [13], circadian rhythm [14], and carbon monoxide [15]. The evolutionarily conserved protein PASKIN is the first mammalian PAS-regulated protein kinase discovered most probably link specific sensing of environmental changes to signaling cascades [4]. Sensing might be facilitated by the PAS domain while signaling occurs through its serine/threonine kinase. The mammalian PAS protein kinase PASKIN was identified by Wenger *et al.* upon a BLAST search using the *B.japonicum* FixL sequence as query [4]. At the same time, S.L. McKnight and co-workers reported the cloning of a human cDNA identical to PASKIN and named the

protein PASK. We designated the protein PASKIN, to avoid confusion with PASK which also stands for a previously discovered unrelated kinase [16].

PASKIN comprises with a size of 144 kDa two PAS domains at its N-terminal part of which the PAS A domain seems to play a pivotal role in modulating the kinase activity. The PAS B domain aligns significantly weaker when comparing to all known PAS domains by using a Hidden Markov model-based algorithm [17]. The C-terminally located kinase domain of PASKIN is a typical catalytic serine/threonine kinase and may constitute a new member of the Snf1/5'AMP-dependent protein kinase subfamily (Fig. 1).

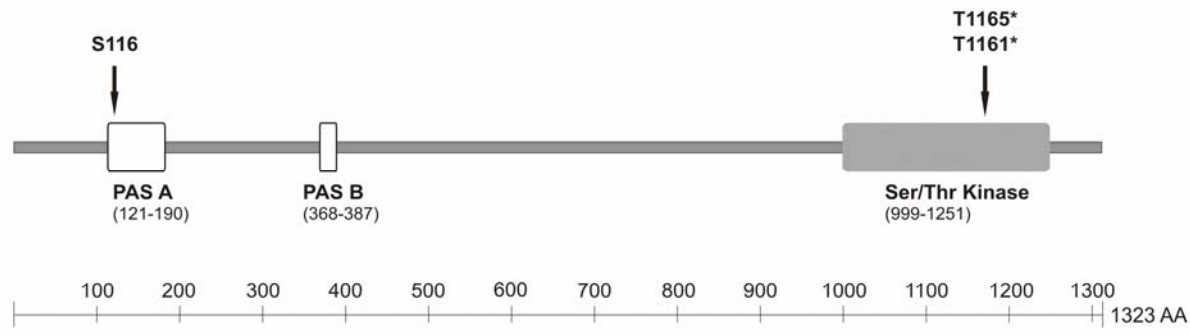

Figure 1: Domain structure of human PASKIN[4].

Most of the PAS proteins are known from archea, bacteria and lower eukarya, where they are known to detect environmental changes in light intensity, oxygen concentration, redox potential and voltage. Prokaryotic PAS proteins rather contain a histidine kinase to couple sensing to signaling, when compared to mammalian PAS proteins. Interestingly, the fold of the PAS domain of PASKIN most strongly resembles the PAS domain of the bacterial oxygen sensor FixL. In the case of FixL, however, signaling is mediated by a histidin kinase.

4.2 The PAS fold and its cofactors

Since PAS domains mediate signal transduction through different mechanisms, detailed information about their sequences and structures is needed. The 3D folds of PAS domains are highly conserved while their amino acid similarity is rather limited. Half of the known PAS domains contain a PAC motif at the C-terminus and split the five-stranded β-sheet into two sections. PAS and PAC motifs do not occur independently of each other, but are parts of the same functional fold, separated by a linker region which is flexible in length. The subdivision into PAS and PAC motifs derives from the major sequential difference in the region

connecting these two motifs. That is the reason, why PAS fold domains range from approximately 60 to 250 amino acids in length [10]. Therefore, Hefti *et al.* aligned six representative 3D-structures and proposed to define the complete structure as the PAS fold including the PAS and the PAC motif defined by Ponting and Aravind [18, 19]. Nevertheless a better annotation of the PAS fold, based upon structural information rather than sequence information is still required. Redefining the PAS fold into several subclasses, depending upon template structure or cofactor, makes sense in terms of the huge variation of PAS proteins occurring in nature; PAS domains are found in serine/threonine kinases, histidine kinases, cyclic nucleotide phosphodiesterases, circadian clock proteins, voltage-activated ion channels, transcription factors, photoreceptors, chemoreceptors as well as regulators of responses to hypoxia and embryological development of the central nervous system. A huge variation in cofactors and ligands, which are partially required for the detection of sensory input signals, is also adding up to the complexity of PAS proteins. The rapid increase in available 3D structures of PAS fold containing proteins provided by the PDB database will help to define

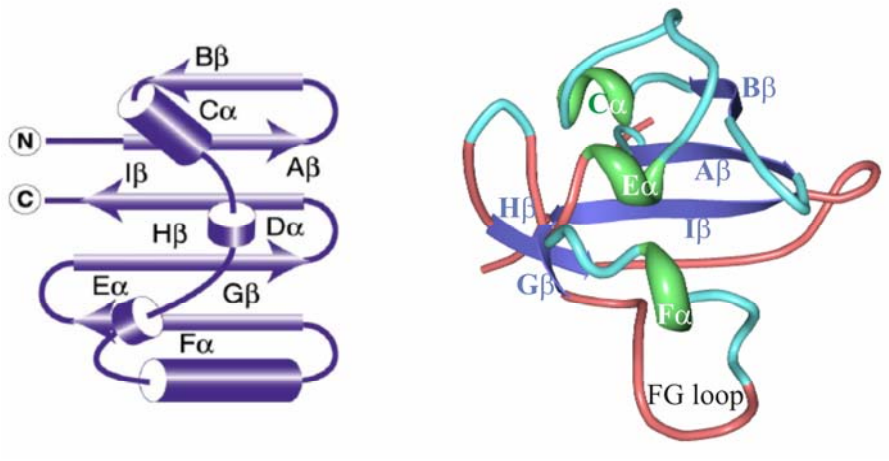

Figure 2: The PAS fold. Typical PAS fold consisting of a five-stranded antiparallel β sheet flanked by several α helices (Left)[2]. Schematic ribbon diagram of the PAS A fold (PDB 1LL8) A to I are the structural elements starting from the N-terminus (Right). Light blue: turn, dark blue: strand, green: helix, red: coil.

the PAS fold more accurately. Up to date there are over 70 3D PAS structures recorded.

PAS domains often serve as protein/protein interaction domains. A cofactor can be necessary for the interaction of such protein/protein interaction domains upon an environmental stimulus. Such organic cofactors might therefore be involved in sensing and are located within the hydrophobic core of the PAS domain. Examples are heme for sensing O_2 in bacterial enzymes [20], FMN (flavin mononucleotide) for blue-light sensing in plant

phototropins [21] and 4-hydroxycinnamic acid for sensing blue light in photoactive yellow protein [22].

Independent of whether or not PAS domains contain a cofactor, they all have the same typical α/β structure fold with several α helices flanking a five-stranded antiparallel β sheet scaffold to form the PAS fold (Fig.2). Therefore folding is independent of ligand binding which has as well been observed when analyzing the crystal structure of the ligand-free human PAS domain gene HERG (human ether-a-go-go-related gene) [11].

Amezcua *et al.* measured an unusual flexibility of the PASKIN backbone amino groups of Fα helix, FG loop and Hβ strand in solution when comparing to other PAS domains indicating that these are sites for binding and interaction [2]. Hβ and Fα are near the ligand binding site of other kinase regulating PAS domains and the FG loop is involved in the interaction of the kinase with the hPASKIN PAS A fold. For FixL a heme is bound within the hydrophobic

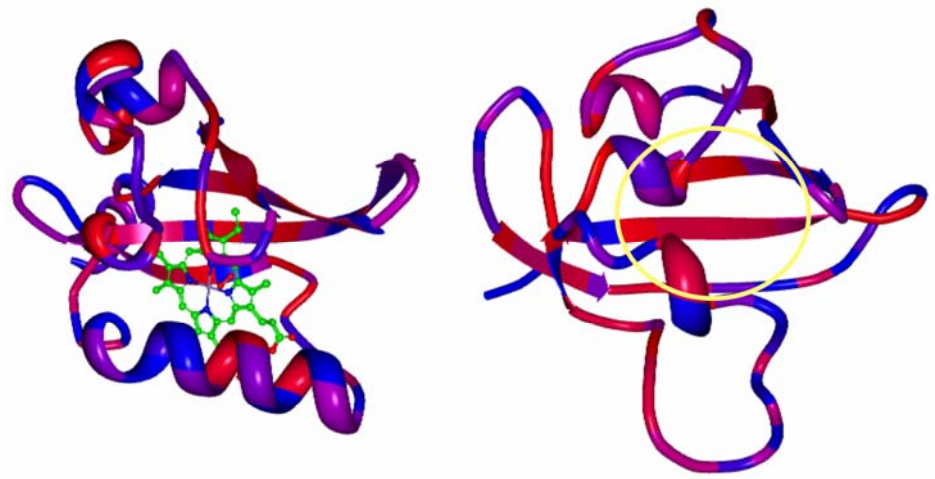

Figure 3: Comparison of binding sites for aromatic compounds. (Left) Oxygen-binding complex of FixL heme domain (PDB 1DP6), green: heme, red: oxygen. (Right) hPASKIN PAS A (PDB1LL8). Hydrophobicity increases from blue to red

core. The propionic acid moieties of heme directly contact the FG loop. (Fig. 3)

Upon screening of over 750 organic compounds for their binding ability to hPASKIN PAS A, Amezcua *et al.* further showed that tightest binding compounds are hydrophobic in character and typically contain one or two aromatic rings substituted with polar groups and separated by a linker of variable length (0-2 atoms). The site of binding corresponds to the pockets used to bind heme in the FixL domain. This hydrophobic core is composed of residues from the flexible Fα helix and Gβ strand including residues essential for discrimination against differently sized ligands. In Fig. 3 the hydrophobic core is marked with a yellow circle. None

of the previously identified ligands for other PAS domains bind to hPASKIN PAS A with significant affinity. Rather a novel compound involved in carbohydrate metabolism or translation could be a candidate, since the yeast relatives of PASKIN regulate those pathways. More genetic and biochemical studies are required to identify an endogenous ligand for PASKIN [2].

4.3 Activation models for PAS domain containing proteins

The prokaryotic histidine kinase FixL

The nitrogen-fixing bacteria *Bradyrhizobium japonicum* [23] and *Rhizobium meliloti* [24] contain an oxygen sensor which is a histidine kinase termed FixL. FixL and PASKIN are, despite their evolutionary distance, very close concerning the PAS fold structure as well as the regulatory mechanism. The nature of the triggering signal, however, differs between these two proteins. While FixL is activated by O_2 interacting with the heme iron, hPASKIN does not contain a heme bearing domain and thus is most likely not able to bind oxygen. Once oxygen binds to the heme, the porphyrin ring undergoes a structural change which subsequently affects as well the FG loop. By this conformational change the kinase domain is inactivated. As the concentration of O_2 drops below 50 μM in symbiotic root nodules, FixL catalyzes a phosphoryl transfer from ATP to the transcription factor FixJ. Subsequently, FixJ activates the transcription of target genes essential to rhizobial nitrogen fixation [25, 26].

The mammalian serine/threonine kinase PASKIN

Among all PAS domains, PASKIN PAS domain shares the highest similarity with the PAS domain of the oxygen sensor FixL. Once a ligand is bound, both proteins alter the structure of the FG loop including surrounding regions. As a consequence, those changes modulate the activity of the kinase domain in cis.

The FixL histidine kinase, however, weakly matches to the intervening domain rather than to the serine/threonine kinase domain of PASKIN. The intervening domain corresponds to the mouse *Paskin* exon 10 to 12 and is assigned to one long open reading frame. Wenger *et al.* therefore speculate that this region is the remnant of an ancestor protein where the histidine kinase-like domain became inactivated during evolution [4]. This hypothesis is further supported by the shortened human exon 10 when compared to the mouse gene. Rutter *et al.* showed that the human PASKIN PAS A domain can specifically inhibit its own kinase domain in trans [17]. Amezcua *et al.* confirmed these data showing that the residues

interacting with the kinase domain are located in the FG loop proximal to the ligand binding cavity [2]. This indicates that modest changes in the binding cavity could regulate kinase activity as confirmed by experiments with site-directed mutagenesis. Small organic molecules regulate enzymatic activity using the PAS domain as a transducer to convert chemical signals into a switch of kinase activity. In an inactive state no bound ligand is present and PASKIN is inactive. In this state the PAS domain is inhibiting the Ser/Thr kinase. Upon ligand binding to the PAS A domain, a conformational change takes place. The Ser/Thr kinase is disinhibited, resulting in autophosphorylation of PASKIN. The activated kinase is now able to phosphorylate downstream targets (Fig. 4).

Phosphorylation dependence and intramolecular PAS domain-mediated inhibition are the two

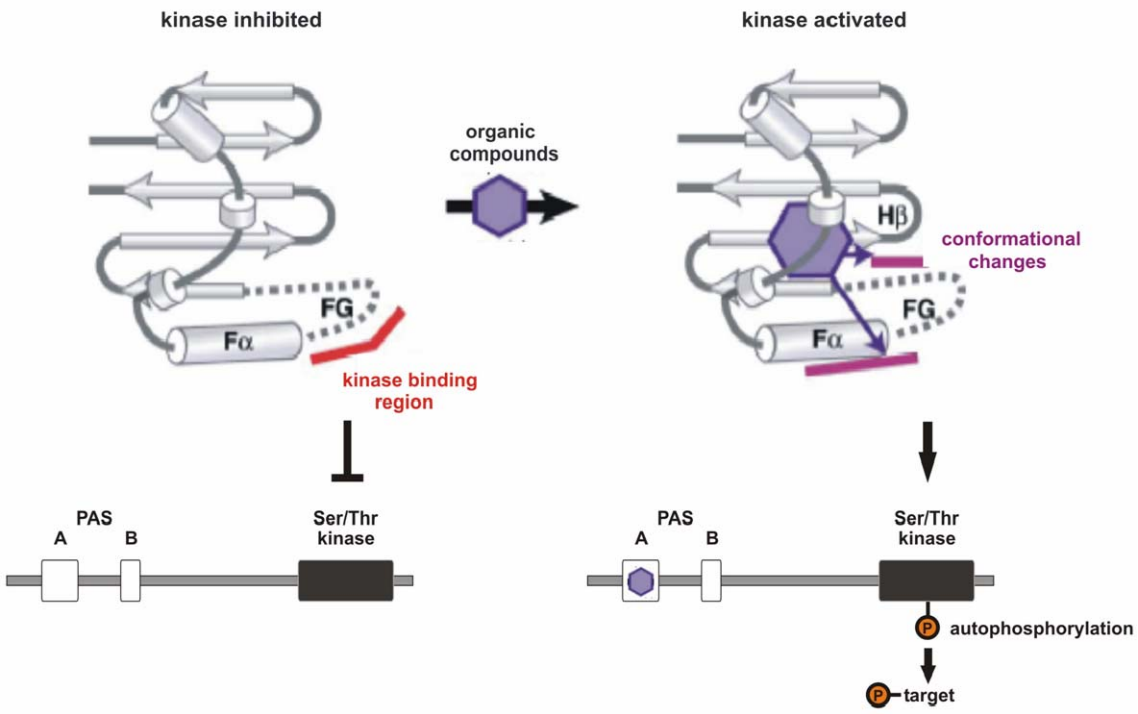

Figure 4: Model for kinase regulation by small-molecule PAS ligands[2].

main mechanisms of PASKIN action. Autophosphorylation of the two threonine residues (Thr1161, Thr1165) is necessary for efficient catalytic activity. The phosphorylation site T1161 corresponds to the phosphorylation residues of Snf1 and AMPK which are necessary for catalytic activity [27]. In nuclear extracts derived from HeLa cells another phosphorylation site (Ser116) of PASKIN in front of the PAS A domain was identified by tandem mass spectroscopy in a large scale characterization of HeLa nuclear phosphoproteins [28]. The N-terminally located PAS domains act as intramolecular inhibitors on the activity.

The role of PAS B however, still needs to be addressed concerning the regulation of kinase activity.

Further work to understand the activation model of PASKIN was performed by our group (Tröger *et al.*, submitted). Tröger *et al.* could identify phospholipids to strongly stimulate PASKIN autophosphorylation in a dose-dependent manner. Phosphatidic acid alone was shown to be sufficient for maximum activation of PASKIN autophosphorylation. The presence of the charged phosphate moiety seems to be required for stimulation of PASKIN kinase activity which is supported by the outcome that PLD, but not PLC, is converting the phospholipids into a high-affinity PASKIN ligand. One therefore might hypothesize that an extracellular ligand is signaling via a receptor-mediated intracellular PLD pathway to regulate PASKIN function.

4.4 Genetics of PASKIN

PASKIN is evolutionarily conserved and located on chromosome 2q37.3 and 1 for human and mouse, respectively. No polymorphism could be tracked and PASKIN is a single-copy gene. Ubiquitous expression of PASKIN was detected by Northern blot analyses as well as by multiple tissues mRNA dot blot. Higher expression levels were found in caudate nucleus and putamen of the brain, in prostate and in testis while reduced levels were expressed in placenta. On the genetic level the intron-exon structure is conserved from mouse to human, consisting of 18 exons except of an untranslated, short mouse first exon at a position similar to the human first exon and some additional base pairs at the end of mouse exon 9 and at the beginning of exon 10. This adds up to additional 71 amino acids in the mouse PASKIN sequence encoding a 1390 amino acid protein. Accordingly, the human *PASKIN* cDNA encodes for a protein of 144 kDa which is not extensively posttranslationally modified.

Human and mouse PASKIN are similar within the two N-terminal consensus PAS repeats and the C-terminal serine/threonine kinase domain, but share less similarity outside of them. The PAS repeats are conserved when compared with the FixL sequence, however the FixL histidine kinase region weakly aligns to the long exon 10 of both human and mouse PASKIN and not to the serine/threonine kinase region. Interestingly, only one kb lies within the start codon of the regulatory subunit 7 gene involved in target protein recognition of type 1 serine/threonine protein phosphatase (PPP1R7 and Ppp1r7, respectively) and the first exon of PASKIN, indicating that they share the promoter region (Fig. 5). Wenger et al assume a bicistronic promoter activity, based on the finding that PPP1R7 as well as PASKIN are

ubiquitously expressed. Moreover a functional role of protein phosphatase-1 in the regulation of PASKIN autophosphorylation was suggested, since Sds22 colocalises with the cell types expressing PASKIN *in vivo* [29]. It might be that Sds22 is responsible for PP1-mediated dephosphorylation of activated PASKIN to switch off the kinase activity. There are at least two Sds22 isoforms coexpressed with PASKIN in mouse testis.

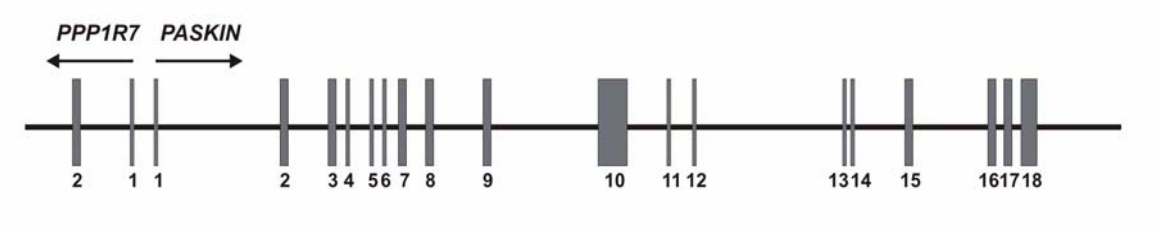

Figure 5: Primary structure of human PASKIN. Gene structure of human *PASKIN*. Exons are indicated by grey boxes numbered according to the human sequence [4].

4.5 Physiological function of PASKIN

Paskin function in yeast

While orthologs of PASKIN are found in yeast, mammals and flies, only in yeast a functional role has been assigned so far. PSK1 and PSK2 are the two PASKIN orthologs in *Saccharomyces cerevisiae* which are regulating protein synthesis and glycolytic flux. However nutrient restriction and high temperature are necessary for the downregulation of protein translation and carbohydrate storage by the active PASKIN kinase. Thereby, PSK1 and PSK2 phosphorylate three translation factors and two enzymes involved in the regulation of glycogen and trehalose synthesis.

S. cerevisiae is able to use galactose as an alternative energy source. When galactose is the only carbon-source available, yeast is converting the sugar into glucose-6-phosphate to allow for glycolytic flux and ATP production. Rutter and colleagues generated a psk1 psk2 double yeast mutant and found a growth defect under galactose utilization combined with elevated temperature (39°C). This temperature-sensitive galactose utilization (gal^{ts}) phenotype of the psk1 psk2 double mutant could be efficiently rescued with the enzymatic activity of the PSK2 protein. In the absence of PASKIN, they conclude that increased formation of storage carbohydrates occurs. Overexpression of the PGM1/2 enzymes is suppressing the gal^{ts} phenotype of the psk1 psk2 double mutant. This makes sense since Pgm enzymes favour conversion of G1P into G6P.

UDP-glucose pyrophosphorylase (Ugp1p) and glycogen synthase (Gsy2p) are both inhibited by PASKIN dependent phosphorylation which leads to enhanced flux of galactose toward glycolysis by inhibiting the accumulation of glycogen. Ugp1p catalyzes the conversion of glucose-1-P to UDP-glucose, which is one step removed from both glycogen and trehalose. Gsy2p is responsible for the direct polymerization of glycogen from UDP-glucose moieties. The double mutant psk1 psk2 leads to the accumulation of abnormally high levels of glycogen therefore maintaining Ugp1p and Gsy2p in hypophosphorylated states to favour the formation of storage carbohydrates. When inactivating the Psk2p phosphorylation sites of Ugp1p and Gsy2p, the phenotype is similar to that observed in the psk1 psk2 double mutant. PASKIN enhances the flux towards glycolysis by negatively regulating Ugp1p and Gsy2p (Fig. 6). A screen for high copy suppressors of the gal^{ts} phenotype revealed a number of genes encoding translation factors and components of the translation apparatus. Moreover, upon screening for Psk2p substrates three different polypeptides involved in protein synthesis were discovered. When overexpressing PASKIN in a yeast strain lacking the translation initiation factor 4B (STM1), the protein synthesis deficits and the vegetative growth are both suppressed. Taken these findings together, PASKIN may also serve to regulate protein synthesis. One of the identified phosphorylation substrates is the product of the Caf20 (Cap-Associated Factor 20) gene which negatively regulates translation by blocking the assembly of the translational apparatus. Furthermore it is known that its mammalian homolog 4E-BP (eIF4E binding protein) is phosphorylated upon stimulation with Insulin and other hormonal signals, thereby releasing eIF4E and subsequently increasing translation rate [30]. The phosphorylation state of the 4E-BP is dependent on nutrient availability. When glucose and amino acid are lacking, 4E-BP phosphorylation is decreased, thereby slowing down protein translation. The other two identified phosphorylation targets are Tif11p (eukaryotic translation initiation factor 1A (eIF1a)) which mediates the transfer of

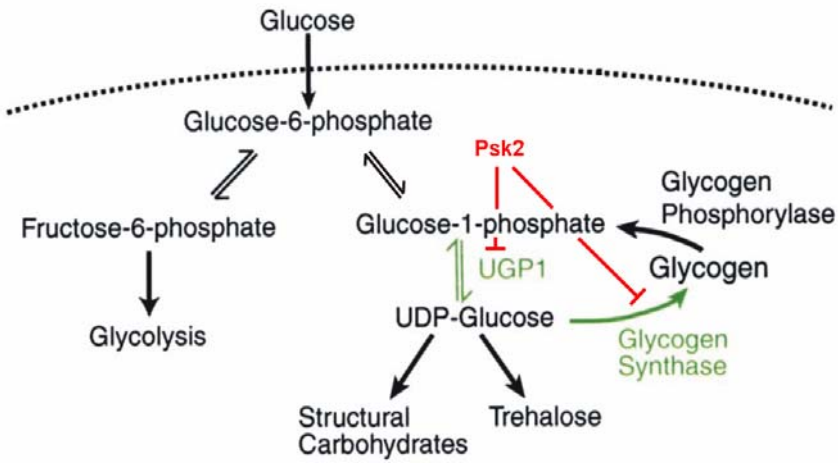

Figure 6: Model for control of metabolic flux by Psk2, modified from reference [1].

Met-tRNA to the 40S ribosomal subunit to form the 40S preinitiation complex and Sro9p which binds RNA in vitro and interacts with translation ribosomes [1].
Products of the PSK1 and PSK2 genes are therefore assigned to regulate sugar flux and translation in the yeast *S. cerevisiae* [1].

PASKIN expression in postmeiotic germ cells during spermatogenesis

In our *Paskin*$^{-/-}$ animals β-galactosidase activity derives from the homologous recombination of exon 10 to 14 with a *lacZ* reporter construct to create knock-out animals. Whole-mount X-Gal staining revealed an unequal staining within different regions of the seminiferous tubules in PASKIN knock-out mice [29]. Since spermatogenesis occurs in synchronized waves of distinct developmental steps, PASKIN expression in germ cells would explain this unequal staining. After analyzing testis sections, PASKIN could be localized in the luminal regions and the interface to the cytoplasm of round and elongated spermatids. PASKIN expression is therefore localized to haploid germ cells. By in situ hybridisation PASKIN mRNA was found in spermatocytes, spermatids, and spermatozoa. With the help of recently generated monoclonal αPASKIN antibodies, subcellular localization was investigated [31]. PASKIN localizes to the cytoplasma and to the nuclei of spermatogonia and spermatocytes with a pattern that might match the nucleoli, at least in spermatogonia. In ejaculated human sperm cells, PASKIN localizes mainly to the midpiece of the tail and is absent in the nucleus. Neither PASKIN mRNA nor PASKIN protein is present in testis at postnatal day 12 to 15. Only at postnatal day 25 PASKIN mRNA levels and β-galactosidase expression strongly increased and the expression is stable until adulthood. PASKIN knock-out animals show normal growth, development and reproduction. Neither sperm production nor fertility or motility is affected.
Interestingly, Sds22 mRNA expression is highest in the testis, increased during mouse puberty, but independent of the *Paskin* genotype. By immunohistochemistry, a similar expression pattern was revealed for Sds22 as it is known for PASKIN.
The investigation of the endogenous function of PASKIN during spermatogenesis in vitro is not possible since no haploid cell culture model is available. To gather more insight into a possible role of PASKIN during spermatogenesis, a yeast two hybrid screening was performed of a human testis cDNA library (Tröger J.; manuscript in preparation). Ku70, inhibitor of activated STAT (iSTAT) and the transcription factor testis zinc finger protein (tZFP) were identified as potential interactors of PASKIN. Ku70, which is involved in a wide range of cellular processes such as apoptosis, DNA repair, tumor development, telomere

maintenance or regulation of specific gene transcription [32], could be confirmed as interactor in a GST pull-down assay. However Ku70, being part of the DNA-repair DNA-PK complex, is not a phosphorylation target of PASKIN in vitro. Its interaction with PASKIN possibly through its protein-protein interaction site (SAP domain) might be necessary to sense the status of the cell, while signaling would occur through a distinct way. A possible signaling cascade could occur through DNA-PKcs, which is as well part of the DNA-repair DNA-PK complex. Interestingly, Ku70 and Ku80 were identified as interaction partners of pancreatic duodenal homeobox-1 (PDX-1), while DNA-PK acts as upstream kinase [33].

PASKIN function in somatic tissues

By a yeast two hybrid screen for novel proteins interacting with PASKIN, our group identified the multifunctional eukaryotic translation elongation factor eEF1A1 in a HeLa cDNA library [31]. eEF1A1 is a GTP-binding protein catalyzing the binding of charged aminoacyl-tRNA to the A-site of the ribosome and is related to the above mentioned eIF1A, a phosphorylation target of the yeast PASKIN homolog. The interaction with the C-terminus of eEF1A1 was mapped to the C-terminal part of the PAS A domain and to the kinase domain of PASKIN. eEF1A1 is not exclusively phosphorylated by PASKIN, but also by PKCδ, Rho-associated kinase and S6 kinase [34-36]. Since Insulin stimulation of protein synthesis involves S6 kinase-dependent eEF1A1 phosphorylation, a possible role for PASKIN at the interface of protein translation and energy metabolism arises, as it has been established for the yeast PASKIN homologs (see above).

eEF1A1 colocalises with PASKIN to the cytoplasm in HeLa cells as well as to the midpiece of the sperm tail. We could show that in a cell-free translation assay PASKIN increases protein translation. We therefore assume that translation can be regulated by PASKIN-dependent eEF1A1 phosphorylation in somatic cells. The functional variety of eEF1A1, including cytoskeletal organization, signal transduction, RNA synthesis, proteasomal degradation of damaged proteins, apoptosis, activation of the heat-shock transcription factor and the implication in major diseases such as diabetes and cancer, leaves possible functional roles open for the PASKIN-dependent eEF1A1 phosphorylation.

On the one hand, PASKIN is detected exclusively in the cytoplasm of baculovirus-infected insect cells and in transiently transfected HEK293[17]. Endogenous PASKIN however was detected as nucleolar pattern in spermatogonia and a more speckled nuclear pattern in spermatocytes and in HeLa cells. In HeLa cells endogenous PASKIN is localized in the cytoplasm as well. The nuclear localization of endogenous PASKIN is further confirmed by a

PASKIN phosphopeptide which was detected in a screen for nuclear phosphopeptides in HeLa cells [28].

On the other hand, although reported to localize to the nucleus in *Trypanosoma cruzi* [37], we detected endogenous eEF1A1 exclusively in the cytoplasm of HeLa cells and of testicular human germ cells [31]. Therefore, a role for the eEF1A1:PASKIN interaction in the cytoplasm seems very likely. More interestingly, however, is the colocalization in mature human spermatozoa. The spermatozoa are in a translation-silent state. Therefore, a translation-unrelated function can be assumed. The midpiece of the sperm tail offers with its highly organized structure several possible roles for the eEF1A1:PASKIN interaction either in cytoskeletal organization or in the regulation of energy flux in combination with the mitochondria. PASKIN staining did not overlap with the markers for the Golgi apparatus or mitochondria. Additionally, in the cytoplasmic liquid of the spermatozoa several testis-specific isoforms of proteins are localized and which might contribute together with the EF1A1 and PASKIN to the response to external stimuli by regulating energy flux, heat-stress response and apoptosis.

As known from the yeast homologs, PASKIN is a regulator of mammalian glycogen synthase. hPASKIN phosphorylates glycogen synthase *in vitro* at Ser-640, which is a known regulatory phosphosite [38]. Interestingly, the midregion of PASKIN is necessary for the phosphorylation of glycogen synthase *in vitro*. This region contains no previously recognized structural or functional domains or sequences. This interaction is negatively regulated by the PAS domain and the glycogen synthase itself. These findings show again that the metabolic status of the cell is playing a key role in activating PASKIN. It could be that hPASKIN maintains free glycogen synthase in a phosphorylated and therefore inactive form until it is properly localized to a glycogen particle.

The human UCK2 protein is a further substrate of hPASK, however nothing is known concerning this interaction so far [38].

The assigned potential roles for PASKIN in somatic tissues might be confirmed and further characterized once the endogenous ligand for PASKIN has been identified.

PASKIN function in pancreatic β-cells

PDX-1 is a major transcription factor involved in the regulation of insulin gene expression in pancreatic β-cells of adults and is furthermore a key factor for normal pancreatic development. When glucose is abundant in the cell, PDX-1 translocates from the nuclear periphery to the nucleoplasm where it is active and can contribute to insulin gene expression

[39]. Disturbed insulin secretion leads to impaired β-cell function and is the main cause for the development of maturity-onset diabetes of the young 4 (MODY 4) [40]. This inherited form of diabetes is as well occurring, when the PDX-1 gene is inactivated. Rutter et al. report that exogenous glucose is involved in regulating PASKIN activity in isolated islet β-cells [41]. Rutter *et al.* microinjected a plasmid coding for WT *PASKIN* and saw increased preproinsulin promoter activity already under low glucose. By deletion of PDX-1 binding sites, the regulation by PASKIN or glucose of both the preproinsulin and PDX-1 promoters was completely absent which implicates PDX-1 as a target of PASKIN action. We showed that PASKIN mRNA and protein levels do not affect glucose-stimulated insulin production in *Paskin* knock-out animals [7]. Neither did in vivo experiments confirm *Paskin*-dependence of insulin regulation nor could we detect positive β-galactosidase staining in organs other than the testis. No differences in basal blood glucose levels and glucose tolerance were observed between wild-type and *Paskin* knock-out mice.

There are some indications, why we did not detect PASKIN to be glucose responsive. First, Rutter *et al.* performed their experiments with overexpressed epitope-tagged kinase. Overexpression of PASKIN hardly had any effect on glucose metabolism and no impact at all on the release of stored insulin. Therefore Rutter *et al.* had to work with microinjected WT *PASKIN* which questions the physiological approach of these experiments. Second, only partly selective was the PASKIN silencing effect, since Rutter *et al.* saw a decrease in the mRNA from PDX-1 as well as from the preproinsulin mRNA in response to high glucose. However, it is still possible that the kinase activity of PASKIN influences energy homeostasis even though mRNA and protein levels do not directly affect insulin production in *Paskin*$^{-/-}$ animals.

It has been reported recently, that PDX-1 is phosphorylated *in vitro* by purified PASKIN on a single threonine residue (Thr 152) [42]. Phosphorylation of PDX-1 by PASKIN seems to drive PDX-1 out of the nucleus. This is opposite to the suggested role of phosphorylated PDX-1 which enters the nucleoplasm [39]. Therefore Rutter and colleagues hypothesise that PASKIN must contribute to the long term stimulation of glucose, when chronic hyperglycaemia is inhibiting insulin secretion. Taken these results together, PASKIN stimulates PDX-1 expression and nuclear import to increase preproinsulin gene expression in pancreatic β-cells [41]. At the same time PASKIN phosphorylates PDX-1 Thr152 in vitro which apparently inhibits PDX-1 nuclear uptake [42]. Our group may contribute with a new model to overcome this contradiction. Glucose might activate an intracellular signaling pathway that involves phospholipase D (PLD) and subsequent increase in phosphatidic acid

(PA) formation. Tröger *et al.* showed that PA stimulates PASKIN autophosphorylation, but inhibits target phosphorylation as shown for eEF1A1 [43]. PDX-1 as another target of PASKIN might therefore as well be inhibited, allowing nuclear translocation.

5 PASKIN FUNCTION IN TESTIS

5.1 Introduction

Function of PASKIN during spermatogenesis

The testis is an organ where profound differentiation processes take place under very low oxygen concentrations. Spermatogenesis is vulnerable to environmental influences, often resulting in male infertility due to toxic pollutants or thermal stress. The molecular mechanisms of these processes are not yet fully understood.

We hypothesise that only under stress conditions PASKIN function becomes apparent, supported by the lack of an obvious phenotype in the *Paskin*$^{-/-}$ animals. In a similar approach, the function of the yeast orthologs PSK1 and PSK2 [1] was elucidated. By perturbation of normal testis homeostasis, PASKIN might sense the altered concentration of a still unknown metabolic ligand, thereby leading to interaction with and subsequent phosphorylation of the target protein.

We mimicked physiological stress leading to apoptosis to simulate stress situation in seminiferous tubuli. Apoptosis assays were established in germinal cell cultures with the objective of implementation in primary cells. We used the knowledge that PAS domains are sensing modules and implemented various stressors in the experimental setups. We hoped to find differences in the susceptibility of *Paskin*$^{+/+}$ versus *Paskin*$^{-/-}$ testis to show that PASKIN serves for the adaptation to environmental/metabolic stress conditions. Note that the testis is a highly organized tissue where spontaneous apoptosis takes place.

Spermatogenesis

The testis is specialized in sperm cell production. Germ cell-specific transcripts are expressed in a developmental stage-specific way [44]. These transcripts are derived from testis-specific genes which have a homolog in somatic cells or result from one or more testis-specific transcriptional start sites or splicing events [45]. In addition, some of the testis-specific proteins are unique to sperm cells. Enzymes and protein isoforms specific to testis include glycolytic enzymes, heat shock proteins, structural proteins, histone like proteins and transcription factors. The testes have, like the ovaries, two functions: they produce the male gametes or spermatozoa as component of the reproductive system, and they produce male sex hormones, thus being endocrine glands. Testosterone is the best-known hormone which stimulates development of the accessory male sexual organs. Both functions of the testicle are under control of gonadotropic hormones (LH, FSH) produced by the anterior pituitary. Under

a thick capsule, the tunica albuginea, the testis contains very fine coiled tubes called the seminiferous tubules. The tubes are lined with a layer of cells that produce sperm cells. The sperm travels from the seminiferous tubules to the rete testis located in the mediastinum testis,

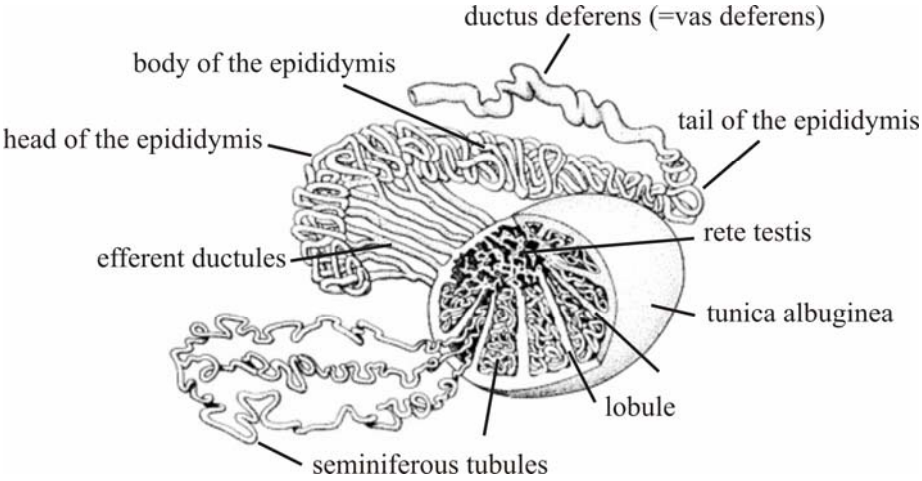

Figure 7: Inside the testis, delicate fibrous septa radiate towards the tunica albuginea and divide the parenchyma of the testis into about 300 lobuli testis, which communicate peripherally. Each lobule contains 1-4 convoluted seminiferous tubules, modified from http://trc.ucdavis.edu.

to the efferent ducts, and then to the epididymis where newly-created sperm cells mature. The sperm moves into the vas deferens and is eventually expelled through the urethra (Fig. 7). Between the seminiferous tubules special cells called Leydig cells are located, where testosterone and other androgens are formed. During puberty, androgen, LH and FSH production increase and the sex cords hollow out, forming the seminiferous tubules, and the germ cells start to differentiate into sperm. Throughout adulthood, androgens and FSH cooperatively act on Sertoli cells in the testes to support sperm production. The testes are located outside of the body, suspended by the spermatic cord within the scrotum. This allows for efficient fertile spermatogenesis in mammals, due to the fact that spermatogenic DNA polymerase beta and recombinase activities exhibit unique temperature optima, at a temperature somewhat less than core body temperature (37 °C).

Seminiferous tubules form the mass of the testes and are the sites of spermatogenesis. Seminiferous tubules are lined by the seminiferous epithelium and contain a fluid-filled lumen, into which fully formed spermatozoa are released. The Sertoli cell cytoplasm extends the entire height of the epithelium because the cell serves to nurture the germ cells through their cycles of development and move them towards the lumen. Interconnecting Sertoli cells create the blood-testis barrier and therefore are able to control the entry and exit of nutrients, hormones etc. into the tubules of the testis. The Sertoli cell also reduces motility and

capacitation (initiation of the acrosome reaction) of the sperm cells so viability is maintained. Leydig cells are located in the interstitial tissue amongst the seminiferous tubules and constitute the endocrine component of the testis. As mentioned above, they synthesize and secrete testosterone. Leydig cells occur in clusters, which are variable in size and richly supplied by capillaries. As the germ cells divide and develop into different types of cells, they move from the basement membrane region through tight junctional complexes of adjacent Sertoli cells until they reside in the adluminal compartment. The germ cells develop as a syncytium or clonal unit connected to one another by intercellular bridges after cell division. This unique process of incomplete division ensures synchronous development and permits rapid communication between the cells by sharing products of their genes [46]. This synchrony of germ cell development results in large areas of the seminiferous tubule containing vast numbers of cells at the same level of development which are represented by the 16 stages of spermatogenesis. Spermatogenesis can be divided into three different phases, spermatocytogenesis, spermatidogenesis and spermiogenesis which is the terminal process. In mice, the first round of spermatogenesis starts at birth and is completed in about 34 up to 40 days postnatally. This process involves cellular proliferation by repeated mitotic divisions, duplication of chromosomes, genetic recombination through cross-over, reduction-division by meiotic division to produce haploid spermatids, and terminal differentiation of the spermatids into spermatozoae.

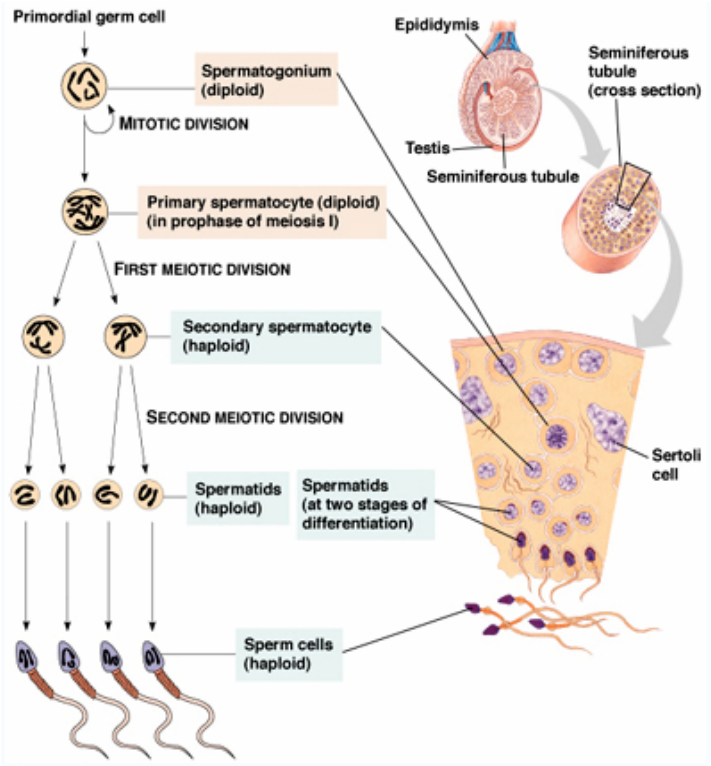

Figure 8: Spermatogenesis

(http://fig.cox.miami.edu/~cmallery/150/mitosis/lifecycle.htm)

Spermatogenesis can as well be divided into three phases: proliferation, reduction-division, and differentiation.

Spermatogonia originate in the 4th week of fetal development in the endodermal walls of the yolk sac and migrate to the primordium of the testis. Spermatogonia remain dormant until puberty and are always in contact with the basal lamina of the tubule. During **spermatocytogenesis**, a diploid

spermatogonium divides mitotically to produce a diploid intermediate cell called a primary spermatocyte. Each primary spermatocyte duplicates its DNA and subsequently undergoes meiosis I to produce two haploid secondary spermatocytes. This division implicates sources of genetic variation, such as random inclusion of both parental chromosomes, and chromosomal crossover, to increase the genetic variability of the gamete. Each cell division from a spermatogonium to a spermatid is incomplete; the cells remain connected to one another by bridges of cytoplasm to allow synchronous development. It should also be noted that not all spermatogonia divide to produce spermatocytes, otherwise the supply would run out. Instead, certain types of spermatogonia divide to produce copies of them, thereby ensuring a constant supply of gametogonia to fuel spermatogenesis. **Spermatidogenesis** is the creation of spermatids from secondary spermatocytes. Secondary spermatocytes produced earlier rapidly enter meiosis II and divide to produce haploid spermatids. The brevity of this stage means that secondary spermatocytes are rarely seen in histological preparations. During **spermiogenesis**, the spermatids begin to grow a tail, and develop a thickened mid-piece, where the mitochondria gather and form an axoneme (highly structured arrangement of microtubules in all cilia). Spermatid DNA also undergoes packaging, becoming highly condensed. The DNA is packaged first with specific nuclear basic proteins, which are subsequently replaced with protamines during spermatid elongation. The resultant tightly packed chromatin is transcriptionally inactive. Specific mRNAs are however stored for later translation of sperm-specific proteins [47]. The Golgi apparatus surrounds the now condensed nucleus, becoming the acrosome. The acrosome contains enzymes important in the process of fertilization. One of the centrioles of the cell elongates to become the tail of the sperm. Maturation then takes place, which removes the remaining unnecessary cytoplasm and organelles. The excess cytoplasm is phagocytosed by surrounding Sertoli cells in the testes. The resulting spermatozoon is now mature but lacks motility, rendering it sterile. The mature spermatozoon is released after about 13.5 d from the protective Sertoli cells into the lumen of the seminiferous tubule in a

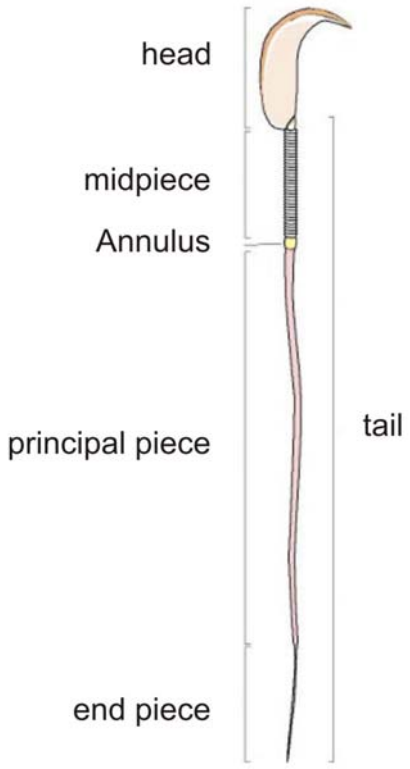

Figure 9: Mouse spermatozoa. (http://www.popcouncil.org/projects/BIO_AnnulusFunction.html)

process called spermiation. The non-motile spermatozoa is transported to the epididymis in testicular fluid secreted by the Sertoli cells with the aid of peristaltic contraction. In the epididymis the spermatozoae only partly acquires motility and becomes capable of fertilization. Transport of the mature spermatozoae through the remainder of the male reproductive system is achieved via muscle contraction rather than the recently acquired motility. The annulus is a ring-shaped structure at the distal end of the midpiece determining the junction between the midpiece and principal piece of the tail (Fig. 9). Sperms missing the annulus are not able to swim [48].

By spermatogenesis, one spermatogonium yields through one round of mitosis and two rounds of meiosis 8 gametes. The overall results of spermatogenesis are cell proliferation, maintenance of a reserve germ cell population, production of haploid gametes and genetic variability due to recombination of chromosomes during meiosis. Note that spermatogenesis in the seminiferous tubuli occurs under a high proliferation rate, suggesting considerable oxygen consumption. Because of the lack of blood vessels, the oxygen partial pressure in the lumen of these tubuli is as low as 2 mmHg [49]. Such low values for oxygen partial pressure are otherwise only found in the vicinity of mitochondria [49]. Therefore the testis represents an unique environment regarding the high division and differentiation rate within a small compartment at low oxygen pressure. With respect to these developmental and environmental challenges, it is not surprising that an unique set of specific genes or splice variants of common genes are expressed exclusively in the testis. For example, testis-specific isoforms of glycolytic enzymes are expressed during the haploid stages of spermatogenesis and are still active in mature spermatozoa, indicating the importance of testis-specific regulation of the glycolytic flux.

During normal spermatogenesis germ cell death occurs spontaneously. On the other hand, induced germ cell death includes for example suppression of hormonal support or increased scrotal temperature. The mechanisms by which these proapoptotic stimuli activate germ cell apoptosis are not well understood. In order to provide some insights, the key molecular components of the effector pathways leading to caspase activation and increased germ cell apoptosis will be summarized in the following chapter.

Molecular players of apoptosis

Apoptosis plays a vital role in the physiological maintenance of most tissues. It is a normal biological process that allows the elimination of unwanted cells through activation of the cell death program. The products of apoptosis are absorbed by neighboring cells without activation of an inflammatory response. Apoptosis may be triggered by a large variety of stimuli including extra-cellular signaling molecules (e.g. cytokines), intracellular signals (e.g. activated oncogenes), or physical stresses (e.g. UV light, gamma radiation). After receipt of an apoptotic signal, intracellular apoptosis-response proteins activate the cell death process through several mechanisms. These include initiating new gene expression, specific protein:protein interactions, and biochemical changes such as phosphorylation. In the second stage of apoptosis, the execution phase, cells undergo the classical changes associated with apoptosis. Cellular events include cleavage of specific cytosolic and structural proteins and fragmentation of DNA. Other cellular changes include the condensation and breakdown of the nucleus as well as mitochondrial membrane permeability changes. Mitochondrial disruption will ultimately result in cell death. The final stage of apoptosis involves the formation of membrane-bound apoptotic bodies. These are completely engulfed by surrounding cells or macrophages through the normal physiologic process of phagocytosis. Disassembly creates changes in the phospholipid content of the plasma membrane outer layer. Phosphatidylserine (PS) is exposed on the outer leaflet to be recognized by phagocytic cells which then engulf the apoptotic bodies. While apoptosis is the ordered disassembly of the cell, it can be distinguished from necrosis, occurring after a severe cellular insult, by the absence of an inflammatory response. The inflammation rises, since immune cells are attracted to the site where cytosolic and organellar contents by lost membrane integrity are spilled. The produced cytokines subsequently generate an inflammatory response. Cytosolic aspartate-specific proteases, called **caspases,** constitute a large protein family that is highly conserved among multicellular organisms. The family can be divided into two major subfamilies: caspases that

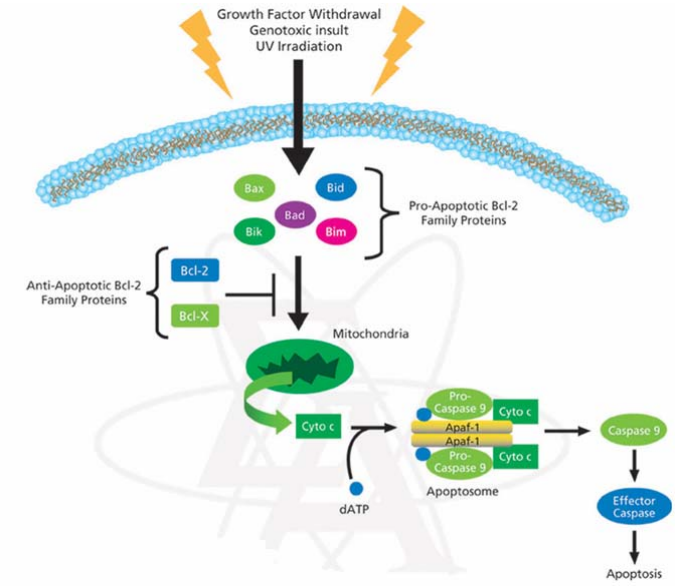

Figure 10: The Bcl-2 family members.
(http://www.sigmaaldrich.com)

are involved primarily in inflammation and have homology to caspase-1 (Interleukin-1β-Converting Enzyme), and those caspases that are related to CED-3 (*Caenorhabditis elegans* cell death abnormality) and are primarily involved in apoptosis. Caspases are constitutively expressed in most cell types as inactive zymogens that are proteolytically processed before they gain full activity. The caspase zymogens contain several domains including an N-terminal prodomain, a large subunit and a small subunit. Caspase activation involves cleaving the zymogen at a specific aspartic acid in the region between the large and small subunits and removing the prodomain. The active site is formed by a heterodimer containing one large and one small subunit, and the fully active caspase protein is a tetramer composed of two heterodimers. Because caspases exist as zymogens, their activity is thought to be regulated primarily on the post-translational level. However recent studies indicate that expression of the caspase-9 gene is regulated on the transcriptional level as well [50], and endoplasmic reticulum (ER) stress can induce expression of mouse caspase-12 in transfected cells [51]. Human caspase-8 and caspase-9 are involved in initiating apoptosis through two different signaling mechanisms and are known as initiator caspases. They can activate effector caspases, including caspase-3, by proteolytic processing. In turn, caspase-3 cleaves downstream targets and irreversibly commits the cell to the apoptotic fate. The initiator and the effector caspases are situated at pivotal junctions in apoptotic pathways. Poly (ADP-ribose) polymerase (PARP) is one of the main cleavage targets of caspase-3 in vivo [52], therefore serving as a marker of cells undergoing apoptosis. Upon cleavage, PARP (116 kDa) is divided into the N-terminal DNA binding domain (24 kDa) and its C-terminal catalytic domain (89 kDa). It is an abundant nuclear enzyme that is involved in a number of cellular processes in response to environmental stress. PARP mediates predominantly the repair of DNA single strand breaks via the activation and recruitment of DNA repair enzymes and is involved in programmed cell death. The **Bcl-2 protein family** includes a large number of proteins that share common BCL-2 homology (BH) domains. Structurally, the Bcl-2 proteins can be divided into three groups. Group I proteins include Bcl-2, and these proteins are anti-apoptotic. Group II and III family members are pro-apoptotic (Fig. 10). The group II family members contain all three of the BH domains (BH-1, BH-2, and BH-3). The group III family members contain only the BH-3 domain. The pro-apoptotic members of the BCL-2 family are implicated in permeabilizing the mitochondria outer membrane (MOM) and allowing leakage of mitochondrial proteins such as cytochrome c. The anti-apoptotic members of the protein family, such as Bcl-2, appear to protect cells from apoptosis by sequestering pro-apoptotic proteins or interfering with their activity [53].

Activation of apoptosis

Apoptosis can be induced in response to many **external stimuli** (extrinsic pathway or positive induction of apoptosis by ligand binding to a plasma membrane receptor) including activation of cell surface receptors such as Fas, TNFR1 (tumor necrosis factor receptor 1), TRAIL-R1 (TNF-related apoptosis-inducing ligand receptor 1), TRAIL-R2, p75-NGFR (p75-nerve growth factor receptor) and others [54]. These death receptors have two distinct signaling motifs: the cytoplasmic death domains (DD) and the death effector domains (DED) that allow them to interact with other proteins involved in the apoptotic cascade. Ligands binding to these cell surface receptors are typically trimeric, related to TNF and cause aggregation of the receptors. This aggregation brings the cytoplasmic domains of the membrane receptors into close proximity and induces a conformational change allowing the assembly of the death inducing signaling complex (DISC) at the cytoplasmic tail of the receptors. The DISC comprises the receptors, the ligands as well as an adaptor protein, the Fas associated death domain protein (FADD). FADD binds through its C-terminal DD to the ligand-bound receptor and recruits procaspase-8. Procaspase-8 in turn binds to the DED of FADD via its own N-terminal DED domains. As a consequence of DISC formation at ligand-bound receptors, several molecules of procaspase-8 are brought into close proximity. One hypothesis suggests that the low intrinsic activity of procaspase-8 allows the procaspase-8 zymogens to cleave and activate each other [55]. On the other hand, it has been reported that activation of caspase-8 requires dimerization [56]. Active caspase-8 heterotetramers are released from DISC and are free to cleave and activate the effector caspase, caspase-3. In some cells, caspase-8 leads to an amplification loop that involves caspase-8 cleavage of the Bcl-2 protein family member, Bid. When Bid is cleaved it can induce Bax-mediated release of cytochrome c from the mitochondria, further committing the cell to apoptosis. Activation of procaspase-8 can be blocked by FLIP which is a caspase-8 homolog without proteolytic activity. FLIP integrates into the DISC inhibiting apoptosis and forming inactive heterodimers with procaspase-8. Alternatively, the mitochondrial pathway is activated by **intrinsic signals** such as DNA damage [57]. The mitochondrial pathway involves members of the Bcl-2 family and can be activated either by the death receptor pathway or by other stimuli that are independent of death receptors including DNA damage, topoisomerase inhibition or withdrawal of trophic factors[58]. Many of the Group II and group II Bcl-2 family members, such as Bax, Bad and Bid, shuttle between the mitochondria and the other parts of the cell. Their activity is regulated by a variety of mechanisms including proteolytic processing, phosphorylation and sequestration by inhibitory proteins. Pro-apoptotic signals direct the Group II and III Bcl-2

family proteins to the mitochondria where the pro-apoptotic members interact with anti-apoptotic Bcl-2 family members, including Bcl-2 and BclXL, to determine whether or not

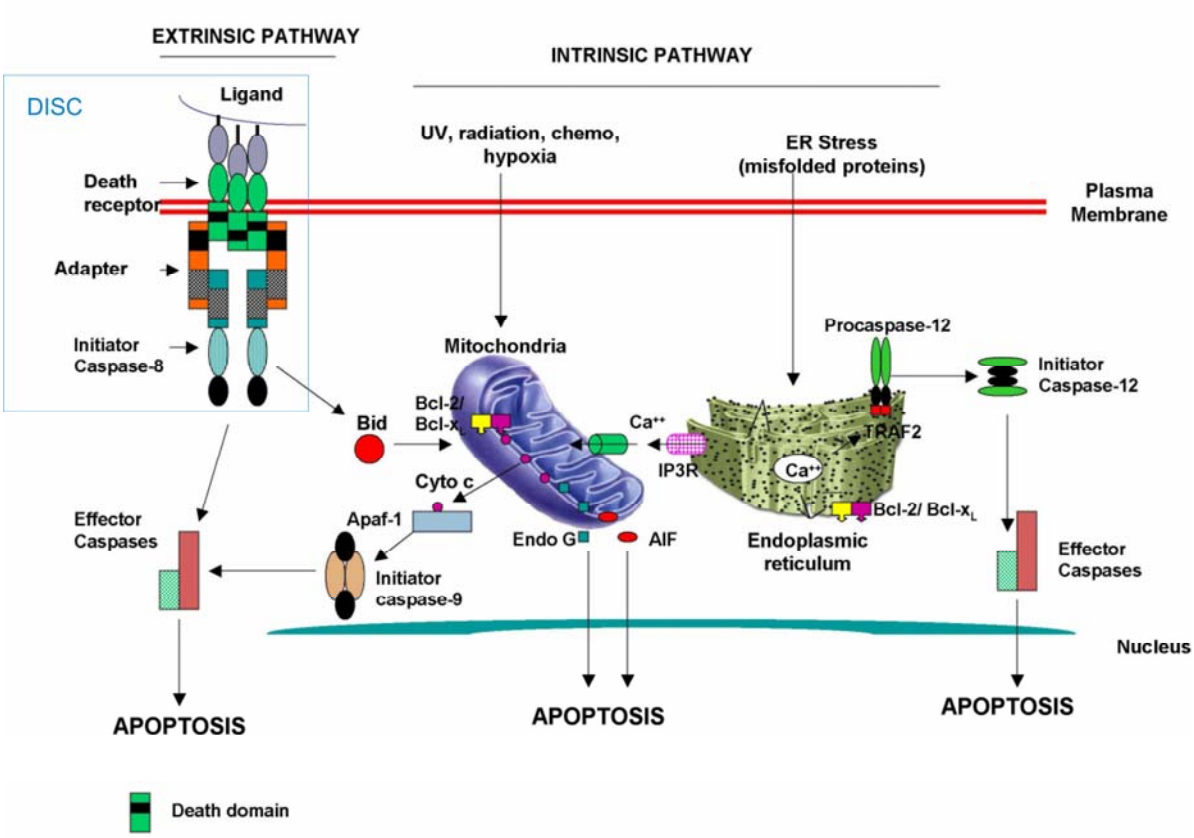

Figure 11: Signaling pathways of apoptosis, modified from Gupta *et al.* Immunity & Ageing 2006 3:5)

apoptosis will be initiated. If the pro-apoptotic proteins win, cytochrome c and other molecules are released from the MOM. Once cytochrome c is released from the mitochondria, it can interact with Apaf-1, dATP and procaspase-9 in a protein complex called the apoptosome. Caspase-9 is processed and activated when it its part of the apoptosome, where it can cleave and activate caspase-3.

Recent studies have suggested that a third pathway for activating apoptosis may involve the ER. In mice, caspase-12 has been implicated in an ER stress pathway that induces apoptosis. Caspase-12 in the mouse localizes to the ER and is cleaved in response to ER stress such as the accumulation of unfolded proteins [59]. Caspase-4 is a potential candidate for activating apoptosis through an ER stress pathway in humans [60]. Granzyme B and perforin, proteins released by cytotoxic T cells form transmembrane pores and trigger apoptosis, perhaps through cleavage of caspases. Caspase independent mechanisms of granzyme B-mediated apoptosis have also been suggested [61] (Fig. 11).

5.2 Methods

Cell lines and culture conditions

The human leukemia cell lines HL-60, the GC-1 spg spermatogonia (CRL-2053), and GC-2 spd spermatocyte (CRL-2196) were cultured in DMEM (high glucose, Life Technologies, Inc., Gaithersburg, MD) supplemented with 10% heat-inactivated FCS (Roche Molecular Biochemicals, Mannheim, Germany), 100 U/ml penicillin, 100 μg/ml streptomycin in a humidified 5% CO2 in air atmosphere at 37°C. For heat exposure cells were splitted and allowed to grow for 24 h, and then exposed to 44°C for 4 h. After heat treatment, cells were returned to 37°C for 3 h so that apoptosis could proceed. All experiments were repeated at least three times. Data shown in the graphs for various parameters represent the means and SEM.

Preparation of cell lysates and determination of DEVD-AMC cleavage

Cells were exposed to 44°C for 4 h and back to 37°C for 3 h. At frequent intervals thereafter, cells were collected by centrifugation and resuspended in lysis buffer (100 mM Hepes, pH 7.5, 10% sucrose, 0.1% CHAPS, 1 mM EDTA, and 1 mM phenylmethylsulfonyl fluoride). Cell lysate (30 mg of protein/sample) was incubated with 12 mM of the fluorogenic peptide substrate DEVD-AMC in a 96-well microtiter plate at room temperature. The cleavage of DEVD-AMC was monitored by AMC liberation in a fluoroscan plate reader using 360 nm excitation and 465 nm emission wavelengths. Fluorescence was measured every 300 s during a 60 min period, and fluorescence units were converted to pmol amounts of AMC using a standard curve generated with free AMC (Sigma). Control experiments confirmed that the release of substrate was linear with DEVD-AMC and protein concentration.

Primary cells and culture conditions

The animals were killed by cervical dislocation. The testis was excised and the capsule removed. The seminiferous tubuli were incubated in BWW media (21.58 mM Na-lactate, 0.50 mM Na-pyruvate, 100 U/ml penicillin and 100 μg/ml streptomycin, 5.56 mM Glc, 5 mg/ml BSA) with or without indicated concentrations of adriamycin in a 6-well plate. The tubuli were incubated in a humidified incubator with 5% CO_2 at 30°C and 44°C, respectively.

Preparation of cell lysates of seminiferous tubuli

Seminiferous tubuli were centrifuged, washed with PBS, and resuspended in 1.5 ml RIPA lysis buffer / g tissue (1% NP40, 0.5% sodium deoxychlate, 1% SDS in PBS, complete mini-protease inhibitor cocktail) and stored at -80°C.

Western Blot Analysis

Total protein extracts of cultured cells were prepared using RIPA lysis buffer. Protein concentration was determined by the Bradford method or BCA assay using bovine serum albumin as a standard [62]. Protein (75 µg) was run on a polyacrylamide gel and blotted onto PVDF membranes by semi-dry electroblotting (Bio-Rad) with a subsequent washing step in TBS; membranes were stained with Ponceau S to verify equal protein loading per lane. After overnight blocking (5% non-fat milk powder, 0.1% Tween 20 in Tris-buffered saline), blots were probed for 2 h with antibodies against PARP (Cell Signaling) or actin (Sigma; diluted 1:1000, 1:5000, respectively) and detected with horseradish peroxidase-conjugated antibodies (Pierce; dilution: 1:2000) and the ECL system (Pierce).

5.3 Results

Caspase activity measurement with DEVD-AMC fluorogenic substrate

Oxidative-stress-induced apoptosis in GC-1/GC-2 cells

The purpose of using GC-1 (spermatogonia) and GC-2 (spermatocytes) cell lines was to establish a functional apoptosis assay to be further used with primary cells of the mouse testis.

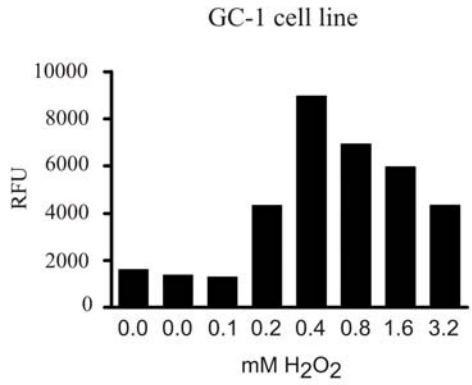

Figure 12: Oxidatively stressed GC-1 cells. Incubation with H_2O_2 for 2 h following 15 min incubation time with DEVD-AMC, as determined by kinetic measurement.

In a first approach the cells were subjected to oxidative stress (H_2O_2) and apoptosis was detected upon active effector caspase-3. Caspase activity was detected by cleavage of a fluorogenic substrate comprising the caspase cleavage site DEVD (Asp-Glu-Val-Asp) linked to a fluorophore. Once the fluorophore is released from the substrate (Ac-DEVD-AMC) the fluorophore can be activated by excitation around its extinction maximum of 346 nm and the emission around its maximum of 442 nm can be detected in a 96-well fluorimeter. Up to

concentrations of 0.5 mM H_2O_2 cells undergo apoptosis and above that concentration cells are becoming necrotic. In Fig. 12 apoptosis is induced up to 0.4 mM as shown by increased RFU. Unfortunately, the reproducibility was poor and showed even less confidence when GC-2 cells were assayed. Therefore we concluded that these cell lines were not adequate to establish an apoptosis assay, since they are genetically instable. Note, that spermatocytes are derived from the transient secondary spermatocytes and lie between the two reduction divisions rendering them genetically instable [63].

Hyperthermia-induced apoptosis in HL-60 cells

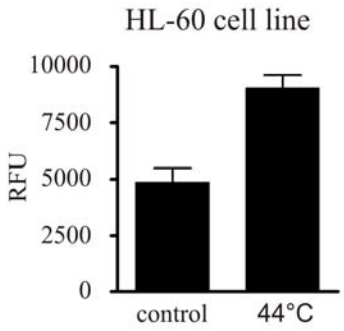

Figure 13: Hyperthermia induced apoptosis in HL-60 cells.

In a further effort to establish an apoptosis assay, the human leukaemia cell line HL-60 was assayed after heat exposure to 44°C according to literature Katschinski *et al.* [64]. Thermal stress resulted in significant apoptotic cell death as demonstrated by caspase 3 activation (Fig. 13). Three independent assays were performed and the optimal endpoint was determined to be 20 min post substrate addition. Subsequently, the testes from *Paskin*$^{-/-}$ and *Paskin*$^{+/+}$ mice were isolated and the seminiferous tubuli were distributed to 6-well plates containing BWW media. Even though various stressors, like hyperthermia, oxidative stress and serum deprivation, were applied, the testicular lysates did not show any caspase activity not even with the double amount of protein used (Fig. 14). We assume that the lysis of the seminiferous tubuli was not complete and therefore the active caspase was not detectable. Harsher detergents were applied (RIPA), however they interfered with the emission measurement.

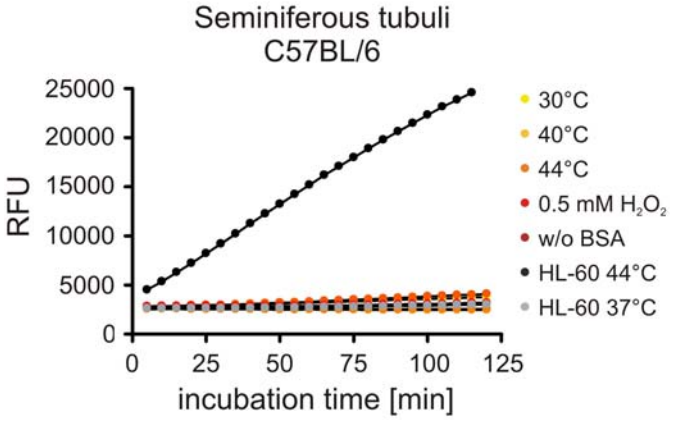

Figure 14: Kinetic measurement of caspase 3 activity. HL-60 cells incubated under 37°C and 44°C, respectively, were used as positive controls.

PARP cleavage detection in stressed seminiferous tubuli

Different lysis buffers were tested to optimize PARP detection via Immunoblotting. When using Chaps as detergent, no band could be visualized for primary cells, in accordance with the fluorometric assay. The reducing capacity of lysis buffer containing 8 M urea (P.J. Ratcliff, Oxford, UK) or 6 M urea [65] precipitated DNA and led to diffuse bands on the Western blots. The addition of DNase I to inhibit the interference of proteins with nucleic acids by degrading the latter did not quite lead to the desired result, even not in combination with lysate sonification. The method of choice implemented RIPA lysis buffer, subsequent homogenization with a douncer in combination with sonification [66]. The seminiferous tubuli were first subjected to hyperthermia for 44°C and then moved back to 30°C for another 3 h. In Fig. 15, the HL-60 control incubated at 44°C show extensively cleaved PARP, indicative of hyperthermic apoptosis, whereas the HL-60 cells incubated at 37°C show only background apoptosis. The seminiferous tubuli derived from *Paskin*$^{-/-}$ and *Paskin*$^{+/+}$ mice did not show differences in PARP cleavage, when they are subjected to hyperthermic conditions versus incubation at physiological temperature. Therefore, further methods to induce apoptosis in seminiferous tubuli were applied. Longer exposure to hyperthermia (72 h) [67], glucose deprivation or hyperglycemia (30 mM) did not show any increase in the apoptotic rate (data not shown). Adriamycin is known to increase apoptosis in seminiferous tubuli [68] and is the trade name for doxorubicin, which is a DNA-interacting drug widely used in chemotherapy of a wide range of cancers. Doxorubicin is known to interact with DNA by intercalation and inhibition of macromolecular biosynthesis [69]. This inhibits the progression of the enzyme topoisomerase II, which unwinds DNA for transcription. Doxorubicin stabilizes the topoisomerase II complex after it has broken the DNA chain for replication, preventing the DNA double helix from being resealed and thereby stopping the process of replication. According to Suominen *et al.*, 8 h treatment of the seminiferous tubuli with 0.1 μM adriamycin shows a two fold increase in apoptotic cells [68]. When these conditions were adapted to *Paskin*$^{-/-}$ and

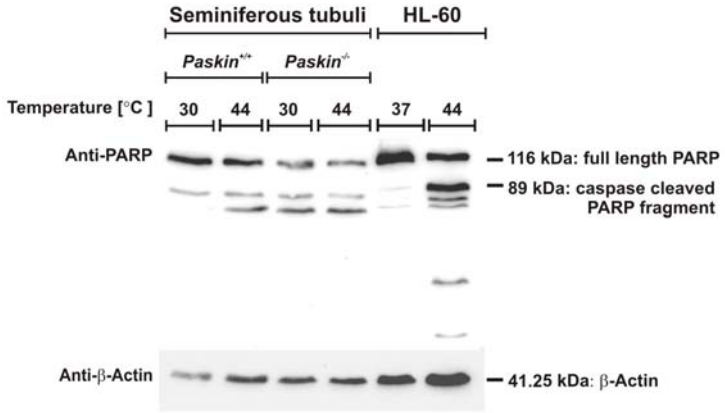

Figure 15: Hyperthermia induced apoptosis in *Paskin*$^{-/-}$ and *Paskin*$^{+/+}$ seminiferous tubuli.

Paskin$^{+/+}$ seminiferous tubuli, no increased PARP cleavage could be verified upon treatment with 0.1 µM adriamycin (Fig. 16). Subsequently adriamycin was titrated up to a concentration of 100 µM. Neither in *Paskin*$^{-/-}$ (Fig. 16) nor in *Paskin*$^{+/+}$ (not shown) seminiferous tubuli a dose-response relationship could be established.

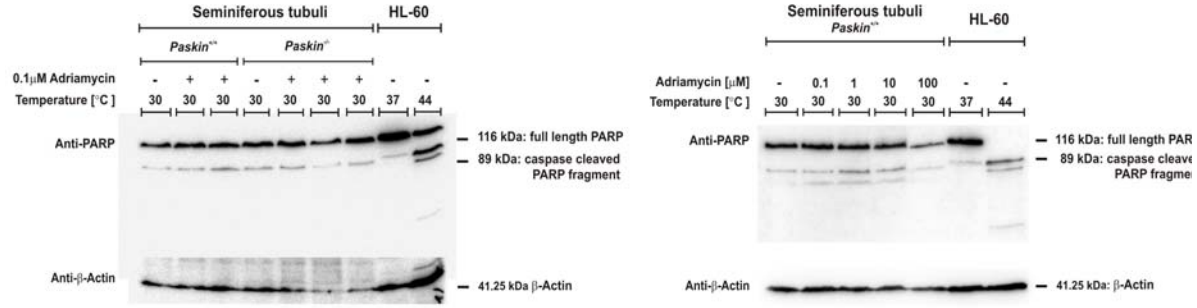

Figure 16: Adriamycin induced apoptosis in *Paskin*$^{-/-}$ and *Paskin*$^{+/+}$ seminiferous tubuli. Administration of 0.1 µM Adriamycin (left) and titrated concentration up to 100 µM (right).

5.4 Discussion

Different methods to quantite apoptosis were established *in vitro*. The first method implied the fluorogenic substrate Ac-DEVD-AMC for measuring cleavage activity of capase 3 after hydrogen peroxide treatment. In spermatogonia and spermatocyte cell lines, the reproducibility failed due to their genetic instability [63]. Using HL-60 cells and hyperthermia the assay was of use. When applied to seminiferous tubuli, the lysis buffer turned out to be not harsh enough for successfully extracting proteins. A harsher detergent could not be used because of the interference with the emission measurement. The second method implied the detection of cleaved PARP by Immunoblotting. Apoptosis can be quantified by comparing the intensity of the cleaved PARP fragment with the full length PARP lane. The basal apoptotic rate in untreated seminiferous tubuli was so strong, that a stressor did not significantly induce more PARP cleavage. In the seminiferous tubuli, where ongoing cell division and differentiation takes place, apoptosis is occurring spontaneously to maintain cell homeostasis. Efforts to lower the background apoptosis by faster handling of the tubuli, for example by switching from CO_2 euthanizing to cervix dislocation, were not effective. Finally, a TUNEL assay was performed with untreated tissue sections embedded in Bouin´s solution (data not shown). No differences could be detected as might be the case when no stress conditions are applied.

The favoured method in use to induce apoptosis in mice in vivo is cryptorchidism. This medical term is referring to the absence from the scrotum of one or both testes. This usually represents failure of the testis to move, to "descend," during fetal development from an abdominal position. In laboratory mice, usually one testis is surgically translocated into the abdominal cavity, which results in temperature elevation and apoptosis induction. After 7 to 14 days the testis is then removed for further experimental procedure, which is a quite long lasting hyperthermic induction when compared to our experimental setup. It is known that spermatocytes are very sensitive to damage at elevated temperatures, which might be as well the case for overall environmental changes. The isolation procedure and the culturing in 6-well plates might already impose too much stress on the tubuli. Suominen *et al.* excised the tubuli and treated them as well in culture, however they used transillumination assisted microdissection [70] to cut 2-mm long segments containing stages III-V, VII-VIII and IX-XI from the mouse seminiferous epithelial cycle [71]. Suominen *et al.* determined apoptosis rate by ISEL staining and the number of apoptotic cells was calculated under light microscope.

5.5 Conclusions

The testis being a complex, heterogeneous tissue and highly susceptible to environmental changes, caused major constraints comparing spontaneous with induced apoptosis. The high expression of PASKIN during the postmeiotic stage of spermatogenesis in mouse testis, the strong nuclear PASKIN signal in spermatogonia and lower PASKIN levels in spermatocytes and spermatids in the mitochondrial sheath of human testis, still points towards a role for PASKIN in spermatozoa function. Even though no significant differences could be detected in sperm motility assays of *Paskin*$^{-/-}$ and *Paskin*$^{+/+}$ sperms under normal laboratory conditions, the co-localisation of PASKIN and eEF1A1 in the mitochondrial sheath, which is implicated in motility of spermatozoa emphasises an implication. Indeed, eEF1A1 is involved in apoptosis [72] besides its role in protein translation. Furthermore, by screening peptide arrays we identified novel putative phosphorylation targets of PASKIN: the inhibitor of PP1 and PKA type II-α regulatory chain. Both proteins are also located to the mitochondrial sheath and have been proposed to play a role in the motility of spermatozoa [73-75]. Protamine is another putative phosphorylation target of PASKIN with a unique role in haploid round spermatids when chromatin is compacted: somatic and testicular histones are replaced by various basic transition proteins that help transform the nucleosomal chromatin into smooth condensed chromatin fibres. The transition proteins are then replaced by the sperm nuclear

proteins, the protamines (Hecht, NB, 1998). Furthermore, transcription is stopped or limited in late elongating spermatids. Specific mRNAs are stored for later translation of sperm-specific proteins. However, the potential phosphorylation targets of PASKIN have first to be confirmed *in vitro* to exclude false positive substrates. Nevertheless, the putative phosphorylation targets open a broad platform to speculate about the possible role(s) of PASKIN.

6 PASKIN FUNCTION IN PANCREAS

6.1 Introduction

Glucose regulated gene expression

Glucose, independently of insulin, can regulate the expression of genes involved in carbohydrate metabolism. Upon entry into the cells, glucose is phosphorylated to G6P by GK in hepatocytes and by hexokinase in all other cells. This step is required for glucose to undergo glycolysis, to be used in the glycogen synthesis pathway, or to enter the pentose phosphate pathway. This first metabolic transformation of glucose is also required for generating the signal that acts in transcriptional regulation. Some reports suggest that G6P itself might be the signaling molecule. Alternatively, other metabolites such as xylitol produced by the pentose phosphate pathway or intermediates of the hexosamine biosynthetic pathway might also act in tissue-specific regulations [76]. The analysis of glucose signaling is, however, often difficult to dissociate from insulin signaling. **First**, the entry of glucose into muscle and adipose tissue cells, which are two main insulin target organs, operates through the translocation of the Glut4 transporter via an insulin-mediated transduction signal. In contrast, the expression of the glucose transporters Glut2 in the liver and pancreas, Glut3 in the brain, and the widely distributed Glut1 are insulin independent, and their translocation is constitutive. **Second**, in the liver and to a lesser extent in the pancreas, the initial metabolic modification of glucose into G6P by GK is required for transcriptional regulation by glucose and is strongly dependent on insulin. Thus, the actions of glucose and insulin often depend on each other.

Therefore, high glucose levels influence gene expression either directly or through the stimulation of insulin production by the β-cells of the pancreas. Insulin acts, in part, by altering the activity of transcription factors and, thus, transcriptional programs in target tissues [11]. Several transcription factors are targets of the insulin-signaling pathways. Of these, SREBP-1c is of particular note [12,13], and the transcription, processing and activity of SREBP-1c are stimulated in the liver in response to insulin [14–16]. The transcriptional activator SREBP-1c, which is expressed in adipose tissue and liver, promotes de novo lipogenesis, so converting excess glucose to triglyceride for storage until periods of energy deficiency. That is how the liver functions as the main buffer, providing glucose when nutrients are scarce and storing glucose into triacylglycerol for longer term storage as fat. By this way, glucose signaling in β-cells is coupled to glucose disposal in the major metabolic tissues.

Glucose regulated gene expression in β-islet cells

The human preproinsulin gene is a single copy gene, while rodents contain two preproinsulin genes. Furthermore, the regulatory DNA elements within the human promoter are different from the rodent orthologs [77]. Glucose stimulates insulin release, transcription of preproinsulin and subsequent processing and translation of the nascent mRNA [78]. These mechanisms are crucial to the cell for maintaining ongoing insulin stores after repeated glucose challenges. Upon glucose stimulation, members of the mitogen-activated protein kinase family, extracellular response kinase-1/2 (ERK1/2), are activated by phosphorylation [79]. As a consequence, the β-cell specific transcription factors PDX-1, MafA, and Beta2/NeuroD1 are translocated to the nucleus, where binding occurs to the promoter sequence of the preproinsulin gene [80]. Recruitment of histone acetyltransferases by these transactivators also leads to increases in histone acetylation at the insulin gene to facilitate transcription [81]. The transcription factors act synergistically to promote insulin gene transcription. PDX-1 is not only involved in the regulation of insulin gene expression in pancreatic β-cells, but it is as well a key factor for normal pancreatic development. Jonsson et al. showed that mice homozygous for a targeted mutation in the PDX-1 gene selectively lack a pancreas. After fetal development the mutant mice die within a few days after birth, while the gastrointestinal part and all other internal organs were normal in appearance [82]. The subcellular localization of PDX-1 is reported to be regulated by phosphorylation, which occurs at glucose concentration, although this model is still controversial [83, 84]. The kinases that regulate glucose-dependent phosphorylation of PDX-1 are not fully identified, but there are several candidates [42, 85]. Glucose can trigger phosphorylation of PDX-1 via phosphatidylinositol 3-kinase (PI3K) which induces nuclear translocation of PDX and increases insulin expression [39]. Other factors activated by glucose likely contribute to PDX-1-mediated response of insulin to glucose [86]. In addition to HNF3b/FOXA2, which positively regulates PDX1 expression [87], other members of the HNF family are expressed in pancreatic β-cells (HNF1a, HNF1b, HNF4a). The maturity-onset diabetes of youth (MODY) is a medical condition and has highlighted the importance of this network of transcription factors, acting directly or indirectly on insulin gene expression [88]. Depending on which of the transcription factors involved in insulin gene expression is genetically mutated, *MODY1*, *MODY3*, *MODY4* or *MODY5* has been assigned. Only *MODY2* is caused by a mutation in the enzyme glucokinase. The fact that mutations in any of these genes result in altered insulin secretion reveals that all of these transcription factors are crucial for the control of cell specificity and metabolic adjustment of insulin expression (Fig. 17).

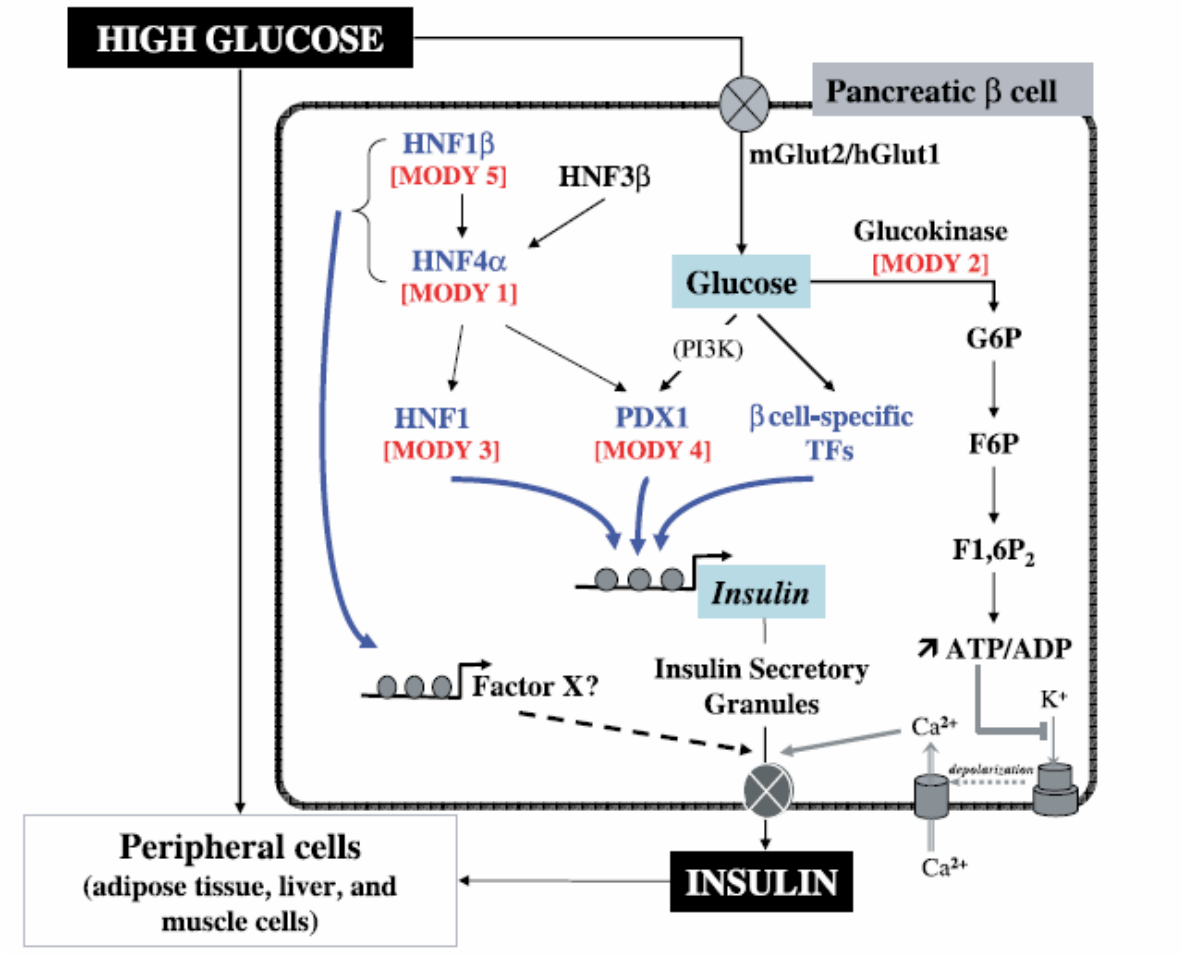

Figure 17: Transcriptional regulation of the insulin gene in the presence of high glucose. The roles of the HNF family of proteins and the central role of the transcription factor PDX1 in the regulation of the expression of the insulin gene are highlighted. Gene alterations responsible for the maturity onset diabetes of the young (MODY) are shown in red. Insulin secretion is triggered by an increase in cytosolic ATP/ADP, which closes K^+- channels in the plasma membrane, thereby causing membrane depolarization and opening of voltage-gated Ca^{2+}-channels. The resulting rise in the cytosolic Ca2_ concentration activates exocytosis of insulin-containing granules. Factor X, hypothetical factor acting on insulin secretion; F6P, fructose-6-phosphate; F1,6-P2, fructose 1,6-diphosphate; Glut, glucose transporter; G6P, glucose-6-phosphate; HNF, hepatocyte nuclear factor; TFs, transcription factors [6].

Glucose regulated gene expression in metabolic tissues

Insulin and glucagon are the central regulators of blood-glucose levels in mammals, however glucose generates independent signals in tissues other than the endocrine pancreas. The role of glucose in altering gene transcription is understood best in the liver, where elevated glucose concentrations increase the production of enzymes that are necessary for lipogenesis

[27,28]. As noted above, the induction of genes that encode lipogenic enzymes depends on insulin and SREBP-1c. However, studies in primary hepatocytes in culture show that in addition to insulin, glucose must also be elevated above the fasting blood level of 5.5 mM. These observations have led to the identification of a specific DNA regulatory sequence in the promoters of several genes that encode lipogenic enzymes, including L-type pyruvate kinase (PK), S14, acetyl-CoA carboxylase and fatty acid synthase (Fig. 18), which has been termed the carbohydrate response element (ChoRE). The ChoRE is composed of two, 6-bp motifs known as E boxes that have a consensus sequence of CACGTG separated by 5 bp [29]. Generally, E-box sequences are recognized by transcription factors that contain basic helix– loop–helix/leucine zipper (bHLH/LZ) DNA-binding domains [30]. A bHLH/LZ protein that is designated the ChoRE-binding protein (ChREBP) binds to ChoRE. Several features of ChREBP are consistent with a role as a glucose-regulated transcription factor. For example, the mRNA that encodes ChREBP is most abundant in liver, small intestine, and white and brown adipose tissue, which are the most active sites of lipogenesis in the body [32]. Most importantly, the cellular localization of ChREBP is influenced by the glucose concentration in primary hepatocytes [33]. In high-glucose conditions, ChREBP is predominantly nuclear, whereas in low glucose most ChREBP is in the cytosol. ChREBP homodimers bind poorly to DNA. Instead, it works in conjunction with another bHLH/LZ protein called Max-like factor X (Mlx) [34,35]. In the presence of Mlx, ChREBP binds to the ChoREs of genes that encode lipogenic enzyme [34]. Two ChREBP–Mlx heterodimers bind to the two E boxes of the ChoRE and appear to interact to provide the unique architecture that is necessary for glucose regulation (Fig. 18).

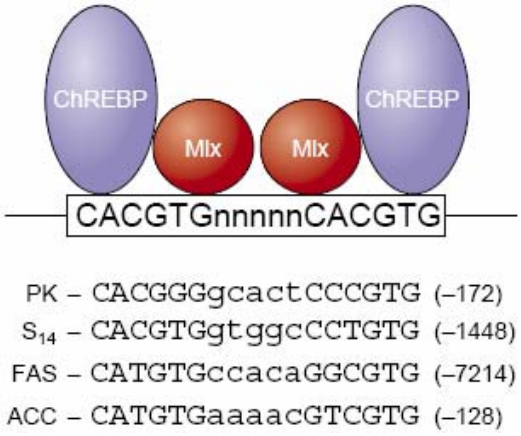

Figure 18: Binding of ChREBP-Mlx to ChoRE activates gene transcription in response to glucose. The E-box-like sequences of these four ChoREs are in capitals and the location of the first base in the sequence relative to the start site of transcription is indicated in brackets [5].

6.2 Publication: Glucose-stimulated insulin production in mice deficient for the PAS kinase PASKIN

Emanuela Borter[1], Markus Niessen[2], Richard Züllig[2], Giatgen A. Spinas[2], Patrick Spielmann[1], Gieri Camenisch[1], and Roland H. Wenger[1]

From the [1]Institute of Physiology and Center for Integrative Human Physiology (CIHP); [2]University Hospital Zürich, Clinic for Endocrinology and Diabetes, University of Zürich, Zürich, Switzerland

Correspondence: Roland H. Wenger, Institute of Physiology, University of Zürich-Irchel, Winterthurerstrasse 190, CH-8057 Zürich, Switzerland. Tel: +41 (0)44 63 55065; Fax: +41 (0)44 63 56814; E-Mail: roland.wenger@access.unizh.ch

ABSTRACT

The PAS domain serine/threonine kinase PASKIN, or PAS kinase, links energy flux and protein synthesis in yeast and regulates glycogen synthase in mammals. A recent report suggested that PASKIN mRNA, protein and kinase activity are increased in pancreatic islet β-cells under hyperglycemic conditions and that PASKIN is necessary for insulin gene expression. We previously generated *Paskin* knock-out mice by targeted replacement of the kinase domain with the β-*geo* fusion gene encoding β-galactosidase reporter activity. Here we show that no X-Gal staining was observed in islet β-cells derived from *Paskin* knock-out mice, irrespective of the ambient glucose concentration, whereas adenoviral expression of the *lacZ* gene in β-cells showed strong X-Gal staining. No induction of PASKIN mRNA could be detected in insulinoma cell lines or in islet β-cells. Increasing glucose concentrations resulted in PASKIN-independent induction of insulin mRNA levels and insulin release. PASKIN mRNA levels were high in testes but undetectable in pancreas and in islet β-cells. Finally, blood glucose levels and glucose tolerance following i.p. glucose injection were indistinguishable between *Paskin* wild-type and knock-out mice. These results suggest that *Paskin* gene expression is not induced by glucose in pancreatic β-cells and that glucose-stimulated insulin production is independent of PASKIN.

INTRODUCTION

Per-ARNT-Sim (PAS) domain proteins often serve as environment sensors, regulating the cellular metabolism and behavior of microorganisms in response to, among others, oxygen or light. In nitrogen-fixing *Rhizobium* species, for example, the oxygen sensor protein FixL contains a heme group within its PAS domain. Oxygen bound to heme inhibits the histidine kinase domain. Under oxygen-free conditions, kinase activity is de-repressed and activates FixJ, the master transcriptional inducer of genes involved in nitrogen fixation.

We and others previously identified a novel mammalian PAS protein, termed PASKIN [4] or PAS kinase [17]. The domain architecture of PASKIN resembles that of FixL. PASKIN contains two PAS domains (PAS A and PAS B) and a serine/threonine kinase domain related to AMP kinases which might be regulated in *cis* by binding of so far unknown (metabolic?) ligands to the PAS domain [2]. Following de-repression, autophosphorylation in *trans* results in the "switch-on" of the kinase domain of PASKIN [17]. The budding yeast PASKIN homologs PSK1 and PSK2 phosphorylate three translation factors and two enzymes involved in the regulation of glycogen and trehalose synthesis, thereby coordinately controlling translation and sugar flux [1]. Under stress conditions (nutrient restriction combined with high temperature), PASKIN kinase activity results in downregulation of protein synthesis and carbohydrate storage in yeast. In mammalian cells, PASKIN-dependent phosphorylation inhibits the activity of the mammalian glycogen synthase [38].

A recent report suggested that PASKIN kinase activity followed by mRNA and protein expression is increased in MIN6 cells and in isolated pancreatic β-cells after exposure to high glucose concentrations [41]. Increased PASKIN activity appeared to be required for glucose-dependent transcriptional induction of the pancreatic duodenum homeobox 1 (PDX-1) transcription factor, leading to transcriptional induction of preproinsulin but not glucokinase or uncoupling protein 2 gene expression. The authors concluded that decreases in PASKIN activity in β cells might contribute to some forms of type 2 diabetes [41]. However, no *in vivo* data were provided in this report.

We previously generated PASKIN null mice by targeted replacement of the kinase domain of the mouse *Paskin* gene by a *lacZ-neo* fusion construct in embryonic stem cells [29, 89]. Surprisingly, PASKIN expression is strongly upregulated in post-meiotic germ cells during spermatogenesis as revealed by both β-galactosidase staining as well as mRNA blotting. In fact, PASKIN mRNA levels in testis are several magnitudes higher than in all other organs tested. No other "sensory" organs, including pancreas, carotid bodies or photoreceptor cells, stained positive for β-galactosidase. At least under laboratory conditions, fertility as well as

sperm production and sperm motility were not affected in PASKIN knock-out mice. To examine the role of PASKIN in glucose-stimulated insulin production, we used pancreatic β-cells derived from wild-type and knock-out mice and performed glucose tolerance tests in these mice.

RESEARCH DESIGN AND METHODS

PASKIN-deficient mice

The generation and genotyping of PASKIN knock-out mice was described previously [29]. Heterozygous *Paskin*$^{+/-}$ mice were crossed with the C57BL/6 inbred strain for ten generations and then bred to homozygosity for the knock-out allele, containing the *lacZ* reporter gene. All animal handling followed the guidelines for the use and care of laboratory animals of the Bundesamt für Veterinärwesen and was approved by the Kantonales Veterinäramt Zürich (Nr. 192/2003).

Islet isolation and β-cell culture

Male *Paskin*$^{+/+}$ and *Paskin*$^{-/-}$ mice were sacrificed by cervical dislocation, the pancreas was excised and islets were either manually picked or isolated by gradient density centrifugation as described before [90]. Briefly, 2 ml ice-cold collagenase solution (1 PZ-U/ml NB-8, 10 mM HEPES, 3.3 mg/ml DNaseI, 10 mM $CaCl_2$ in Hank's balanced salt solution (HBSS), pH 7.4) was injected into several sites of the pancreas which was then incubated for 10 to 14 minutes in a 37°C shaking waterbath. The digestion was stopped by adding ice-cold FCS-quenching buffer (10% FCS in 22 mM HEPES, HBSS). After two washing steps with BSA-quenching buffer (0.5% BSA in 22 mM HEPES, HBSS) and following centrifugation at 1200 rpm/2 minutes/4°C, the digested pancreas was filtered through medical gauze. Following centrifugation as above, the pellet was resuspended either in 35 ml RPMI1640 media for manual picking or in 5 ml 1.119 g/ml histopaque (Sigma, Buchs, Switzerland) in a 50 ml tube and overlaid with 5 ml 1.100 g/ml histopaque, 10 ml 1.077g/ml histopaque and 10 ml HBSS. The tube was centrifuged (1200 rpm/25 minutes/4°C) and the islets were collected from the interphase, diluted 1:1 with BSA-quenching buffer, centrifuged (1200 rpm/10 minutes/4°C), washed once in HBSS and resuspended in RPMI1640 supplemented with 10% FCS, 100 U/ml penicillin, 100 μg/ml streptomycin, 10 mM HEPES, 11 mM D-glucose (Invitrogen, Basel, Switzerland). Medium was changed every 24 hours for 2 to 3 days until the islets spread and flattened on 35 mm plates coated with extracellular matrix (ECM) derived from bovine

corneal endothelial cells (Novamed, Jerusalem, Israel). To control for β-galactosidase expression, islets were infected with adenovirus constitutively expressing the *lacZ* reporter gene [90].

Insulin determination

Islets were cultured in pyruvate-free RPMI1640 as above. Before glucose stimulation, islets were starved in medium containing 1.6 mM glucose for 30 minutes, medium was replaced and the islets incubated for another hour. The medium was replaced by fresh medium containing the desired glucose concentrations and the islets were incubated for 6 hours at 37°C. The supernatant was collected for insulin measurments and the islets were prepared for X-Gal staining. Insulin concentrations were determined by RIA using the insulin-CT kit according to the instructions provided by the manufacturer (Schering, Baar, Switzerland).

X-Gal staining and β-galactosidase assay

Excised mouse testes or cultured, glucose-treated islets were fixed with 0.2% glutaraldehyde, 5 mM EGTA, 2 mM $MgCl_2$, 0.1 M Na-phosphate buffer pH 7.3, permeabilised with 0.01% Na-deoxycholate, 0.02% NP-40, 2 mM $MgCl_2$, 0.1 M Na-phosphate buffer pH 7.3, and incubated in X-gal solution (5 mM $K_3Fe(CN)_6$, 5 mM $K_4Fe(CN)_6$, 2 mM $MgCl_2$, 0.02% NP-40, 0.01% Na-deoxycholate, 0.1 M Na-phosphate buffer pH 7.3, 0.1% X-Gal) at 37°C. β-Galactosidase activity was determined in tissue extracts by the ONPG assay and normalized to protein content as described before [91].

Cell culture and glucose stimulation

Mouse spermatogonia GC-1 and spermatocyte GC-2 [92], human testicular germ cell tumor NCCIT and embryonal carcinoma NTERA-2 cl.D1 (provided by S. Schweyer, Göttingen, Germany), mouse insulinoma MIN6 and the B1-MIN6 subline (provided by W. Moritz, Zürich, Switzerland; J. Rutter, Utah, USA; and P.A. Halban, Geneva, Switzerland, respectively), and rat insulinoma INS-1E (provided by C.B. Wollheim, Geneva, Switzerland) cell lines were cultured in high glucose Dulbecco's modified Eagle's medium (Sigma) as described previously [93]. The glucose concentration was lowered to 3 mM for 16 hours before incubation of cells with 3 mM or 30 mM glucose for 6 hours.

mRNA quantification

Total RNA from mouse organs or cultured cells was isolated as described previously [92]. Mouse PASKIN, insulin and L28 mRNA was determined by RT-qPCR. Briefly, 8 μg of total RNA was reverse transcribed with StrataScript III (Stratagene, Amsterdam, The Netherlands) and qPCR was performed in duplicates with 8% of the cDNA reaction mixture using a SYBRGreen qPCR reagent kit on a MX3000P PCR light cycler according to the manufacturer's instructions (Stratagene). Primers (synthesized by Microsynth, Balgach, Switzerland) used were: PASKIN, hPASKINfwd 5'-ggaactgctccagtttcctg-3' and hPASKINrev 5'-ggatctccgcttaatgacca-3'; mPASKINfwd 5'-agggtccaagaattgacgtg-3' and mPASKINrev 5'-tgactgctcaccatcctctg-3'; rPASKINfwd 5'-tgtggactgcagtggagaag-3' and rPASKINrev 5'-caaagaggtccaagccagag-3'; ribosomal protein L28, hL28fwd 5'-ggaactgctccagtttcctg-3' and hL28rev 5'-ggatctccgcttaatgacca-3'; mL28fwd 5'-ggcaaaggggtcgtggtagt-3' and mL28rev 5'-tcagggcggtacttgttctt-3'; rL28fwd 5'-cggagcccaataatctgaag-3' and rL28rev 5'-ttgatggtggtcctcacgta-3'; PDX-1, mPDX-1fwd 5'-gaaatccaccaaagctcacg-3' and mPDX-1rev 5'-ttcaacatcactgccagctc-3'; glucokinase, mGckfwd 5'-tatgaagaccgccaatgtga-3' and mGckrev 5'-tttccgccaatgatcttttc-3'; rGckfwd 5'-cagtggagcgtgaagacaaa-3' and rGckrev 5'-cttggtccaattgaggagga-3'; insulin, mmInsfwd 5'-tggcttcttctacacacccaag-3' and mmInsrev 5'-acaatgccacgcttctgcc-3'; rmIns1fwd 5'-caccttttgtggtcctcacct-3' and rmIns1rev 5'-ccagttggtagagggagcag-3'; mPKfwd 5'-ttctgtctcgctaccgacct-3' and mPKrev 5'-cctgtcaccacaatcaccag-3'; rPKfwd 5'-cgttcagcccagcttctatc-3' and rPKrev 5'-cctgtcaccacaatcaccag-3'. Dilution series of the corresponding plasmids or gel-isolated PCR products were used to obtain standard curves.

Immunofluorescence

Flattened islet β-cells on ECM dishes were washed with PBS, fixed with 4% paraformaldehyde, permeabilized with 0.5% TritonX-100, blocked with 10% normal goat serum (NGS) in PBS and stained with polyclonal guinea-pig anti-insulin antibodies (Sigma) diluted 1:100 in 1% NGS in PBS for 30 minutes at 37°C. Bound antibodies were detected with FITC-conjugated goat anti-guinea-pig antibodies at 1:20 dilution (Sigma). The ECM plates were mounted with Kaiser's glycerol gelatine (Merck, Darmstadt, Germany) and analyzed by fluorescence microscopy.

Intraperitoneal glucose tolerance tests

Glucose tolerance tests were performed in 6-8 and 14-16 weeks old male mice. Mice were fasted overnight (16 hours) and injected intraperitoneally with a saline glucose solution of 2 g/kg body weight. Blood was obtained by puncturing the tail vein and glucose levels were measured using ACCU-CHEK Aviva (Roche Diagnostics, Basel, Switzerland). Measurements were performed before and 30, 60, 90, 120 and 150 minutes after glucose injection.

RESULTS

PASKIN mRNA is not induced by high glucose treatment of cultured cell lines

PASKIN mRNA has been previously suggested to be induced by glucose in pancreas-derived MIN6 cells [41]. However, following exposure to high glucose levels (30 mM) for 6 hours, we could not confirm PASKIN mRNA induction in mouse MIN6 cells or rat INS-1E cells, while insulin secretion by MIN6 cells or pyruvate kinase mRNA in INS-1E cells were readily increased under high glucose concentrations. Real-time RT-PCR also did not reveal any glucose-dependent increase in expression of PDX-1 or the two mouse or rat insulin genes (data not shown). A similar pattern of constitutive insulin and PDX-1 gene expression as well as the glucose-dependent pyruvate kinase gene expression in INS-1E cells has been reported previously [94]. Moreover, neither testis-derived mouse spermatogonia GC-1 and spermatocyte GC-2 nor human testicular germ cell tumor cell lines NTERA and NCCIT significantly increased PASKIN mRNA expression following treatment with 30 mM glucose (data not shown). Generally, the PASKIN mRNA levels were very low in all of these cell culture models, suggesting that they might not represent appropriate models for PASKIN expression.

The mouse *Paskin* gene is not transcriptionally activated by high glucose in cultured islets

To obtain a physiologically more relevant cell culture model, pancreatic islets were isolated from *Paskin* wild-type mice as well as from *Paskin* knock-out mice containing a *lacZ-neo* fusion gene replacing exons 10 to 14 of the *Paskin* gene [29]. Expression and activity of the β-galactosidase reporter gene in these mice was consistent with PASKIN mRNA levels as analyzed by Northern blotting, demonstrating adequate representation of *Paskin* gene activity [29]. However, staining of β-cells derived from *Paskin*$^{-/-}$ mice with X-Gal did not reveal any

signal when compared with wild-type mice (Fig. 1*A*). In contrast, β-cells infected with adenovirus expressing a *lacZ* reporter gene (Fig. 1*A*), or testes derived from the same knock-out but not from the wild-type mice (Fig. 1*B*), readily stained blue. The identity of the primary β-cells was confirmed by immunostaining for insulin using immunofluorescence and immunohistochemistry (Fig. 1*C*). In another set of experiments, pools of islets were prepared from groups of 6 *Paskin*$^{+/+}$ or *Paskin*$^{-/-}$ mice, split into aliquots of 20 islets, exposed to various glucose concentrations for 6 hours, extracted and assayed for specific β-galactosidase activities using an *in vitro* assay. As shown in Fig. 1*D*, only background levels could be detected in *Paskin*$^{-/-}$ islets, corresponding to *Paskin*$^{+/+}$ islets, which were not induced by treatment with high glucose concentrations. In contrast, simultaneously prepared testis extracts derived from *Paskin*$^{-/-}$ mice displayed at least 14-fold higher β-galactosidase activities than the background levels observed in *Paskin*$^{+/+}$ testes.

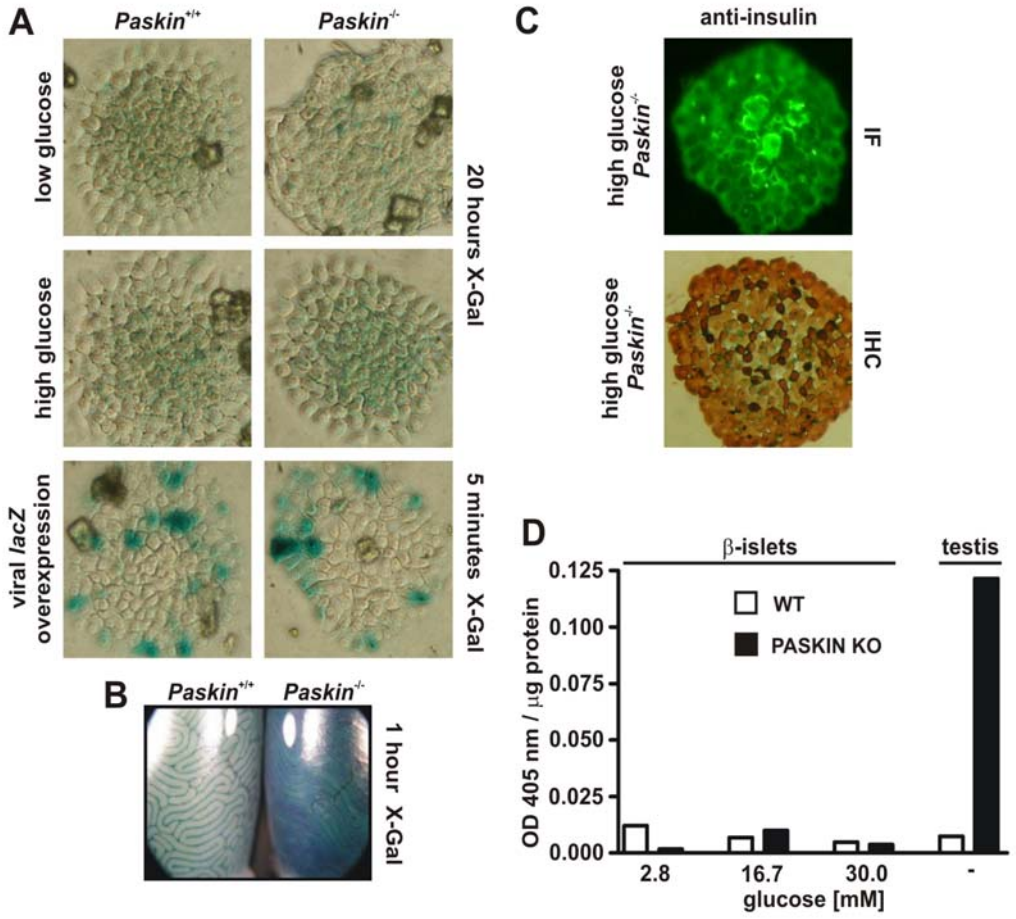

Figure 1: *Paskin* gene expression in pancreatic islet β-cells derived from *Paskin* wild-type or knock-out mice. Pancreata and testes were excised from the same male mice at 6-8 weeks of age. Islets were prepared, cultured under high or low glucose conditions, and stained as described in Research Design and Methods. *A*: X-gal staining of islets to determine β-galactosidase activity derived from *lacZ* gene expression used as reporter gene within the *Paskin* locus in the *Paskin*$^{-/-}$ mice, or derived from adenoviral *lacZ* expression as control. The different X-gal incubation times are indicated. *B*: Examples of a control X-gal staining of testes derived from the same animals. *C*: Examples of insulin immunodetection by immunofluorescence (IF) or immunohistochemistry (IHC), following X-gal staining, to confirm the identity and integrity of the β-cells. *D*: In another set of experiments, β-galactosidase activities were quantitatively determined by a colorimetric assay using protein extracts derived from pooled β-cells kept under various glucose concentrations as indicated or from testes as control. The $OD_{405\ nm}$ values were normalized to 1 µg of protein.

Insulin gene expression is independent of PASKIN in cultured primary β-cells

Because not only PASKIN mRNA levels but also kinase activity has been reported to be induced by high glucose [29], insulin gene expression could still be regulated in a PASKIN-dependent manner, even if the *Paskin* gene itself is not glucose-responsive. Therefore, pools of islets were prepared from groups of 8 *Paskin*$^{+/+}$ or *Paskin*$^{-/-}$ mice, split, exposed to high or low glucose concentrations for 6 hours, and mRNA levels were determined by real-time RT-PCR. However, neither glucose-induction of insulin mRNA (Fig. 2*A*) nor insulin release into the supernatant (Fig. 2*B*) were dependent on the presence of a functional *Paskin* gene. The genotype of the mice was confirmed by simultaneous PASKIN RT-PCR using testis-derived RNA which, as expected, had high PASKIN mRNA levels when isolated from *Paskin*$^{+/+}$ mice, but undetectable levels when isolated from *Paskin*$^{-/-}$ mice (Fig. 2*C*). To test whether PASKIN mRNA could be induced by glucose in the major organ expressing PASKIN, seminiferous tubuli were excised from testis and cultured *in vitro* under various glucose conditions. Again, no significant glucose-dependent PASKIN mRNA induction could be observed by real-time RT-PCR (Fig. 2*D*). Of note, the copy number of PASKIN mRNA in testis is approx. $1x10^6/\mu g$ total RNA whereas it was below the detection limit in pancreatic islets (data not shown).

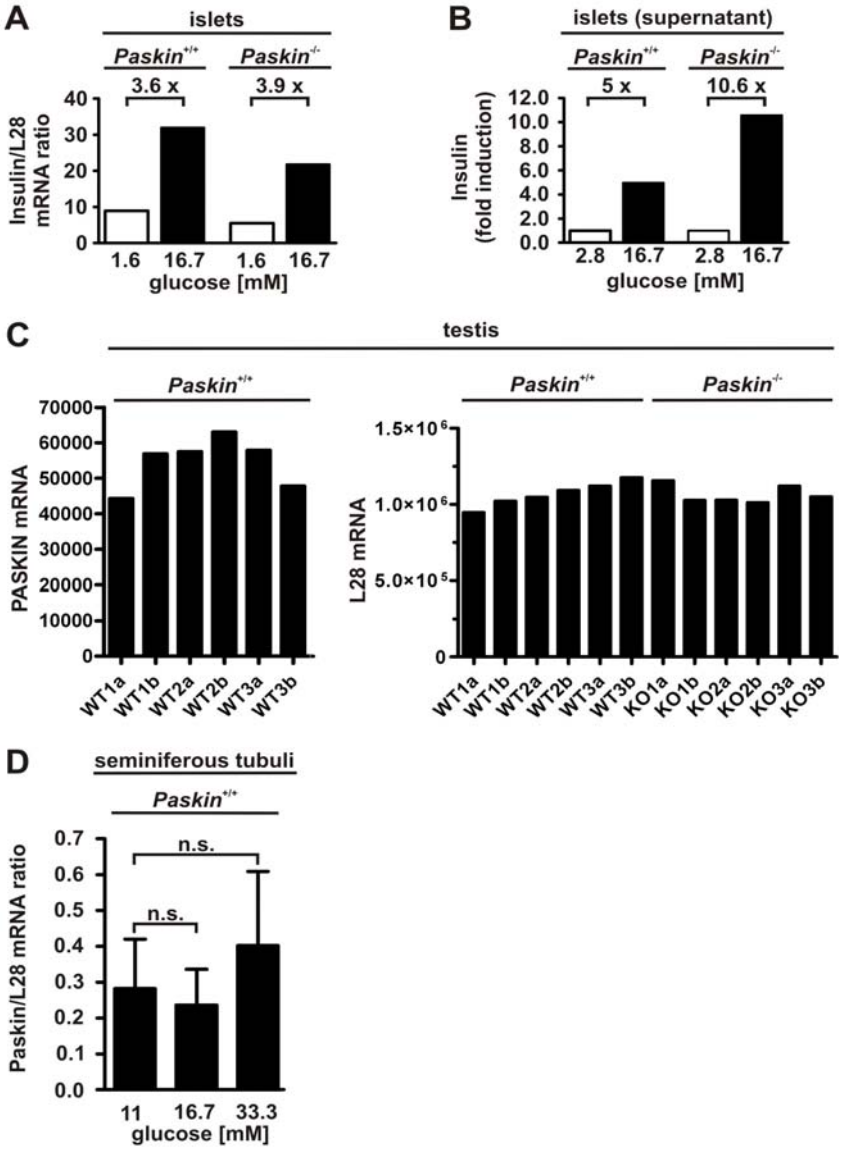

Figure 2: *Insulin* gene expression and insulin secretion by pancreatic islet β-cells pooled from groups of 8 *Paskin* wild-type (WT) or knock-out (KO) mice. Pancreata and testes were excised from the same male mice at 6-8 weeks of age. Islets were prepared, cultured under high or low glucose conditions, and insulin mRNA and protein secretion determined by real-time RT-PCR and RIA, respectively. Glucose induction of insulin mRNA (*A*) and insulin secretion (*B*) were equal in β-cells derived from *Paskin* wild-type and knock-out mice. *C*: Example of simultaneous PASKIN mRNA determination in testes derived from the same mice as used for islet preparation. "a" and "b" refer to left and right testis of the same animal. PASKIN mRNA was undetectable in knock-out mice (not shown). *D*: Lack of PASKIN mRNA induction by glucose in cultured tubuli seminiferi derived from 14 week old mice (mean ± SEM of n = 3 independent experiments; n.s., not significant with p=0.80 and 0.65, respectively, using unpaired t-tests).

Normal glucose tolerance in *Paskin*$^{-/-}$ mice

In order to rule out that the *in vitro* cultivation of islets inadequately reflected PASKIN function, *in vivo* experiments were performed. First, endogenous PASKIN and insulin expression levels in organs derived from mice fed normal chow diet *ad libitum* were determined by real-time RT-PCR. As shown in Fig. 3*A* (top panel), PASKIN mRNA levels were at least 50-fold higher in the testis than in every other organ tested, confirming previous Northern blotting data [29]. PASKIN mRNA was undetectable in pancreas. While mRNA derived from pancreas, as expected, generally was of worse quality than from other organs, PASKIN could not be detected even when 10-fold more RNA was used for the RT reactions. However, high insulin mRNA levels were found in the same pancreas cDNA samples (Fig. 3*A*, bottom panel).

Glucose (2 g/kg body weight) was injected intraperitoneally into 6-8 weeks (n = 5-6 per group) or 14-16 weeks (n = 7 per group) old *Paskin*$^{+/+}$ or *Paskin*$^{-/-}$ mice and blood glucose levels were followed at 30 minute intervals for 2.5 hours. There was no significant difference in glucose tolerance between *Paskin* wild-type and knock-out mice in either of the age groups (Fig. 3*B*). To examine basal blood glucose levels, groups of 6-8 weeks or 14-16 weeks old mice were either fed *ad libitum* or fasted overnight for 16 hours. As shown in Fig. 3*C*, there was again no significant difference between *Paskin* wild-type and knock-out mice, irrespective of their food supply.

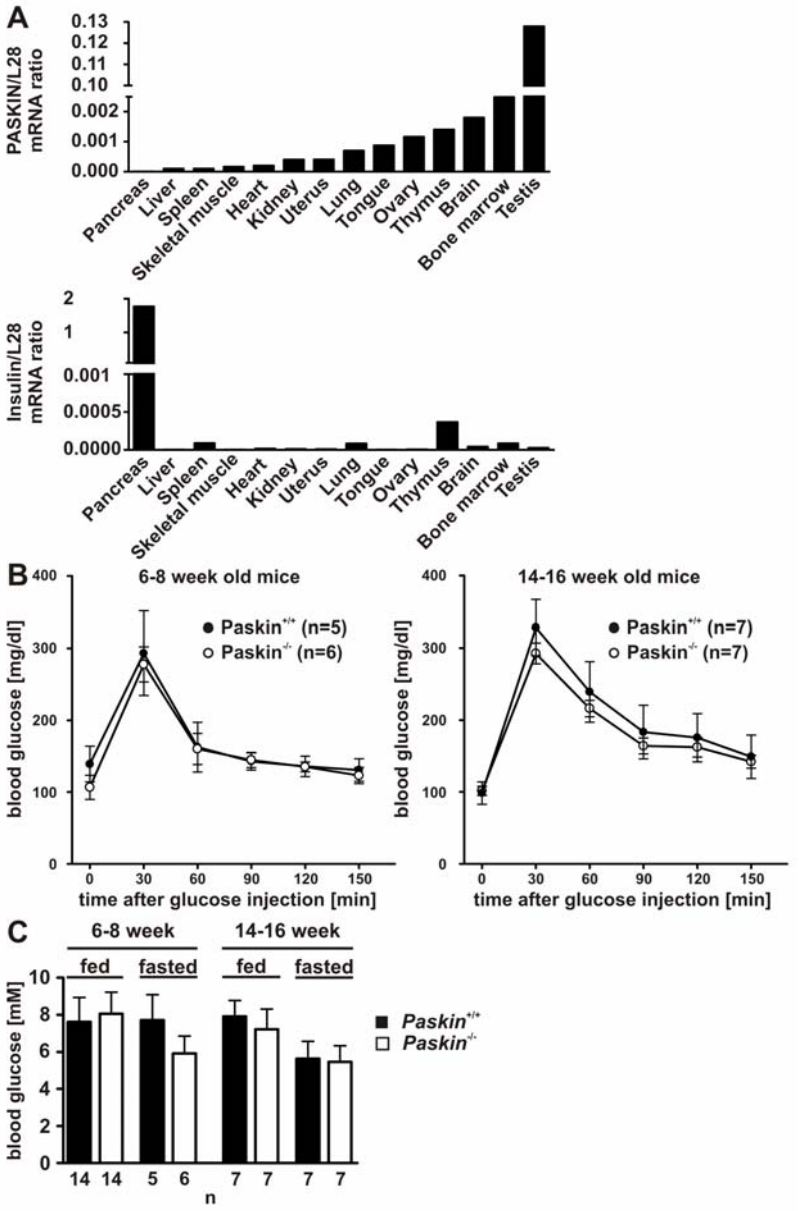

Figure 3: Normal blood glucose concentrations and glucose tolerance in *Paskin* wild-type and knock-out mice. *A*: PASKIN and insulin mRNA levels in various organs derived from C57BL/6 mice determined by real-time RT-PCR. *B*: Intraperitoneal glucose tolerance tests in 6-8 or 14-16 weeks old *Paskin* wild-type or knock-out mice. *C*: Blood glucose concentrations in 6-8 or 14-16 weeks old *Paskin* wild-type or knock-out mice either fed *ad libitum* or fasted overnight for 16 hours (shown are mean ± SD values of the indicated number n of male mice).

DISCUSSION

PASKIN is highly expressed in the testis and *Paskin* knock-out mice display no obvious phenotype and a normal fertility and lifespan [29]. Therefore, a recent report suggesting that PASKIN is required for glucose-induced PDX-1 and insulin gene expression was quite unexpected [41]. We thus back-crossed our initial *Paskin* knock-out strain ten times with C57BL/6 inbred mice in order to obtain a more homogenous genetic background and repeated the experiments reported by da Silva Xavier et al. [41]. We neither found PASKIN mRNA regulation by high glucose in various pancreatic β-cell or testicular cell lines, nor in isolated islets or tubuli seminiferi. One explanation for this difference might be that we used real-time RT-PCR rather than the probably less reliable Northern blotting for mRNA determination. While we were unable to demonstrate glucose-dependent induction of PDX-1 and insulin mRNA expression, glucose readily induced insulin release into the supernatant of MIN6 cells and glucose also stimulated pyruvate kinase gene expression in INS-1E cells, demonstrating adequate cell culture conditions. Currently, we do have no explanation for this discrepancy. We obtained MIN6 cells from three distinct sources, but obtained similar results with all batches. However, probably more important than the cultured cell lines are the results with cultured islets. Importantly, increasing the ambient glucose concentration resulted in a similar increase in insulin mRNA and insulin secretion, whether the β-cells were derived from *Paskin* wild-type or knock-out mice. This experiment probably provides the most convincing evidence that glucose-stimulated insulin gene expression is independent of PASKIN. Another argument was provided by glucose tolerance tests which showed equal blood glucose clearance in young as well as older *Paskin* wild-type and knock-out mice. We extended the determination of blood glucose levels to additional groups of mice fed with normal chow diet or fasted overnight, but again could not observe any significant difference in blood glucose concentrations. Thus these experiments demonstrated normal acute and chronic insulin function in *Paskin* knock-out mice *in vivo*, further supporting our notion that insulin expression is independent of PASKIN.

PASKIN clearly has a metabolic function in yeast, and the regulation of glycogen synthase supports the idea of a similar function also in mammals [1, 38]. In addition, we recently identified enzymes of the glycolytic pathway as potential PASKIN targets (Tröger J., Eckhardt K., Wenger R.H.; unpublished observations). Thus, even when the PASKIN mRNA expression levels are rather low in all tissues except testis, a PASKIN function outside of the testis certainly cannot be excluded. However, considering its structural architecture, PASKIN kinase activity probably represents the metabolically regulated effector rather than PASKIN

mRNA and/or protein induction. While we can exclude glucose from being a direct activator of PASKIN *in vitro* (Tröger J., Eckhardt K., Wenger R.H.; unpublished observations), it appears to be likely that another, yet unidentified metabolic ligand induces PASKIN kinase activity and target protein phosphorylation. Such an activator also would explain the lack of an obvious phenotype in *Paskin* knock-out mice. Like in yeast, PASKIN function might become apparent only under altered environmental conditions such as nutrient stress. Emphasis hence must be put on the identification of PASKIN-activating conditions. Apparently, high glucose alone is not sufficient to induce PASKIN.

ACKNOWLEDGEMENTS

Supported by grants from the University Research Priority Program "Integrative Human Physiology" (to E.B.), the *Stiftung für wissenschaftliche Forschung an der Universität Zürich* (to R.H.W.), and the Swiss National Science Foundation (3100A0-104219 to R.H.W. and G.C.). The authors wish to thank S. Schweyer, W. Moritz, J. Rutter, P.A. Halban and C.B. Wollheim for the kind gift of cell lines; and C. Wagner and J.A. Ehses for helpful advice.

6.3 Conclusions

PASKIN mRNA is not regulated under hyperglycaemic conditions, neither in various pancreatic β-cell lines, testicular cell lines nor in isolated islets or tubuli seminiferi. Exposure to high glucose levels (30 mM) for 6 hours did not confirm PASKIN mRNA induction in mouse MIN6 cells or rat INS-1E cells as suggested by da Silva Xavier *et al.* [41]. Insulin secretion by MIN6 cells and pyruvate kinase gene expression in INS-1E were increased under high glucose concentrations, indicative of adequate cell culture conditions. Real-time RT-PCR also did not reveal any glucose-dependent increase in expression of PDX-1 or the two mouse or rat insulin genes. MIN6 cells were obtained from three different sources and the results were similar for all batches, including the B1-MIN6 subclone [95]. Moreover, neither testis-derived mouse spermatogonia GC-1 and spermatocyte GC-2 nor human testicular germ cell tumor cell lines NTERA and NCCIT increased PASKIN mRNA expression following treatment with 30 mM glucose. Furthermore, we performed alignments of all known glucose response elements with the PASKIN promoter and the introns 1 to 5 of *Mus musculus*, *Rattus norvegicus* and *Homo sapiens*. No conserved glucose response element was found within the promoter or the introns. Most convincingly an increase in insulin mRNA and insulin secretion in both *Paskin*$^{-/-}$ and *Paskin*$^{+/+}$ pancreatic β-cells after exposure to high glucose but no increase in PASKIN mRNA was observed. Thus insulin gene expression is independent of PASKIN under these conditions. Glucose tolerance tests showed no evidence of deficient insulin secretion in PASKIN animals independent of their age. This was further supported by normal blood glucose in *Paskin*$^{-/-}$ and *Paskin*$^{+/+}$ animals in fed or fasted state. We reason that the acute and chronic insulin function in *Paskin*$^{-/-}$ animals is normal. PASKIN mRNA expression levels are low in all tissues, indicating that PASKIN might play a role in energy homeostasis once it is activated by its corresponding ligand. However, considering PASKIN as a mammalian sensor protein, the kinase activity might represent the metabolically regulated effector rather than PASKIN mRNA and protein induction. By this model, the lack of an obvious phenotype in *Paskin*$^{-/-}$ animals further supports the assumption that a ligand is needed which activates PASKIN activity under special nutrient conditions.

7 PASKIN FUNCTION IN ENERGY HOMEOSTASIS

7.1 Introduction

The role of AMP kinase in energy homeostasis

Based on the known effects of AMPK on carbohydrate and lipid metabolism, it becomes clear that this system is a major player in the development and/or treatment of obesity, diabetes, and the metabolic syndrome, which have reached epidemic proportions in modern industrialized society. AMPK is probably involved in the beneficial effects of regular exercise and appears to mediate many of the effects of the adipokines leptin and adiponectin, as well as the antidiabetic drug metformin. AMPK also appears to be involved in cancer because LKB1 as a direct upstream kinase of AMPK acts as tumor suppressor, and because of the roles of the AMPK pathway in angiogenesis, apoptosis, and senescence of tumors. There are also indications that the AMPK system is involved in the effects of caloric restriction on life span. Note, that AMPK is involved in regulating energy homeostasis on the whole body level as well as on the cellular levels.

The protein structure

AMPK is a heterotrimer comprising α, β, and γ subunits. Two genes each encode the catalytic α subunit and the regulatory β subunit. The regulatory γ subunit is encoded by 3 genes. In total 12 heterotrimeric combinations are possible, while splice variants give rise to further diversity. The 2 isoforms of the α subunit, α_1 and α_2, contain the kinase domain in their N-terminal half, with the C-terminal regions being required to form a complex with the β and γ subunits [96]. The α subunits appear to have rather similar substrate specificities, but the α_2 isoform is enriched in the nucleus of several cell types, including pancreatic β cells [97], neurons [98], and skeletal muscle [99], whereas α_1 is predominantly cytoplasmic. The α_1 isoform is associated with the plasma membrane in carotid body type 1 cells [100] and airway epithelial cells [101]. The eukaryotic β subunits contain 2 conserved regions, located in the central and C-terminal regions. The C-terminal domain is responsible for the formation of a functional αβγ complex that is regulated by AMP [102]. The central conserved region is recognized to be a glycogen-binding domain, however the functions of this domain remain unclear, although it is present in the β subunits of all eukaryotic species [103]. The γ subunits (γ_1, γ_2, and γ_3) contain variable N-terminal regions followed by 4 tandem repeats of a 60-aa sequence named the CBS motif by Bateman [104]. These act in pairs to form 2 domains (now

termed Bateman domains), each of which binds one molecule of AMP, being the regulatory binding sites for the nucleotides [105]. The Bateman domains also antagonistically bind ATP on a distinct site with a lower affinity than AMP, so that high concentrations of ATP oppose activation of the AMPK complex by AMP [106].

Activation model

AMP exerts its activation of AMPK by different mechanisms. On the one hand, AMP activates AMPK allosterically by binding to the γ subunit. On the other hand, AMP also promotes phosphorylation [107] at a specific threonine residue on the α subunit (Thr172) [108] by an upstream kinase that has recently been identified as a complex between the tumor suppressor protein LKB1 and 2 accessory subunits, termed STRAD and MO25 [109, 110] (Fig. 20). Phosphorylation of Thr172 produces at least 100-fold activation in contrast to the 5-fold activation of the allosteric mechanism. The high increase in activation derives from the inhibitory effect of AMP on phosphatases that dephosphorylate Thr172 and at the same time making AMPK a better substrate for LKB1 [109]. The latter mechanism is not acting on the LKB1 complex, but only affects AMPK. These three effects of AMP make the system very sensitive to small increases in AMP. All 3 effects are also antagonized by high concentrations of ATP. Note that in cells lacking LKB1, such as HeLa cells, there is still some basal phosphorylation of Thr172 and AMPK activity [109]. Interestingly, phosphorylation of Thr172 as well as AMPK activity can be increased by addition of a Ca^{2+} ionophore. This led to the identification of Ca^{2+}/calmodulin-dependent protein kinase kinase (CaMKK) as the responsible kinase for phosphorylation of Thr172 [111-113]. Indeed, Heller and colleagues have provided evidence that thrombin, which is acting through a Gq-coupled receptor (Gq couples the receptor to phospholipase C which produces inositol-1,4,5-triphosphate) stimulates AMPK through the Ca^{2+}-mediated pathway [114]. This pathway also operates in other cells of the endothelial/hematopoietic lineage, such as T lymphocytes [115].

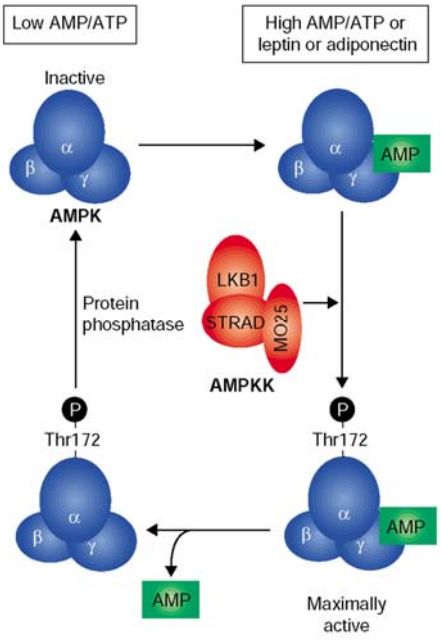

Figure 20: Activation of AMPK.
(http://jbiol.com/content/)

Regulation of AMPK

AMPK is an exquisite sensor of the metabolic energy status of the cell. Any metabolic stress that inhibits ATP production or that accelerates ATP consumption increases the cellular ADP:ATP ration. Consequently, AMPK is activated and can phosphorylate downstream targets. Physiological stress that activates AMPK in skeletal muscle is exercise or contraction. Upon inhibited oxidative phosphorylation in cells, caused by hypoxia or during pathological ischemia, the increased ADP:ATP ratio activates AMPK. This increase was reported in many tissues and organs, such as the heart, in pulmonary artery smooth muscle or in glomus cells of the carotid body, which sense the oxygen level in arterial blood supplying the brain [100]. Most mammalian cells express glucose transporters and hexokinase isoforms that have a very low Km for glucose, so that the rate of ATP synthesis from glucose only drops when blood glucose falls to pathologically low levels. Accordingly, physiological glucose stress is not activating AMPK in these cells. However cells that are specialized for glucose sensing express the GLUT2 isoform or hexokinase (hexokinase IV, glucokinase) with a much higher Km for glucose, so that the rate of ATP synthesis falls in response to decreases in blood glucose within the physiological range. Accordingly, physiological glucose stress is activating AMPK in these cells. Thus, in pancreatic β-cells and in neurons of the hypothalamus that controls feeding behaviour, AMPK is activated by low glucose levels [116, 117]. Accordingly, in lower eukaryotes, where no complex processes such as hormone release and feeding behaviour occur, the primary role of the AMPK homolog is the response to glucose starvation. The cytokines leptin and adiponectin are both adipokines released from adipocytes. These two adipokines are main players in the control of whole body energy homeostasis. Leptin, the product of the obese gene (ob), conciliates that fat stores are adequate, and exerts a feedback inhibition of food intake via effects on hypothalamic neurons which express the leptin receptor [118]. However, as well as inhibiting energy intake, leptin also stimulates energy expenditure by promoting uptake and oxidation of glucose [119] and fatty acids [120] in skeletal muscle. Leptin can directly activate the α_2 subunit of AMPK in muscle [121]. The same group showed that leptin inhibited AMPK-α_2 activity in the hypothalamus of fasted mice. It is known that anorexigenic agents, such as leptin and insulin inhibit AMPK-α_2 in the paraventricular region of the hypothalamus [122], whereas orexigenic agents, such as the gut hormone ghrelin and cannabinoids increase α_2 activity in the same region in fed mice [123, 124]. AMPK has been reported to be activated by adiponectin in skeletal muscle, where it stimulates glucose uptake and fatty acid oxidation and in liver, where it inhibits expression of gluconeogenic genes [125, 126]. Liver AMPK,

especially the α_2 isoform, is necessary for the ability of adiponectin to lower blood glucose [127].

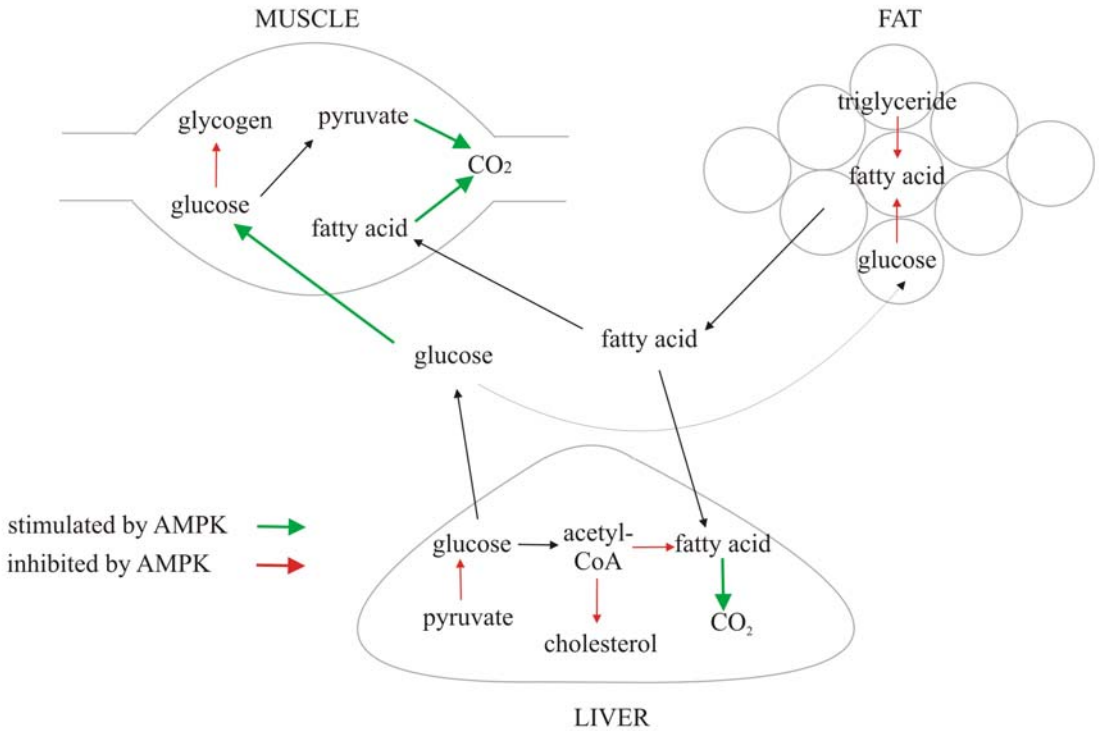

Figure 21: Major effects of AMPK activation on glucose and lipid metabolism in liver, muscle, and adipose tissue. Effects of AMPK on pyruvate oxidation are mediated by upregulation of mitochondrial biogenesis, whereas effects on fatty acid oxidation are mediated by both phosphorylation of ACC2 and activation of fatty acid entry into mitochondria, as well as upregulation of mitochondrial biogenesis [5].

Metabolic pathways regulated by AMPK

In general, AMPK switches on catabolic pathways that generate ATP (eg, glucose uptake, glycolysis) while switching off ATP-consuming anabolic pathways (fatty acid, cholesterol, glycogen, and protein synthesis). Fig. 21 summarizes the major effects of AMPK activation on glucose and lipid metabolism in liver, muscle, and adipose tissue, as well as its acute and long-term effects on metabolism. It is becoming increasingly clear that AMPK is involved in regulating other cellular processes. For example, if cells are running short of ATP, it does not make sense for them to grow and proliferate. AMPK inhibits cell growth and proliferation by inhibiting both the activity and expression of biosynthetic enzymes involved in lipid, carbohydrate, and protein synthesis, and also by switching off the target-of-rapamycin (TOR)⇒S6 kinase I pathway [128-130] that appears to be crucial in the regulation of cell

growth and cell size. AMPK seems to achieve this by phosphorylation of tuberous sclerosis complex-2 (TSC2) (tuberin), an upstream regulator of mTOR [131] (Fig. 22). AMPK activation also halts progress through the cell cycle at the G1-S phase transition, which is associated with accumulation of the tumor suppressor p53 and of the cyclin-dependent kinase

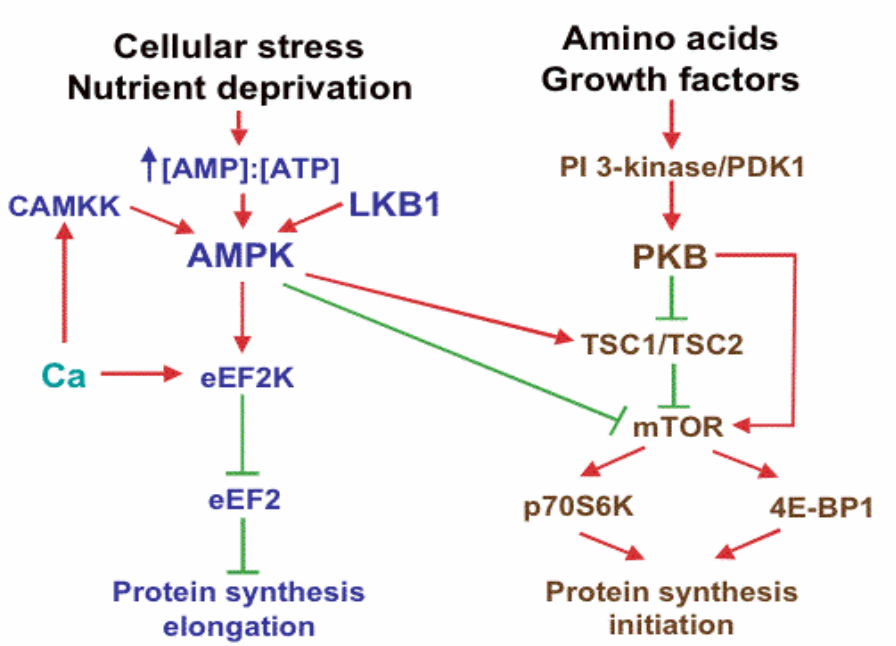

Figure 22: Interaction of AMPK and mTOR signaling pathways. (www.icp.ucl.ac.be)

inhibitors p21 and p27, which act downstream of p53 [132-134]. Under these conditions, p53 becomes phosphorylated on Ser15 [134, 135], although it is not clear whether this is a direct phosphorylation by AMPK. AMPK activation also has complex effects on apoptosis. In some situations, it prevents the process [136-138], whereas in others it induces it [139-142]. Successful apoptosis requires ATP, and an explanation for these conflicting findings may be that AMPK activation sometimes allows cells to recover from an energy crisis that would otherwise have triggered cell death. However, if the cells go past the "point of no return," AMPK may become proapoptotic. AMPK also has a role in cell senescence. Increased cellular AMP:ATP and AMPK activity appear to contribute to the senescence observed in human fibroblasts after a high number of passages in culture [143].

AMPK and IGF-1 signaling pathways

The insulin/insulin-like growth factor-1 signaling pathway is activated when nutrients are available, whereas the AMPK pathway is activated when cells lack a carbon source. Therefore these two pathways oppose each other. In mammals, insulin promotes lipid, protein, and

glycogen synthesis, whereas AMPK inhibits these biosynthetic pathways. The effect of insulin on protein synthesis is mediated in part by activation of the TOR pathway via phosphorylation of TSC2, whereas activation of AMPK causes phosphorylation of different sites on TSC2 and inhibits TOR [131, 144]. There also appears to be direct crosstalk between the two pathways. In some tissues, such as cardiac muscle, insulin antagonizes activation of AMPK [145, 146], and this appears to involve activation of the protein kinase Akt [147]. Indeed, Akt is able to phosphorylate both AMPKα subunits at a Ser residue, which antagonizes AMPK activation via phosphorylation at Thr172 [148]. In other cases, the insulin and AMPK signaling pathways work in the same direction, particularly in processes that regulate plasma glucose levels. In skeletal muscle, both insulin and AMPK activation stimulate glucose uptake by increased translocation of GLUT4 to the plasma membrane, although the subsequent fate of the glucose is different (glycogen synthesis in the case of insulin, which is anabolic; glycolysis/oxidation in the case of AMPK, which is catabolic). The two pathways appear to converge on the phosphorylation of AS160 [149, 150], a protein with a Rab-GTPase–activating protein (Rab-GAP) domain that is involved in regulation of GLUT4 translocation. Activation of AMPK plays a major part in the well-known ability of muscle contraction to stimulate glucose uptake. AMPK activation may also be involved in the effects of repeated exercise (ie, training) to improve insulin-sensitive glucose uptake, because of its ability to increase expression of GLUT4 [151] and perhaps other effects. A second case in which insulin and AMPK act in the same direction occurs in the liver, in which both proteins repress the expression of enzymes involved in gluconeogenesis, such as phosphoenolpyruvate carboxykinase and glucose-6-phosphatase [152]. It makes sense that insulin, a hormone released in response to high blood glucose, should repress hepatic glucose production, whereas in the case of AMPK it may have evolved because of its catabolic actions. Gene repression by AMPK is thought to occur via phosphorylation and consequent cytoplasmic sequestration of the transcriptional coactivator TORC2 [153]. Repression of gluconeogenesis appears to be the major cause of the plasma glucose-lowering effects of the adipokine adiponectin and the antidiabetic drug metformin on plasma glucose levels. In both cases, there is evidence that the mechanism involves activation of AMPK [125, 154]. A final case in which insulin and AMPK act in the same direction occurs in adipocytes, where insulin and AMPK suppress activation of hormone-sensitive lipase, and hence lipolysis, by cAMP elevating agonists [106, 155, 156]. While insulin causes phosphorylation and activation of phosphodiesterase 3B by Akt to lower cAMP [157], AMPK phosphorylates hormone-sensitive lipase at a site (Ser565) that antagonizes activation by cAMP-dependent protein

kinase [158]. This makes sense regarding the anabolic actions of insulin, but the reason why AMPK should suppress lipolysis requires explanation. If fatty acids released by lipolysis are not removed from the cell rapidly enough, they are known to recycle into triglyceride, thus consuming ATP. Inhibition of lipolysis by AMPK has been proposed as a mechanism to limit this recycling, ensuring that the rate of lipolysis does not exceed the rate at which fatty acids can be removed or metabolized by other routes, such as fatty acid oxidation [159].

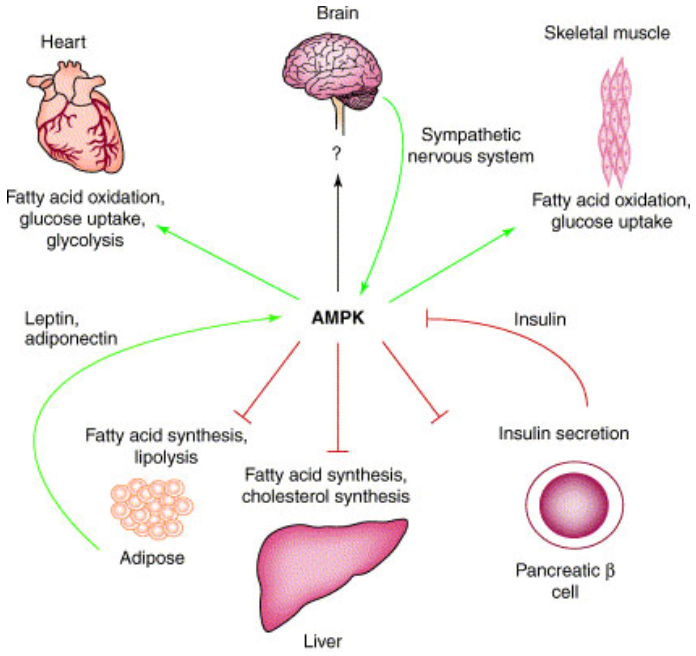

Figure 23: Roles of AMPK in the control of whole-body energy metabolism [3].

7.2 Decreased body weight gain by high fat diet in PASKIN-deficient mice

Emanuela Borter[1], Philipp Schläfli[1], Bettina Alder[2], Peter Wielinga[2], Thomas Lutz[2] Patrick Spielmann[1], Gieri Camenisch[1] and Roland H. Wenger[1]

[1]Institute of Physiology and Center for Integrative Human Physiology, University of Zürich, CH-8057 Zürich, Switzerland

[2] Institute of Veterinary Physiology and Zurich Center for Integrative Human Physiology, Vetsuisse Faculty University of Zürich, CH-8057 Zürich, Switzerland

ABSTRACT

PASKIN is a PAS domain serine/threonine AMP-related sensory kinase which is ubiquitously expressed at low levels with highest expression in the testis. We recently generated PASKIN knock-out mice which did not show any obvious phenotype. Yeast data suggest that PASKIN is involved in energy homeostasis. Thus, PASKIN might sense the altered concentration of a (unknown) metabolic ligand which triggers the interaction and / or phosphorylation of target proteins such as glycogen synthase. We found that *Paskin*$^{-/-}$ mice are protected from weight gain and triglyceride increases when fed with a high fat diet. Glucose tolerance was not impaired under high fat diet conditions. These effects might be attributed to the increased activity of AMPK because there was more phospho-AMPK present in skeletal muscle tissue of PASKIN than wild type mice. These data suggest that PASKIN might be an antagonist of AMPK and contributes to balancing energy homeostasis by AMPK. We detected a decreased spontaneous activity of *Paskin*$^{-/-}$ mice and assume that PASKIN is implicated in AMPK-dependent energy homeostasis of skeletal muscle.

INTRODUCTION

PAS (Per-Arnt-Sim) proteins are known from all three kingdoms of life where they represent protein sensors involved in the perception of light intensity, oxygen partial pressure, redox potentials, voltage and certain ligands [9] [10] [19]. The mammalian PAS domain-containing proteins can also serve as heterodimerization interfaces of transcription factors involved in the xenobiotic response, adaptation to hypoxia and circadian rhythm generation [12] [13] [12, 160]. By database searches using the PAS sequence as a bait, we and others identified a novel mammalian PAS protein termed PASKIN [4] or PASK [17]. PASKIN contains two PAS domains showing a high sequence similarity to the oxygen sensor protein FixL of *Rhizobium* species, and a serine/threonine kinase domain related to AMP-kinases. As known from FixL, the PAS domain represses the kinase activity in *cis*. Upon ligand-binding to the PAS domain, the kinase domain is activated in *trans*, resulting in auto-phosphorylation of the kinase domain [17]. Ligand binding as well as mutation of the PAS A domain result in activation of the kinase domain. Synthetic ligands were identified and show a structural similarity to dioxin, known to bind to the PAS domain of the aryl hydrocarbon receptor [2]. However, an endogenous ligand for PASKIN activation has not been identified so far.

To elucidate the function of PASKIN, our lab previously generated PASKIN deficient knock-out mice. Surprisingly, PASKIN is highly upregulated in the testis during the post-meiotic stages of spermatogenesis. PASKIN mRNA expression is remarkably higher in the testis than in all other tissues. However, neither male fertility nor sperm production or motility was affected in PASKIN knock-out mice [29].

From the yeast PASKIN homologs PSK1 and PSK2 we know that the psk1 psk2 double-mutant strain shows a decreased growth at elevated temperature (39°C) and galactose supply. PSK1 and PSK2 phosphorylate three translation factors (Caf20, Tif11 and Sro9) and two enzymes involved in glycogen and trehalose synthesis (Ugp1, Gsy2), thus controlling translation and sugar flux [1]. Recently, it has been shown that the mammalian glycogen synthase interacts with the midregion of human PASKIN and is phosphorylated at Ser-640 [38].

AMPK is a well-conserved serine/threonine protein kinase that has been proposed to act as a cellular fuel gauge [161]. It is formed by a catalytic subunit (α) and two regulatory subunits (β and γ). Each subunit exists as multiple isoforms (α1, α2, β1, β2, γ1, γ2 and γ3), each encoded by a different gene [162]. AMPK is activated allosterically by an increase in the intracellular AMP/ATP ratio and also by phosphorylation of the threonine 172 residue, a residue located in

the activation loop of the α subunit [159]. Once activated, AMPK leads to a concomitant inhibition of energy-consuming biosynthetic pathways and activation of ATP-producing catabolic pathways.

In this work we show that PASKIN is to some extent a direct counterplayer of the AMPK signaling pathway. When the diet was changed from 5% to 45% fat, *Paskin*$^{-/-}$ mice resisted to fat accumulation and glucose intolerance. Significantly decreased spontaneous activity of *Paskin*$^{-/-}$ mice led us to focus on the involvement of PASKIN in AMPK signaling of skeletal muscle.

Methods

Primary cells and culture conditions

MEFs were prepared from 13.5-day-old *Paskin*$^{-/-}$ and *Paskin*$^{+/+}$ embryos. Following removal of the head and inner organs, embryos were rinsed with ice cold phosphate-buffered saline (PBS) and 2% FCS, minced, and digested with trypsin (0.05% solution containing 0.53 mM EDTA) for 15 min at 37°C, using 2 ml per embryo. Cells were resuspended before and after addition of 5 ml MEF media (DMEM, 10% FCS, 1% glutamine, 100 IU/ml penicillin, 100 μg/ml streptomycin, 200 μM β-mercaptoethanol). The resulting suspension from one single embryo was plated into one 10 cm diameter culture dish and incubated at 37°C and supplied with in a 5% CO_2 humidified chamber. Cells were grown ~2 days, until the culture was 90% confluent, split once, harvested, frozen, and labeled as passage 1.

Cell culture and transient transfection

HEK293 embryonic kidney carcinoma cell lines were cultured in high-glucose Dulbecco's modified Eagle's medium (DMEM) (Sigma) as described previously [163]. Transient transfections were performed with the polyethylenimine (Polysciences) method [164].

Animals

Paskin$^{-/-}$ mice [29] were backcrossed into C57BL/6J (The Jackson Laboratory) for 10 generations. C57BL/6J animals were raised in the same room under the same conditions. Mice were maintained on a normal chow diet (4.5% fat, KLIBA NAFAG) or a high fat diet (45% fat, Research Diets) beginning at 12 weeks of age. In each experiment, age-matched wild type mice were used as controls. All animal handling followed the guidelines for the use

and care of laboratory animals of the Bundesamt für Veterinärwesen and was approved by the Kantonales Veterinäramt Zürich (Nr. 192/2003).

Immunoblotting

Total protein extracts of cultured cells were prepared using cell lysis buffer (10 mM Tris-HCl pH 8.0, 1 mM EDTA, 400 mM NaCl, 0.1% NP-40, protease inhibitor cocktail (Roche)). Following incubation on ice for 5-10 min, the lysate was centrifuged (5 min / 15´000 rpm / 4°C) and the supernatant stored at -80°C. Protein concentrations were determined by the Bradford method using bovine serum albumin as a standard [62]. For immunoblot analysis, cellular protein was electrophoresed through SDS-polyacrylamide gels and electrotransferred onto nitrocellulose membranes (Schleicher & Schuell) by semi-dry blotting. Membranes were stained with Ponceau S (Sigma) to confirm equal protein loading and transfer. All washing steps were performed with Tris buffered saline (TBS) containing 0.1% Tween-20. Membranes were incubated for 2 h in blocking buffer (0.1% Tween-20 with 5% w/v nonfat dry milk in TBS). The following antibodies were used for incubation in primary antibody dilution buffer (0.1% Tween-20 with 5% BSA in TBS): rabbit monoclonal antibody (mAb) anti-AMPKα (Cell Signaling) and rabbit mAb anti-phospho-AMPKα (Cell Signaling); rabbit polyclonal anti-β-actin (Sigma); and secondary polyclonal goat anti-mouse or anti-rabbit antibodies coupled to horseradish peroxidase (Pierce, Perbio, Lausanne, Switzerland). Chemiluminescence detection was performed with the Supersignal West Dura kit (Pierce) and chemiluminescence was recorded with a CCD camera (FluorChem8900, AlphaInnotech, Witec, Littau, Switzerland) or by exposure to X-ray films (Fuji, Düsseldorf, Germany)

Running wheel

A flexible computer-controlled running wheel system (TSE Systems International Group) was used to detect spontaneous activity with following dimensions for use with mice: drum diameter: 115 mm, drum depth: 40 mm, drum rods: 4 mm diameter and 5 mm distance between two rods. In total, 16 *Paskin*$^{-/-}$ and 16 *Paskin*$^{+/+}$ mice at the age of 16 weeks (8 males and 8 females) were measured during a time period of two weeks. Animals got adapted to the new environment for 2 days.

Glucose / insulin tolerance test *in vivo*

Glucose tolerance test (GTT) - animals were fasted 16 h, after which 20% glucose in 0.9% NaCl (2 g glucose/kg body weight) was injected intraperitoneally. At the indicated times, tail vein blood was sampled for glucose determination by electrochemical measurements (Accu-Chek Aviva, Roche Diagnostics). When performing GTT the animals were 9 months old and the HFD group was on HFD for 6 months.

Insulin tolerance test (ITT) - human recombinant insulin (0.75 U/kg body weight) was intraperitoneally injected to fasted mice (16 h) and blood glucose levels were determined at the indicated times. When performing ITT the animals were 10 months old and the HFD group was on HFD for 7 months.

Indirect calorimetry

Measurements were performed in an open circuit calorimetry system (AccuScan Inc., Columbus, OH). Room air was passed through each cage with a flow rate controlled at approximately 2 l/min. Every 2 min, out-coming air was sampled during 20 s for each individual cage and analyzed for $V(O_2)$ (ml / kg / min) and $V(CO_2)$ (ml / kg / min). Simultaneously, physical activity was monitored by 3 arrays of 16 infrared light beam sensors. Furthermore, food intake and water intake were measured continuously. All data were analyzed with AccuScan Integra ME software. Energy expenditure was calculated for each 2 min sample according to Weir [165] using the following equation: total energy expenditure (kcal/h) = $3.9 \times V(O_2)$ ml/h + $1.1 \times V(CO_2)$ ml/h. The average over 60 min was calculated for each individual animal and expressed as kcal/h. The respiratory quotient (RQ) is defined as the quotient between CO_2 production and O_2 consumption. The light beam breaks were converted into distance travelled in centimeter. In the first measurement the *Paskin*$^{-/-}$ and *Paskin*$^{+/+}$ mice were all on NCD and were at the age of 12 weeks. Subsequent switch of one group to HFD and further two measurements after 6 and 12 weeks on HFD, respectively, were performed.

Blood analysis

Paskin$^{-/-}$ and *Paskin*$^{+/+}$ mice were 11 months old and one group had been fed HFD for the last 8 months. Animals were fasted for 6 hours before anaesthesia (200 mg/kg ketamine, 10 mg/kg xylazine). Up to 1 ml blood was removed from the portal vein into a 1 ml heparin rinsed syringe using a 25 G needle. After centrifugation (5 min / 8000 g / 25°C) the plasma was

collected and frozen at -80°C. Measurements of indicated analytes were performed by the Institute for Clinical Chemistry (IKC, USZ Zürich).

Results

Body weight of *Paskin*$^{-/-}$ and *Paskin*$^{+/+}$ mice

First, we backcrossed *Paskin*$^{-/-}$ mice for 10 generations to have a genetically homogenous C57BL/6 background. Then we weighed the *Paskin*$^{-/-}$ and C57/BL6 wild-type mice on a daily base from day 6 on and after weaning on a weekly base until the age of three months. The graphs in Fig. 1 represent the mean weight of indicated numbers of animals at an age of 65 days. Male but not female *Paskin*$^{-/-}$ mice were significantly heavier with $p < 0.05$ as calculated by an unpaired t-test.

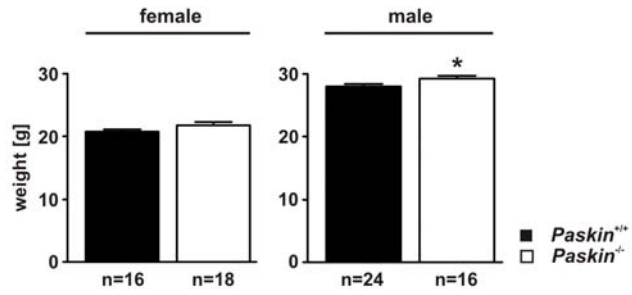

Figure 1: Body weight of *Paskin*$^{+/+}$ and *Paskin*$^{-/-}$ mice. The body weight at the age of 65 days is shown for the indicated numbers of animals. Data are expressed as mean values±SEM.

Running wheel performance of *Paskin*$^{-/-}$ and *Paskin*$^{+/+}$ mice

We next examined the spontaneous running wheel activity of *Paskin*$^{-/-}$ and *Paskin*$^{+/+}$ mice. The fact that male *Paskin*$^{-/-}$ mice are slightly heavier might be caused by a lower spontaneous activity. We let the animals accommodate for one week in the new cage containing the running wheels. We then measured the running distance during 14 subsequent days. As expected, the animals did not run during the light phase, therefore the run distance in the dark phase is shown. The average distance ran during these 13 nights was calculated per animal. The mean values of eight animals for each group are shown in Fig. 2a. Sex is a significant factor in daily running wheel activity, with female mice known to run an average of 20% farther and 38% faster than male mice [166]. One reason might be that in cycling female mice the second part of the proestrus night is often characterized by increased motor activity (over 100%) compared to the remaining estrus cycle nights [167]. Surprisingly we found that *Paskin*$^{-/-}$ animals ran significantly shorter distances during the night when compared with *Paskin*$^{+/+}$ mice. This behavior is even more pronounced for male mice ($p<0.01$) than for female mice ($p<0.05$). When analyzing the data in more detail we found various animals

which suddenly stopped running without any obvious reason and suddenly started using the running wheel again after a couple of nights or alternatively did not enter the wheels anymore. Therefore, Fig. 2b shows the same experiment as in Fig. 2a, but only representing mice which used the wheel every night. This led to a smaller number in animals and the mean values for the distances ran per night per animal were calculated only from 6 nights and 7 nights for female and male animals, respectively. Female ($p< 0.05$) and male ($p<0.05$) *Paskin*$^{-/-}$ animals still ran significantly less than *Paskin*$^{+/+}$ animals. The measurement resolution in the running wheel experiment is 2 h, meaning that the wheel rotations during the 2 h are added to one value. With our running wheels, the raw data do not provide detailed information about the behavior of the animals in the running wheel when compared to systems that use a resolution of 1 minute. Nevertheless, all raw data points derived from *Paskin*$^{-/-}$ animals are smaller when compared to *Paskin*$^{+/+}$ animals.

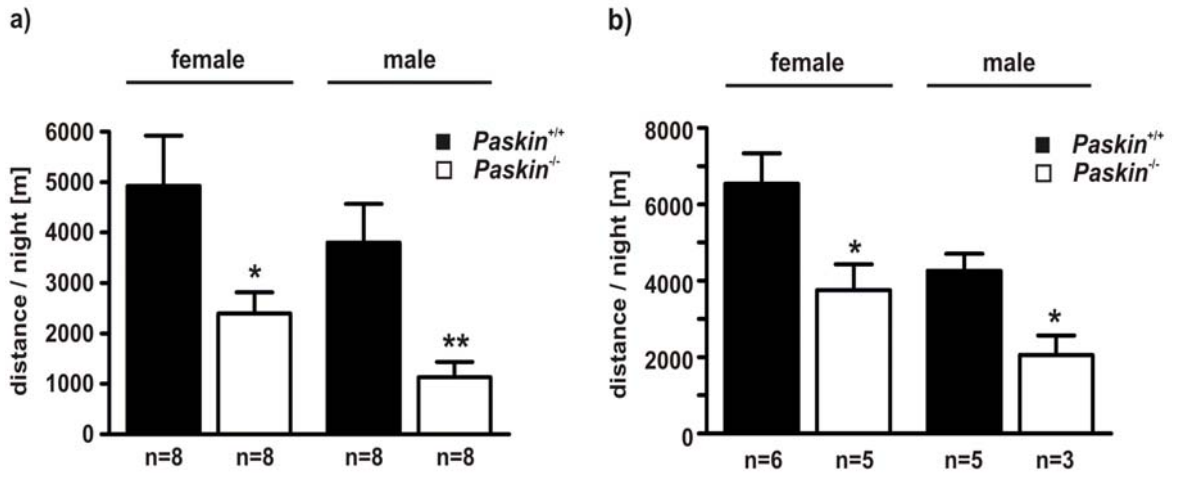

Figure 2: Running wheel distance of *Paskin*$^{-/-}$ and *Paskin*$^{+/+}$ mice. (a) Average distance run during 14 subsequent dark phases of 8 animals per group. (b) The same experiment as in (a) but animals which were not active every night during the measured period of time were removed from statistics.

AMPK expression in *Paskin*$^{-/-}$ and *Paskin*$^{+/+}$ mouse embryonic fibroblasts

We generated mouse embryonic fibroblast (MEF) from our *Paskin*$^{-/-}$ and *Paskin*$^{+/+}$ mice to examine whether PASKIN might have an effect on AMPK, the sensor of the metabolic energy status of the cell. We kept primary MEFs in culture until cells spontaneously immortalized. Immunoblots were performed with primary MEFs and with MEFs that spontaneously immortalized. Lower protein levels of phospho-AMPK were detected in primary *Paskin*$^{+/+}$ MEFs. No changes in AMPK protein levels were visible with immortalized MEFs (data not shown). It is possible, that this discrepancy in the protein levels of AMPK

derives from a clonal artefact which possibly was induced by the spontaneous immortalization. Phosphorylation of AMPK was almost absent in spontaneously immortalized *Paskin*$^{+/+}$ MEF when compared to *Paskin*$^{-/-}$ MEF (Fig. 3). By quantitative RT-PCR to detect AMPK mRNA levels in *Paskin*$^{-/-}$ and *Paskin*$^{+/+}$ MEFs, the presence of AMPK subunit α_1 and not AMPK subunit α_2 in these cells was shown. Furthermore we could confirm in both the spontaneously immortalized and the primary MEFs that a possible regulation of AMPK through PASKIN does not occur on the mRNA level (data not shown).

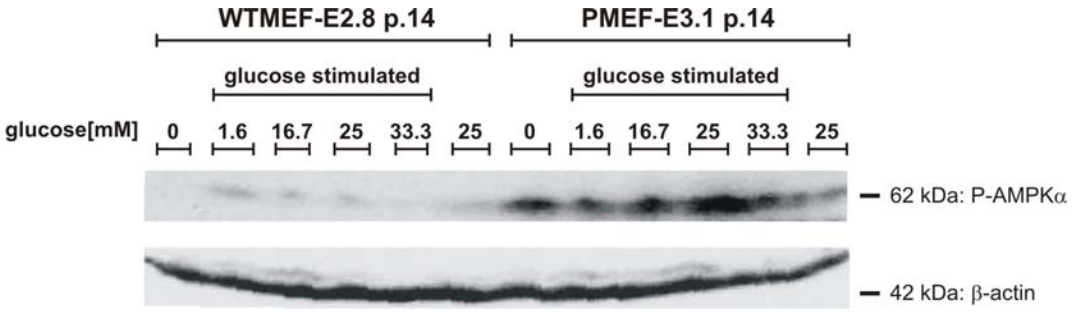

Figure 3: P-AMPKα detection in glucose stimulated *Paskin*$^{-/-}$ and *Paskin*$^{+/+}$ MEFs. Before glucose stimulation, MEFs were starved in medium containing 1.6 mM glucose for 30 minutes, medium was exchanged and the MEFs incubated for another hour in 1.6 mM glucose. The medium was replaced by fresh medium containing 0 mM, 1.6 mM, 16.7 mM, 25 mM or 33.3 mM glucose and the MEFs were incubated for 24 hours at 37°C. Additionally, lysates from non-stimulated MEFs in DMEM supplied with 25 mM glucose were loaded. (WTMEF-E2.8 p.14: *Paskin*$^{+/+}$ MEF from embryo number 2.8 after 14 passages, PMEF-E-3.1 p.14: *Paskin*$^{-/-}$ MEF from embryo number 3.1 after 14 passages)

To further investigate AMPK protein levels and phosphorylation in PASKIN deficient cells, we transiently transfected HEK293 with 4 different shRNA plasmids (pLKO.1-puro). The transient transfection of HEK293 did not down-regulate PASKIN protein levels (Fig. 4).

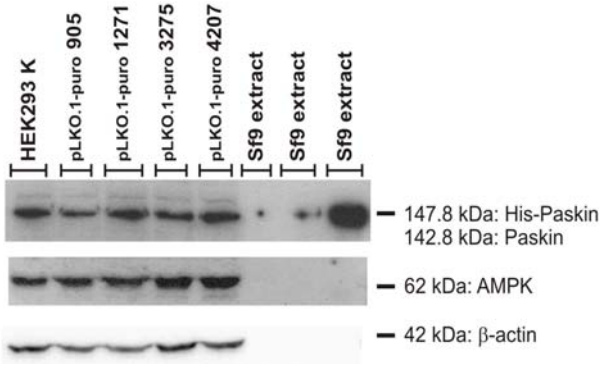

Figure 4: Transiently transfected HEK293. HEK293 cells were transfected with 4 different PASKIN shRNA pLKO.1-puro plasmids (905, 1271, 3275, 4207) and protein were extracted after 42 hours. Lysates of Sf9 cells transfected with a plasmid containing His-tagged PASKIN were used as positive controls in a dilution series for PASKIN expression.

Effect of high fat diet on body weight of *Paskin*$^{-/-}$ and *Paskin*$^{+/+}$ mice

To challenge metabolic homeostasis, we fed *Paskin*$^{-/-}$ and *Paskin*$^{+/+}$ mice with a diet consisting of 45% fat versus 4.5% fat supplied in the normal chow diet (NCD). At the age of 14 weeks, 16 *Paskin*$^{-/-}$ mice (8 female and 8 male) were fed either high fat diet (HFD) or NCD. Analogously, 16 *Paskin*$^{+/+}$ control animals were included. Food uptake of each mouse was measured three times per week. The animals were weighed once per week. The left panel of Fig. 5 represents the body weight, the cumulative body weight increase and the cumulative food uptake under NCD, while on the right panel the same evaluation is illustrated under HFD condition. Male *Paskin*$^{-/-}$ mice showed significantly increased body weight under NCD when compared to male *Paskin*$^{+/+}$ mice (two tailed unpaired t-test, $p<0.0001$) while the cumulative body weight gain did not significantly differ between *Paskin*$^{+/+}$ and *Paskin*$^{-/-}$ mice . Food intake was linear and implicates that the male animals ate equal amounts of NCD. Interestingly, under HFD the body weight of male *Paskin*$^{-/-}$ mice increased less than male *Paskin*$^{+/+}$ mice fed HFD. Female *Paskin*$^{-/-}$ mice fed NCD have increased body weight compared to female *Paskin*$^{+/+}$ mice (two-tailed unpaired t-test, $p<0.005$) (Fig. 6). When fed HFD female *Paskin*$^{+/+}$ mice significantly gain more body weight (two-tailed unpaired t-test, $p<0.05$) than female *Paskin*$^{-/-}$ mice (Fig. 6). Comparably, the body weight gain is increased in female *Paskin*$^{+/+}$ mice, while the food intake is identical between female *Paskin*$^{+/+}$ and *Paskin*$^{-/-}$ mice (Fig. 6).

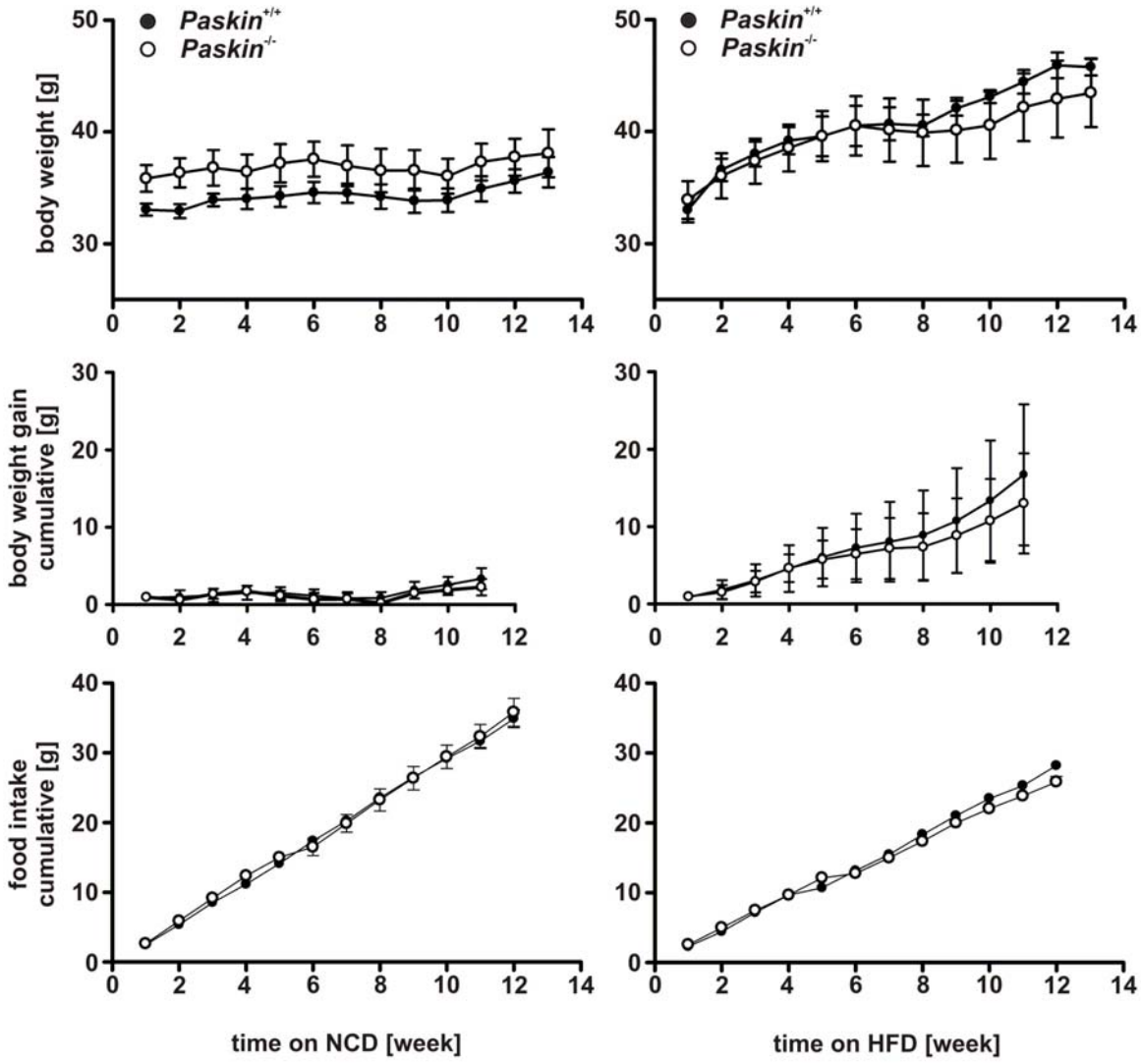

Figure 5: Male *Paskin*$^{-/-}$ and *Paskin*$^{+/+}$ body weight, cumulative body weight gain and cumulative food intake. Male *Paskin*$^{-/-}$ (n=8) and male *Paskin*$^{+/+}$ (n=8) mice were fed NCD (left panel) or HFD (right panel) starting at the age of 12 weeks. Body weight measurements were performed on a weekly base for 14 weeks. During the same period, for each mouse food intake was measured 3 times per week. Data are expressed as mean±SEM per week.

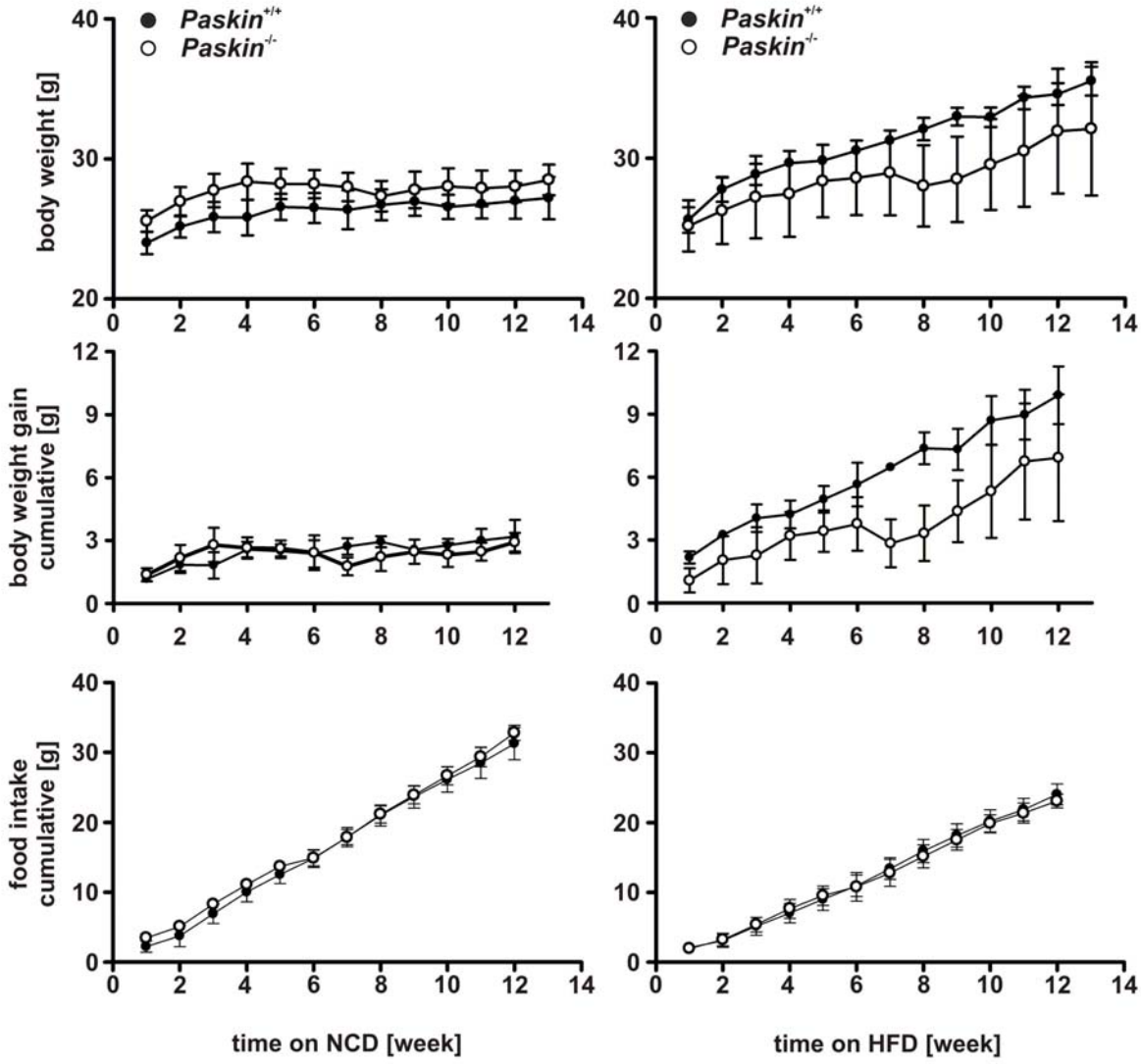

Figure 6: Female *Paskin*$^{-/-}$ and female *Paskin*$^{+/+}$ body weight, cumulative body weight gain and cumulative food intake. Female *Paskin*$^{-/-}$ (n=8) and female *Paskin*$^{+/+}$ (n=8) mice were fed NCD (left panel) or HFD (right panel) starting at the age of 12 weeks. Body weight measurements were performed on a weekly base for 12 weeks. During the same period, for each mouse food intake was measured 3 times per week. Data are expressed as mean±SEM per week.

Intraperitoneal glucose tolerance tests with HFD fed mice

Feeding of HFD results in impaired overall glucose homeostasis and is finally leading to the metabolic syndrome [168]. To asses whether *Paskin*$^{-/-}$ mice are prone to diabetes, intraperitoneal (i.p.) glucose tolerance tests (IPGTT) were performed, in which plasma glucose levels were monitored over time following i.p. glucose injection. Note that under NCD the ability to clear glucose was not obviously different between *Paskin*$^{+/+}$ and *Paskin*$^{-/-}$ mice [7]. The left panel of Fig. 7 represents the results of IPGTT under NCD for male mice (top) and female mice (bottom). As shown before, there were no differences in glucose clearance, either in female or in male NCD-fed mice. However, HFD-fed *Paskin*$^{-/-}$ males (right panel) showed significantly better glucose clearance relative to *Paskin*$^{+/+}$ males. Surprisingly this phenotype could not be confirmed with *Paskin*$^{-/-}$ females (Fig. 7).

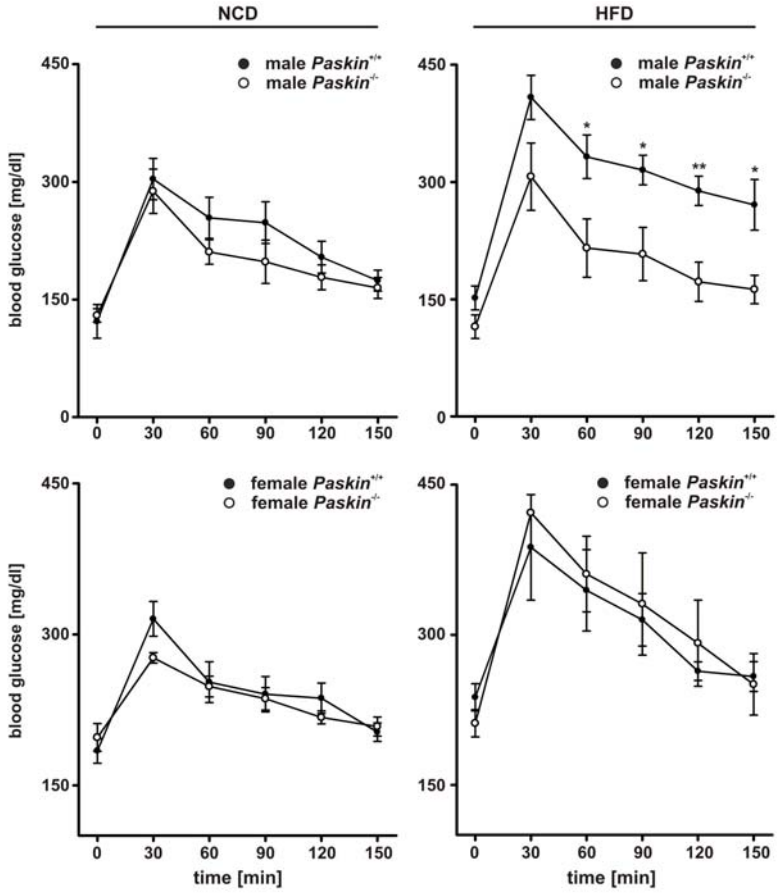

Figure 7: Intraperitoneal glucose tolerance tests in *Paskin*$^{+/+}$ and *Paskin*$^{-/-}$ male and female mice fed NCD or HFD. Mice were fasted for 16 hours before i.p. administration of 2 g/kg body weight D-glucose. Blood glucose was measured every 30 minutes. Left panel: IPGTT in mice fed NCD (male ***Paskin***$^{+/+}$, n=3; male ***Paskin***$^{-/-}$, n=3; female ***Paskin***$^{+/+}$, n=3; female ***Paskin***$^{-/-}$, n=4), right panel: IPGTT in mice fed HFD for 7 months (male ***Paskin***$^{+/+}$, n=4; male ***Paskin***$^{-/-}$, n=4; female ***Paskin***$^{+/+}$, n=3; female ***Paskin***$^{-/-}$, n=3). All animals were 9 months old, when IPGTT was performed. Data are expressed as mean ± SEM. * = $p < 0.05$, ** = $p < 0.01$ (two-tailed unpaired t-test).

Insulin tolerance tests were performed with the same animals one week later. The animals did not respond accurately to the i.p. administered 0.75 U insulin per kg of body weight. Especially male animals hardly lowered their blood glucose levels independent of their genotype. Female mice showed a drop of 40 mg/dl, however the fasted blood glucose level was already low in NCD animals (80 mg/dl). We saw a significant lower blood glucose level in fasted male *Paskin*$^{-/-}$ mice when compared to *Paskin*$^{+/+}$ males.

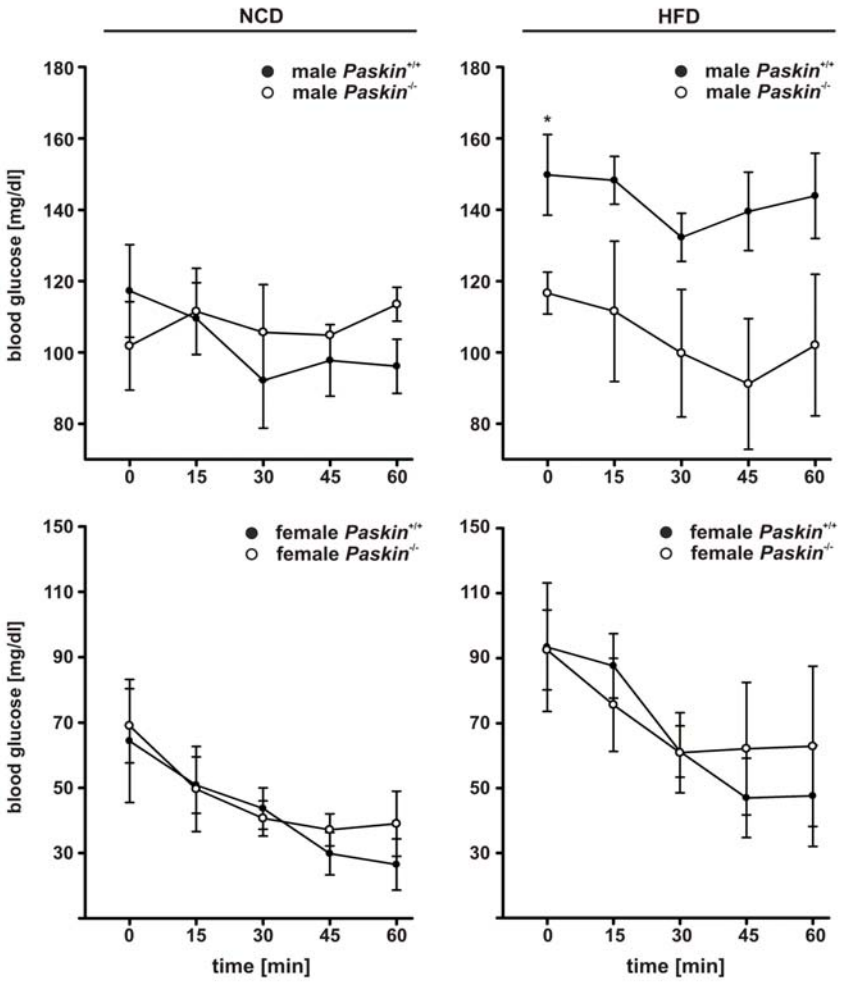

Figure 8: Intraperitoneal insulin tolerance tests in *Paskin*$^{+/+}$ and *Paskin*$^{-/-}$ male and female mice fed NCD or HFD. Mice were fasted for 16 hours before i.p. administration of 0.75 U/kg body weight insulin. Blood glucose was measured every 15 minutes. Left panel: IPITT in mice fed NCD (male *Paskin*$^{+/+}$, n=3; male *Paskin*$^{-/-}$, n=3; female *Paskin*$^{+/+}$, n=3; female *Paskin*$^{-/-}$, n=4), right panel: IPITT in mice fed HFD for 7 months (male *Paskin*$^{+/+}$, n=4; male *Paskin*$^{-/-}$, n=4; female *Paskin*$^{+/+}$, n=3; female *Paskin*$^{-/-}$, n=3). All animals were 10 months old, when IPITT was performed. Data are expressed as mean±SEM. * = $p < 0.05$ (two-tailed unpaired t-test).

Indirect calorimetry measurements with *Paskin*$^{-/-}$ and *Paskin*$^{+/+}$ mice

HFD leads to obesity and other metabolic syndrome related diseases [168]. Obesity occurs from an inbalance between energy intake (food intake) and energy expenditure (basal metabolism and physical activity) [169]. *Paskin*$^{-/-}$ animals are partially resistant to body weight increase and impaired glucose clearing upon HFD. Under NCD, though, they show a lower running wheel activity compared with *Paskin*$^{+/+}$ mice. To further elucidate a possible connection between these two phenotypes, we measured food intake, water intake, locomotor activity, O_2 consumption and CO_2 emission by indirect calorimetry using metabolic cages. From these data energy expenditure and respiratory quotient (RQ) were calculated. The animals got adapted for 24 hours to the new cages before measurements were started. The whole experiment lasted 24 hours, while during the active phase (12 h) food was given ad libitum and during the inactive (12 h) phase food was not available. In total 32 animals were measured (16 *Paskin*$^{+/+}$ mice and 16 *Paskin*$^{-/-}$ mice). Each group consisted of 8 female and 8 male animals, while 4 of each gender received HFD. The first measurement was performed before the administration of HFD to obtain basal values. Two subsequent measurements were performed after 6 and 12 weeks of HFD feeding, respectively. No differences at all in energy expenditure, oxygen consumption or water intake were detected between *Paskin*$^{+/+}$ mice and *Paskin*$^{-/-}$ mice (data not shown, two-tailed unpaired t-test). No significant differences were found in locomoter activity, food intake or the respiratory quotient (data not shown, two-tailed unpaired t-test).

Blood plasma analysis of *Paskin*$^{-/-}$ and *Paskin*$^{+/+}$ mice

After the experiments in the metabolic cage were completed, blood was collected. Because these parameters have never been determined in these mice so far, various electrolytes, including sodium, potassium, chloride, total calcium and phosphate were estimated. Moreover urea, uric acid and creatinine were measured, which reflect proper kidney function, and creatin kinase, representing heart and muscle performance, were determined. Further marker enzymes were measured to detect proper liver function like alanin-aminotransferase (ALT), aspartate-aminotransferase (AST) and the activity of alkaline phosphatase, as marker for liver function and skeletal muscle performance was measured. Markers for the lipid homeostasis like cholesterol and triglyceride were estimated. Alkaline phosphatase activity was significantly increased in *Paskin*$^{-/-}$ males when fed NCD (Fig. 9a). However the values for the females were unchanged between *Paskin*$^{-/-}$ and *Paskin*$^{+/+}$ mice. Total cholesterol blood levels are expected to be elevated under HFD [170]. This was true for *Paskin*$^{+/+}$ female mice (Fig.

9b). *Paskin*$^{-/-}$ females, however, had less cholesterol in their blood which is consistent with the finding that under high fat diet their body weight was not elevated to the same extent as the *Paskin*$^{+/+}$ body weight. However, for male animals the contrary was found leading to very moderate effects when male and female values were taken together (Fig. 9b). High triglyceride blood levels arise as a consequence of secondary hyperlipemia and are associated with diabetes mellitus [171]. Although not significant, triglyceride levels were elevated in HFD fed male *Paskin*$^{+/+}$ animals when compared to *Paskin*$^{-/-}$ male mice. The contrary was true for female animals (Fig. 9c). We detected increased free fatty acid levels in HFD and NCD *Paskin*$^{-/-}$ females versus *Paskin*$^{+/+}$ females (Fig. 9d). In Fig 10 other blood metabolites are taken together. No significant differences could be detected.

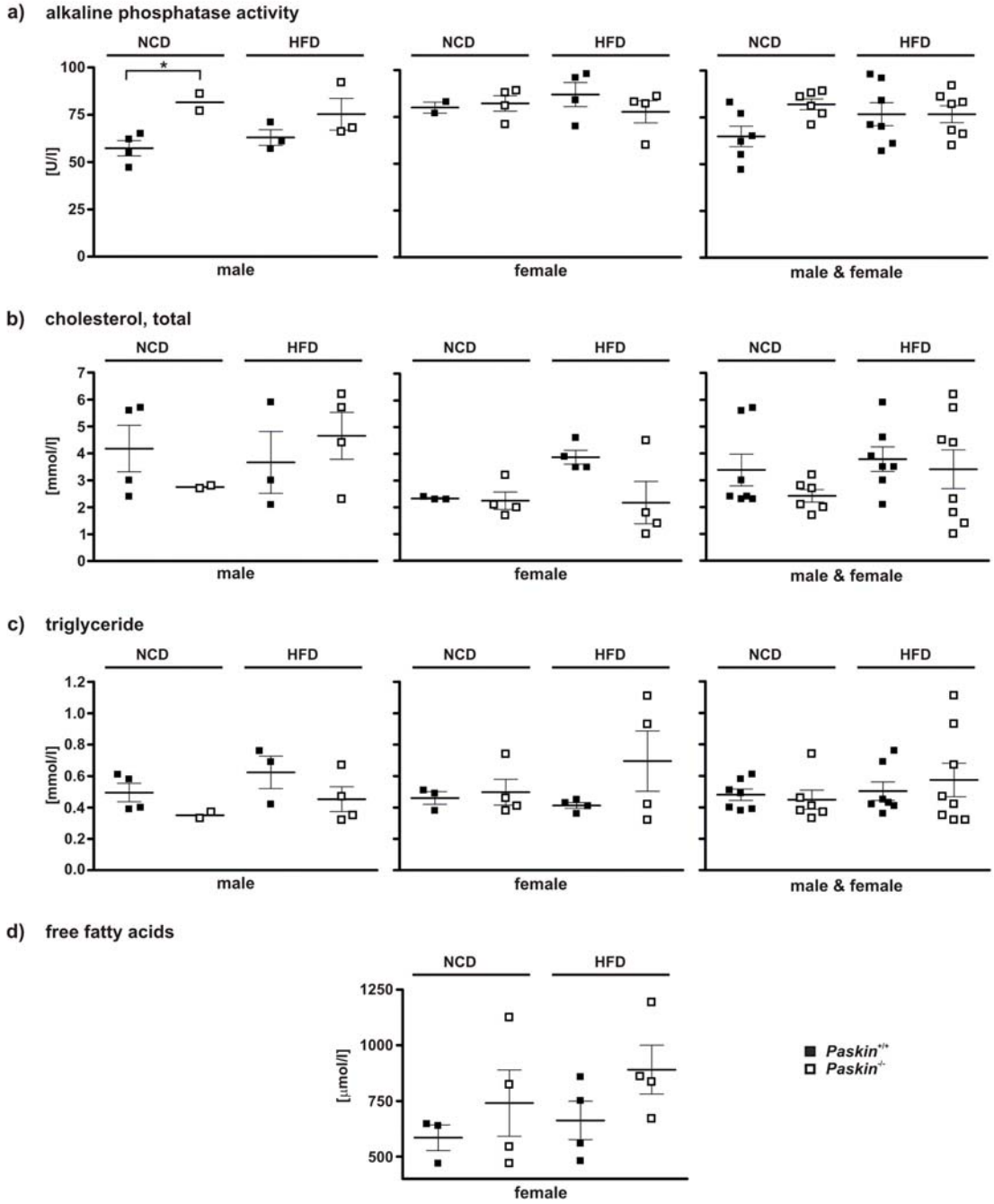

Figure 9: Alkaline phosphatase activity and Lipid homeostasis in *Paskin*$^{+/+}$ and *Paskin*$^{-/-}$ male and female mice under NCD and HFD. Mice were fasted for 6 h before blood was taken from the portal vein. Data are expressed as mean±SEM. * = $p < 0.05$ (two-tailed unpaired t-test).

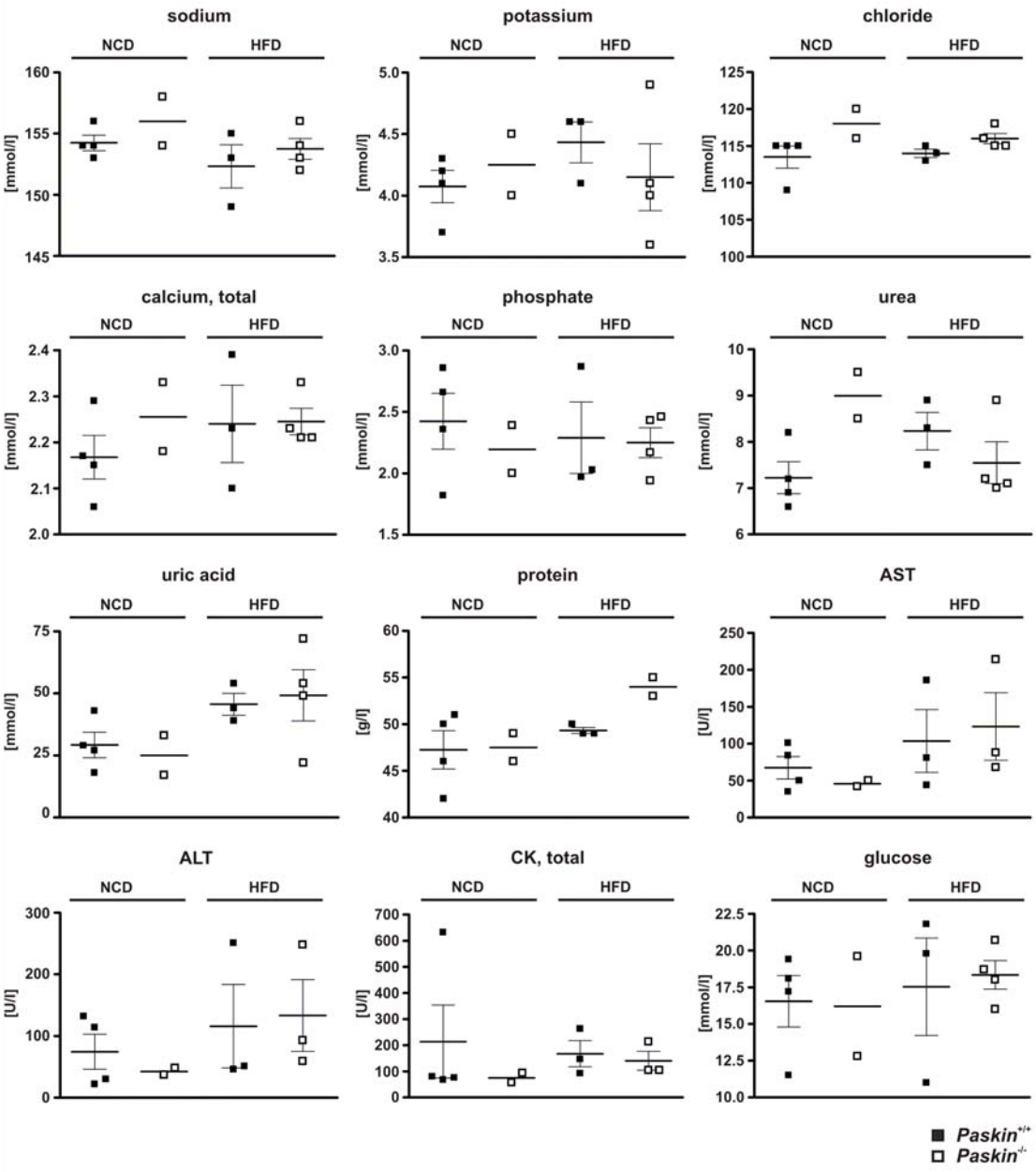

Figure 10: Electrolytes, kidney parameters, total protein, liver enzymes, muscle enzymes and glucose in *Paskin*$^{+/+}$ and *Paskin*$^{-/-}$ male mice under NCD and HFD. Mice were fasted for 6 h before blood was taken from the portal vein. Data are expressed as mean±SEM. * = $p < 0.05$ (two-tailed unpaired t-test).

DISCUSSION

When fed a high-fat diet (HFD), C57BL/6J mice are known to develop obesity and a number of symptoms reminiscent of the metabolic syndrome, including insulin resistance [168]. Unpublished data from Rutter´s group suggest that PASKIN is an inhibitor of AMPK expression and therefore acts as a regulator of energy homeostasis [172]. Rutter´s main preliminary finding is that *Paskin*$^{-/-}$ mice are protected from the effects of a HFD, and he suggested that this phenotype originates from increased AMPK expression and activity in *Paskin*$^{-/-}$ mice. We could confirm that under HFD female *Paskin*$^{-/-}$ mice gain significantly less body weight when compared to *Paskin*$^{+/+}$ mice. The same observations were made for male mice, but data were not significant. Importantly, this retention in body weight gain under HFD does not arise because of different feeding behaviour. Furthermore, male *Paskin*$^{-/-}$ mice under NCD are significantly heavier than *Paskin*$^{+/+}$ mice, consistent with the decreased running activity of *Paskin*$^{-/-}$ mice.

Concerning AMPK protein levels and activity we could so far see stronger protein phosphorylation of AMPKα in MEFs derived from *Paskin*$^{-/-}$ mice than in *Paskin*$^{+/+}$ MEFs. Most probably due to clonal differences in our *Paskin*$^{-/-}$ and *Paskin*$^{+/+}$ MEFs, we did not detect elevated AMPKα protein levels in *Paskin*$^{-/-}$ MEF. Rutter and colleagues did not measure AMPKα protein level or phosphorylation in MEFs but found AMPKα protein levels elevated in *Paskin*$^{-/-}$ gastrocnemius muscle, soleus muscle and in pancreatic islets. Furthermore they found AMPKα protein levels and phosphorylation to be elevated in liver extracts of *Paskin*$^{-/-}$ [172]. In order to elucidate the effect PASKIN might have on AMPKα we are in the process of generating stable *Paskin*$^{-/-}$ HEK293 shRNA-mediated knock-down cell lines.

Rutter *et al.* found triglyceride accumulation in liver of male mice only for the control wild-type animals on high-fat diet and the fat mass was accordingly decreased in the knock-out animals compared to the control animals [172]. By blood analysis we did not find significantly increased triglyceride levels. Therefore, more animals need to be analyzed for triglyceride levels in the blood, since in male *Paskin*$^{+/+}$ when compared with *Paskin*$^{-/-}$ the higher triglyceride levels might become significantly higher with representative numbers of animals measured. Moreover a gender specific effect could then either be confirmed or disproved, as in females we did not measure a difference in triglyceride levels. The decreased body weight in *Paskin*$^{-/-}$ mice might originate from a decreased fat mass [172], therefore a lower triglyceride level would represent a convenient explanation why the body weight of

Paskin$^{-/-}$ mice is lower under HFD. Measurement of free fatty acid is error-prone due to high autohydrolysis of lipids and strongly depends on the fasted state. It might be that 6 hours fasting is too short for adequate free fatty acid determination.

As obesity results from the imbalance between energy intake and energy expenditure, metabolic chambers were used to examine the mechanisms that are partially protecting *Paskin*$^{-/-}$ mice from obesity. Rutter *et al.* found *Paskin*$^{-/-}$ mice to consume more oxygen, to emit more carbon dioxide and to generate more heat during the day and the night [172]. Rutter *et al.* confirmed this hypermetabolic phenotype by the finding that the ATP production rate was higher in *Paskin*$^{-/-}$ than in *Paskin*$^{+/+}$ soleus muscle fibres. However neither increased mitochondrial number, mitochondrial mass, nor citrate synthase activity accounted for this difference. A discrepancy was encountered with our experiments where we applied indirect calorimetry to *Paskin*$^{+/+}$ and *Paskin*$^{-/-}$ mice. We did not find any hypermetabolic phenotype in *Paskin*$^{-/-}$ mice. This could be explained by the finding that the animals did not get used to the metabolic chambers during the 24 h adaptation time. Hence, a longer adaptation time is needed. A recent publication shows that rats are being adapted for two weeks to the metabolic cages before measurements were started [173]. The mice were scared and therefore lost weight in these metabolic cages. This weight loss can be seen in Fig. 5 and Fig. 6, respectively. Surprisingly Rutter *et al.* allowed the animals to adapt only for 4 hours to the new surrounding, although measurements went on for 3 days. Rutter *et al.* used only 3 male animals for this setup while we performed indirect calorimetry with 32 animals.

Since diet-induced obesity is accompanied by increased triglyceride accumulation in peripheral tissues and strongly associates with the development of insulin resistance, glucose and insulin tolerance tests were performed. Rutter *et al.* found lower basal insulin levels in *Paskin*$^{-/-}$ mice already under NCD. The fasted insulin levels of HFD-fed *Paskin*$^{-/-}$ mice were half the value of wild-type mice [172]. Under HFD *Paskin*$^{-/-}$ animals showed better glucose tolerance and increased insulin sensitivity compared to *Paskin*$^{+/+}$ animals [172]. We detected increased glucose tolerance in HFD-fed *Paskin*$^{-/-}$ male as well, since they cleared glucose significantly faster than the control animals. Surprisingly in females we could not confirm these findings. Rutter *et al.* performed IPITT on fed animals and saw increased insulin sensitivity in male *Paskin*$^{-/-}$ mice [172]. We did not find increased insulin sensitivity in *Paskin*$^{-/-}$ mice. However, it could be that the advanced age of our animals was responsible for the lack of an adequate insulin response.

S6 Kinase 1 (S6K1) deficient mice are hypoinsulinaemic, glucose intolerant and have a reduced β-cell mass, although their glucose levels are normal [174]. Thus Um et al. suggest a

hypersensitivity to insulin owing to the apparent loss of a negative feedback loop from S6K1 to insulin receptor substrate (IRS1). Since PASKIN mice show reduced insulin levels [172] and do show an increased insulin sensitivity under HFD [172] the S6K1 might be involved in the energy metabolism of PASKIN mice. Furthermore when fed HFD mice are known to increase S6K1 acitvity, therefore negatively regulating insulin signalling[174]. Thus levels of S6K1 need to be addressed in our PASKIN mice for further understanding the pathways leading to a obesity suppressed phenotype.

It will be important to examine whether the detected decreased running wheel activity of *Paskin*$^{-/-}$ mice is due to an inability of long lasting work affected by muscle dystrophy, or whether *Paskin*$^{-/-}$ mice have defects in the peripheral and / or central nervous system. To understand this behaviour, circadian rhythm experiments coupled with running wheel activity are currently being performed with 11 *Paskin*$^{-/-}$ and 11 *Paskin*$^{+/+}$ male mice. A special role for PASKIN in skeletal muscle in correlation with AMPK might be an explanation for the demonstrated phenotype.

7.3 Conclusions

We found that PASKIN deletion suppresses phenotypes associated with a high-fat diet. This is supported by the finding that *Paskin*$^{-/-}$ mice were partially protected from obesity when high-fat diet was fed. Furthermore lower triglyceride plasma levels and better glucose clearance point towards a role of PASKIN in whole body energy metabolism. These phenotypes suggest that AMPK signaling might be suppressed to some extent by PASKIN.

Fujii *et al.* [175] recently examined muscle AMPK in maximal exercise capacity. In transgenic mice carrying cDNAs of inactive AMPK $\alpha 2$, the maximal exercise capacity was dramatically reduced and a faster decrease of muscle glycogen by in situ muscle contraction was measured. If PASKIN inhibits AMPK activity, our *Paskin*$^{-/-}$ mice should perform better in a maximal exercise test. On the other hand we know from the yeast homologs that glycogen accumulation is inhibited by active PASKIN. Therefore the decreased spontaneous activity of *Paskin*$^{-/-}$ mice needs further examination. It is necessary to perform exercise tolerance tests with *Paskin*$^{-/-}$ mice or to perform muscle contraction experiments *in vitro* to see whether the phenotype of decreased spontaneous activity has its origin in muscle function or whether the CNS is responsible for this phenotype.

Intriguingly, in at least 3 animal models that are resistant to diet-induced obesity, ie, mice overexpressing the uncoupling proteins UCP1141 or UCP3, [176] or mice with a knockout of stearoyl- CoA desaturase-1 [177], a persistent activation of AMPK in the affected cell types appears. The ability of AMPK to inhibit adipocyte lipolysis and to stimulate fatty acid oxidation in many tissues, both acutely via phosphorylation of ACC2 [178] and chronically by up regulating peroxisome proliferator-activated receptor gamma coactivator-1α (PGC-1α) and mitochondrial biogenesis, [179, 180] is also likely to be beneficial in insulin resistance and type 2 diabetes. There is much evidence that these conditions are partly caused by abnormal accumulation of triglyceride in muscle and liver and that this can be at least partly caused by a defect in mitochondrial function [181]. Interestingly, incubation of cultured cells with high levels of the saturated fatty acid palmitate affected the integrity of the endoplasmic reticulum and led to cell death, and this was ameliorated using 5-amino-4-imidazolecarboxamide riboside (AICAR) an AMP analogue to activate AMPK and stimulate fatty acid oxidation [182]. One objection is that it has also been proposed that high rates of fatty acid oxidation can be damaging because of oxidative stress, for example, in ischemic heart following reperfusion [183] and in endothelial cells [184]. It will be important to establish whether any adverse effects of AMPK activation in certain cell types are compensated by the overall improvements in metabolic status. PASKIN might be implicated to keep this balance and to protect from oxidative stress and therefore might play a regulatory role in the redundant regulatory mechanisms to maintain energy homeostasis through multiple signaling pathways.

Our model for PASKIN activation could to some extent be confirmed, since an obvious phenotype arises when the *Paskin*$^{-/-}$ mice are challenged by HFD. Only under HFD, when the phosphorylation of AMPK is decreased [185], *Paskin*$^{-/-}$ mice can maintain AMPK phosphorylation due to the lack of PASKIN dependent inhibition. So far, there is no evidence that PASKIN directly inhibits AMPK phosphorylation or interacts with AMPK. Peptide and protein arrays were screened in our lab for novel phosphorylation targets of PASKIN. However AMPK was not detected. Therefore, an *in vitro* phosphorylation or co-immunoprecipitation assay is necessary to gain more insight into the molecular interplay of PASKIN with AMPK and to find out whether PASKIN can phosphorylate and thereby inhibit AMPK. Another approach would be to see whether an activator of AMPK, like LKB1 or PPARδ [186] are as well able to be phosphorylated by or interact with PASKIN. Furthermore, it might be that the regulation of PASKIN implies the melanocortin system. Melanocortin can potently restore AMPK phosphorylation in skeletal muscle of HFD fed mice [185].

Intracerebroventricular treatment with a melanocortin antagonist of HFD fed *Paskin*$^{-/-}$ mice would provide an insight whether PASKIN affects the central regulation of skeletal muscle AMPK activity. Antecedent it would make sense to check PASKIN expression in the brain stem, where endogenous agonists of melanocortin are synthesized [187]. Possibilities to see significant differences between *Paskin*$^{+/+}$ and *Paskin*$^{-/-}$ mice fed HFD would imply to apply more stringent stress conditions, i.e. to increase the fat-diet to 60% fat by calories.

8 CONCLUSIONS

PASKIN as a novel PAS serine/threonine kinase might participate in a multitude of cellular processes. The ubiquitous expression, the AMP-kinase related kinase domain and the high similarity to the FixL PAS domain, suggest PASKIN as a mammalian cellular sensor protein. Indeed, using protein and peptide arrays we identified possible phosphorylation targets which are involved in spermatogenesis, glycolysis, and glycogen metabolism. The present work brings together all these aspects and specifically addresses a role for PASKIN in whole body energy metabolism.

The function of PASKIN in the testis might so far be the most obscure question to be solved. Although PASKIN is most prominently expressed in the testis, even after backcrossing into a homogenous C57BL/6 background, neither impaired fertility nor other apparent phenotypes arose. Measurement of testosterone levels or the determination of apoptosis in seminiferous tubuli *in vitro* were not yet successful. Interestingly, it has been reported, that insulin and leptin are expressed in and secreted by human ejaculated spermatozoa [188]. Ando *et al.* assume that leptin and insulin are needed to manage the energy status in ejaculated spermatozoa. Surprisingly, PASKIN and insulin are located in the midpiece of the uncapacitated spermatozoa.

We could show, that hyperglycemia is neither increasing PASKIN mRNA nor protein in pancreatic islet β-cells. Not only PASKIN mRNA levels but also kinase activity was reported to be induced by high glucose. We disproved this by showing that neither glucose induction of insulin mRNA nor insulin secretion was dependent on the presence of a functional PASKIN gene. In vivo experiments like glucose and insulin tolerance tests performed with both genders and variously aged *Paskin*$^{+/+}$ and *Paskin*$^{-/-}$ mice further underline that PASKIN is not implicated in insulin secretion or production. A function for PASKIN in the immediate answer of insulin secretion can therefore be excluded. In addition, we did not detect PASKIN mRNA levels in pancreas neither in islet β-cells.

The administration of high fat diet to *Paskin*$^{+/+}$ and *Paskin*$^{-/-}$ mice shed light on a possible implication of PASKIN in energy homeostasis. HFD-fed *Paskin*$^{-/-}$ mice are not gaining weight to the same extent as HFD-fed *Paskin*$^{+/+}$ mice. Indeed, the significantly heavier NCD-fed *Paskin*$^{-/-}$ mice, when compared to NCD-fed *Paskin*$^{+/+}$ mice, turn into the lighter weighing group once HFD is applied to *Paskin*$^{+/+}$ and *Paskin*$^{-/-}$ mice. We assume that the differences in body weight derives from a higher body fat content of the HFD-fed *Paskin*$^{+/+}$ mice which show an increased level of triglyceride in their blood plasma when compared to the HFD-fed

Paskin$^{-/-}$ male mice. The glucose clearing ability in *Paskin*$^{+/+}$ mice was significantly lower versus *Paskin*$^{-/-}$ mice, pointing towards a role for PASKIN in maintaining the balance in energy homeostasis. This leads to the question: What might be the counterplayer of PASKIN? AMPK phosphorylation was found to be increased in *Paskin*$^{-/-}$ mouse embryonic fibroblasts, although AMPK has abundant regulatory effects in energy homeostasis and it is a difficult task to solve the effect PASKIN exerts on the signaling pathway of AMPK. AMPK signaling pathway and the insulin signaling pathway share common as well as opposite regulatory mechanisms (see introduction). This might be an explanation why PASKIN was thought to play a role in pancreatic islet β-cells. Other factors like cell culture handling and discrepancies arising when validating *in vitro* results with *in vivo* experiments, were contributing to the results concerning PASKIN function in pancreatic islet β-cells presented in this work.

The significantly decreased running activity of Paskin$^{-/-}$ might lead towards a role for PASKIN in skeletal muscle. Since AMPK can easily be stimulated by exercise, either in vivo or in vitro experiments will shed light on possible implication of PASKIN in the metabolism of skeletal muscle. Another hint that PASKIN might play a role in skeletal muscle is its putative interaction partner Ryanodine receptor 2 which belongs to a class of calcium channels in various forms of muscle and other excitable animal tissue (Eckhardt K., Wenger R.H.; unpublished data). Ryanodine receptors (RyRs) are the major cellular mediator of calcium induced calcium release in animal cells.

In conclusion, we found that PASKIN deletion suppresses phenotypes associated with a high-fat diet. Thus we assume the involvement of PASKIN in keeping the energy balance. To elucidate the exact mechanism of PASKIN action on cellular level further *in vivo* and *in vitro* experiments are required. Whether PASKIN interacts with AMPK or PARPδ remains to be elucidated, however we suggest a role for PASKIN in metabolic energy homeostasis.

9 CV AND PUBLICATION LIST

PARTICULARS

Full Name	**Emanuela BORTER**
Date of birth	28.06.1978
Native place	Interlaken (BE)

EDUCATION

06.2004 – 06.2007	**Dissertation** Institute of Physiology, University of Zurich (Prof. R.H. Wenger) and Zurich Center for Integrative Human Physiology (ZIHP) **"**PASKIN function in testis, pancreas and energy homeostasis"
10.1998 – 10.2003	**Master in Biotechnology** Swiss Federal Institute of Technology, (ETH) Zurich Master Thesis (Dr. Gregg Whited, metabolic pathway engineering): "Electricity generation in microbial fuel cells" (Genencor Int., Inc., CA, USA)
08.1991 – 06.1998	**High school**, type B (latin), Zug

POSTERS AND PRESENTATIONS

03.2007	86th Congress of the DPG (Deutsche Physiologische Gesellschaft), Hannover (D). Oral presentation
10.2006, 09.2005	ZIHP Symposium, University of Zurich (CH). Poster
10.2006	Annual Meeting of the Swiss Physiological Society. Fribourg (CH) Oral presentation
09.2005	Symposium of the Zurich Center for Integrative Human Physiology (ZIHP), University of Zurich (CH). Poster
04.2005	International meeting "stress signals and cellular responses" at the Martin-Luther-University of Halle-Wittenberg (D). Poster

FELLOWSHIPS AND GRANTS

05.2004-05.2007	Swiss National Science Foundation (3100A0-104219 to R.H.W. and G.C.)
10.2005, 09.2007	University Research Priority Program "Integrative Human Physiology" (to E.B., 25´000 CHF)

PUBLICATION LIST

Eckhardt K, Tröger J, Reissmann J, Katschinski DM, Wagner KF, Stengel P, Paasch U, Hunziker P, **Borter E**, Barth S, Spielmann P, Stiehl DP, Camenisch G, and Wenger RH, **2007**, Localization of the PAS domain kinase PASKIN and its novel target eukaryotic translation elongation factor eEF1A1 in male germ cells. Cell Physiol Biochem. **20**, 227 (2007)

Borter E, Niessen M, Zuellig R, Spinas GA, Spielmann P, Camenisch G, Wenger RH, Glucose-stimulated insulin production in mice deficient for the PAS kinase PASKIN. Diabetes. **56**, 113 (2007)

Hägele S, Behnam B, **Borter E**, Wolfe J, Paasch U, Lukashev D, Sitkovsky M, Wenger RH, Katschinski DM, The fibrous sheath protein TSGA10 prevents nuclear accumulation of testis-specific hypoxia-inducible factor (HIF)-1αI.1. FEBS Lett. **580**, 3731 (2006)

Tröger J, Eckhardt K, Spielmann P, Schläfli P, **Borter E** and Wenger RH, **2007**, Phospholipid stimulation and downstream target identification of the PAS domain kinase PASKIN, submitted

10 ACKNOWLEDGEMENTS

I would like to thank

my Doktorvater Dr. Roland Wenger for his guidance, his outstanding scientific support and for being an excellent teacher.

Dr. Gieri Camenisch and Dr. Uwe Paasch for joining my promotionskommittee and for their project inputs.

Prof. Giatgen Spinas, Dr. Markus Niessen and Dr. Richard Züllig from the Clinic for Endocrinology and Diabetes, University Hospital Zürich for the collaboration.

Prof. Thomas Lutz, Dr. Peter Wielinga and Bettina Alder from the Institute of Veterinary Physiology, University Zürich for the collaboration.

the University Research Priority Program “Integrative Human Physiology” for its supporting grant.

Patrick for always having a helping hand for handling the mice during the last three years.

Dr. Carsten Wagner for his precious advices whenever mouse experiments were concerned.

Juliane, Patrick, Katrin and Philippe for their support and relaxing moments.

All other group members for diverting talks in the cell culture and for amusing moments in the lab, especially Daniel and Patrick for sharing pieces of their lab wisdom.

My parents and my sister for their encouragement before and during my PhD.

last but not least Stephan, Bert, Ivana, Bettina and Sophie for listening to me talking about my projects and giving me inputs for all situations.

11 REFERENCES

1. Rutter, J., B.L. Probst, and S.L. McKnight, *Coordinate regulation of sugar flux and translation by PAS kinase.* Cell, 2002. **111**(1): p. 17-28.
2. Amezcua, C.A., et al., *Structure and interactions of PAS kinase N-terminal PAS domain: model for intramolecular kinase regulation.* Structure, 2002. **10**(10): p. 1349-1361.
3. Carling, D., *The AMP-activated protein kinase cascade--a unifying system for energy control.* Trends Biochem Sci, 2004. **29**(1): p. 18-24.
4. Hofer, T., et al., *Mammalian PASKIN, a PAS-serine/threonine kinase related to bacterial oxygen sensors.* Biochem Biophys Res Commun, 2001. **288**(4): p. 757-64.
5. Towle, H.C., *Glucose as a regulator of eukaryotic gene transcription.* Trends Endocrinol Metab, 2005. **16**(10): p. 489-94.
6. Desvergne, B., L. Michalik, and W. Wahli, *Transcriptional regulation of metabolism.* Physiol Rev, 2006. **86**(2): p. 465-514.
7. Borter, E., et al., *Glucose-stimulated insulin production in mice deficient for the PAS kinase PASKIN.* Diabetes, 2007. **56**(1): p. 113-7.
8. Nambu, J.R., et al., *The Drosophila single-minded gene encodes a helix-loop-helix protein that acts as a master regulator of CNS midline development.* Cell, 1991. **67**(6): p. 1157-67.
9. Gu, Y.Z., J.B. Hogenesch, and C.A. Bradfield, *The PAS superfamily: sensors of environmental and developmental signals.* Annu Rev Pharmacol Toxicol, 2000. **40**: p. 519-61.
10. Taylor, B.L. and I.B. Zhulin, *PAS domains: internal sensors of oxygen, redox potential, and light.* Microbiol Mol Biol Rev, 1999. **63**(2): p. 479-506.
11. Morais Cabral, J.H., et al., *Crystal structure and functional analysis of the HERG potassium channel N terminus: a eukaryotic PAS domain.* Cell, 1998. **95**(5): p. 649-55.
12. Schmidt, J.V. and C.A. Bradfield, *Ah receptor signaling pathways.* Ann Rev Cell Dev Biol, 1996. **12**: p. 55-89.
13. Wenger, R.H., *Cellular adaptation to hypoxia: O_2-sensing protein hydroxylases, hypoxia-inducible transcription factors, and O_2-regulated gene expression.* FASEB J, 2002. **16**(10): p. 1151-62.
14. Reppert, S.M. and D.R. Weaver, *Coordination of circadian timing in mammals.* Nature, 2002. **418**(6901): p. 935-41.
15. Dioum, E.M., et al., *NPAS2: a gas-responsive transcription factor.* Science, 2002. **298**(5602): p. 2385-7.
16. Ushiro, H., et al., *Molecular cloning and characterization of a novel Ste20-related protein kinase enriched in neurons and transporting epithelia.* Arch Biochem Biophys, 1998. **355**(2): p. 233-40.
17. Rutter, J., et al., *PAS kinase: An evolutionarily conserved PAS domain-regulated serine/threonine kinase.* Proc Natl Acad Sci U S A, 2001. **98**: p. 8991-8996.
18. Ponting, C.P. and L. Aravind, *PAS: a multifunctional domain family comes to light.* Current Biology, 1997. **7**(11): p. R 674-R 677.
19. Hefti, M.H., et al., *The PAS fold. A redefinition of the PAS domain based upon structural prediction.* Eur J Biochem, 2004. **271**(6): p. 1198-208.
20. Gilles-Gonzalez, M.A., *Oxygen signal transduction.* IUBMB Life, 2001. **51**(3): p. 165-73.

21. Christie, J.M., et al., *Arabidopsis NPH1: a flavoprotein with the properties of a photoreceptor for phototropism.* Science, 1998. **282**(5394): p. 1698-701.
22. Borgstahl, G.E., D.R. Williams, and E.D. Getzoff, *1.4 A structure of photoactive yellow protein, a cytosolic photoreceptor: unusual fold, active site, and chromophore.* Biochemistry, 1995. **34**(19): p. 6278-87.
23. Gong, W., et al., *Structure of a biological oxygen sensor: a new mechanism for heme-driven signal transduction.* Proc Natl Acad Sci U S A, 1998. **95**(26): p. 15177-82.
24. Miyatake, H., et al., *Dynamic light-scattering and preliminary crystallographic studies of the sensor domain of the haem-based oxygen sensor FixL from Rhizobium meliloti.* Acta Crystallogr D Biol Crystallogr, 1999. **55**(Pt 6): p. 1215-8.
25. Gilles-Gonzalez, M.A., G.S. Ditta, and D.R. Helinski, *A haemoprotein with kinase activity encoded by the oxygen sensor of Rhizobium meliloti.* Nature, 1991. **350**(6314): p. 170-2.
26. Sousa, E.H., G. Gonzalez, and M.A. Gilles-Gonzalez, *Oxygen blocks the reaction of the FixL-FixJ complex with ATP but does not influence binding of FixJ or ATP to FixL.* Biochemistry, 2005. **44**(46): p. 15359-65.
27. Stein, S.C., et al., *The regulation of AMP-activated protein kinase by phosphorylation.* Biochem J, 2000. **345 Pt 3**: p. 437-43.
28. Beausoleil, S.A., et al., *Large-scale characterization of HeLa cell nuclear phosphoproteins.* Proc Natl Acad Sci U S A, 2004. **101**(33): p. 12130-5.
29. Katschinski, D.M., et al., *Targeted disruption of the mouse PAS domain serine/threonine kinase PASKIN.* Mol. Cell. Biol., 2003. **23**(19): p. 6780-6789.
30. Gingras, A.C., B. Raught, and N. Sonenberg, *eIF4 initiation factors: effectors of mRNA recruitment to ribosomes and regulators of translation.* Annu Rev Biochem, 1999. **68**: p. 913-63.
31. Eckhardt, K., et al., *Male germ cell expression of the PAS domain kinase PASKIN and its novel target eukaryotic translation elongation factor eEF1A1.* Cell Physiol Biochem, 2007. **20**: p. *227-240*.
32. Downs, J.A. and S.P. Jackson, *A means to a DNA end: the many roles of Ku.* Nat Rev Mol Cell Biol, 2004. **5**(5): p. 367-78.
33. Lebrun, P., M.R. Montminy, and E. Van Obberghen, *Regulation of the pancreatic duodenal homeobox-1 protein by DNA-dependent protein kinase.* J Biol Chem, 2005. **280**(46): p. 38203-10.
34. Kielbassa, K., et al., *Protein kinase Cδ-specific phosphorylation of the elongation factor eEF-α and an eEF-1α peptide at threonine 431.* J Biol Chem, 1995. **270**(11): p. 6156-62.
35. Izawa, T., et al., *Elongation factor-1α is a novel substrate of Rho-associated kinase.* Biochem Biophys Res Commun, 2000. **278**(1): p. 72-8.
36. Chang, Y.W. and J.A. Traugh, *Phosphorylation of elongation factor 1 and ribosomal protein S6 by multipotential S6 kinase and insulin stimulation of translational elongation.* J Biol Chem, 1997. **272**(45): p. 28252-7.
37. Ejiri, S., *Moonlighting functions of polypeptide elongation factor 1: from actin bundling to zinc finger protein R1-associated nuclear localization.* Biosci Biotechnol Biochem, 2002. **66**(1): p. 1-21.
38. Wilson, W.A., et al., *Control of mammalian glycogen synthase by PAS kinase.* Proc Natl Acad Sci U S A, 2005. **102**(46): p. 16596-16601.
39. Rafiq, I., H.J. Kennedy, and G.A. Rutter, *Glucose-dependent translocation of insulin promoter factor-1 (IPF-1) between the nuclear periphery and the nucleoplasm of single MIN6 beta-cells.* J Biol Chem, 1998. **273**(36): p. 23241-7.

40. Winckler, W., et al., *Evaluation of common variants in the six known maturity-onset diabetes of the young (MODY) genes for association with type 2 diabetes.* Diabetes, 2007. **56**(3): p. 685-93.
41. da Silva Xavier, G., J. Rutter, and G.A. Rutter, *Involvement of Per-Arnt-Sim (PAS) kinase in the stimulation of preproinsulin and pancreatic duodenum homeobox 1 gene expression by glucose.* Proc Natl Acad Sci U S A, 2004. **101**(22): p. 8319-24.
42. An, R., et al., *Regulation by Per-Arnt-Sim (PAS) kinase of pancreatic duodenal homeobox-1 nuclear import in pancreatic beta-cells.* Biochem Soc Trans, 2006. **34**(Pt 5): p. 791-3.
43. Troeger, J., *Phospholipids stimulate the autophosphorylation of the PAS domain kinase PASKIN.* Lipid research, 2007: p. *submitted*.
44. Eddy, E.M., *Male germ cell gene expression.* Recent Prog Horm Res, 2002. **57**: p. 103-28.
45. Hecht, N.B., *Molecular mechanisms of male germ cell differentiation.* Bioessays, 1998. **20**(7): p. 555-61.
46. Braun, R.E., et al., *Genetically haploid spermatids are phenotypically diploid.* Nature, 1989. **337**(6205): p. 373-6.
47. Dadoune, J.P., J.P. Siffroi, and M.F. Alfonsi, *Transcription in haploid male germ cells.* Int Rev Cytol, 2004. **237**: p. 1-56.
48. Kissel, H., et al., *The Sept4 septin locus is required for sperm terminal differentiation in mice.* Dev Cell, 2005. **8**(3): p. 353-64.
49. Max, B., *This and that: hair pigments, the hypoxic basis of life and the Virgilian journey of the spermatozoon.* Trends Pharmacol Sci, 1992. **13**(7): p. 272-6.
50. Csiszar, A., et al., *Proinflammatory phenotype of coronary arteries promotes endothelial apoptosis in aging.* Physiol Genomics, 2004. **17**(1): p. 21-30.
51. Rao, R.V., et al., *Coupling endoplasmic reticulum stress to the cell death program. Mechanism of caspase activation.* J Biol Chem, 2001. **276**(36): p. 33869-74.
52. Nicholson, D.W., et al., *Identification and inhibition of the ICE/CED-3 protease necessary for mammalian apoptosis.* Nature, 1995. **376**(6535): p. 37-43.
53. Daniel, P.T., et al., *Guardians of cell death: the Bcl-2 family proteins.* Essays Biochem, 2003. **39**: p. 73-88.
54. Wajant, H., *Death receptors.* Essays Biochem, 2003. **39**: p. 53-71.
55. Hengartner, M.O., *The biochemistry of apoptosis.* Nature, 2000. **407**(6805): p. 770-6.
56. Boatright, K.M., et al., *A unified model for apical caspase activation.* Mol Cell, 2003. **11**(2): p. 529-41.
57. Rich, T., C.J. Watson, and A. Wyllie, *Apoptosis: the germs of death.* Nat Cell Biol, 1999. **1**(3): p. E69-71.
58. Parone, P., et al., *Apoptosis: bombarding the mitochondria.* Essays Biochem, 2003. **39**: p. 41-51.
59. Nakagawa, T., et al., *Caspase-12 mediates endoplasmic-reticulum-specific apoptosis and cytotoxicity by amyloid-beta.* Nature, 2000. **403**(6765): p. 98-103.
60. Hitomi, J., et al., *Involvement of caspase-4 in endoplasmic reticulum stress-induced apoptosis and Abeta-induced cell death.* J Cell Biol, 2004. **165**(3): p. 347-56.
61. Adrain, C. and S.J. Martin, *The mitochondrial apoptosome: a killer unleashed by the cytochrome seas.* Trends Biochem Sci, 2001. **26**(6): p. 390-7.
62. Bradford, M.M., *A rapid and sensitive method for the quantitation of microgram quantities of protein utilizing the principle of protein-dye binding.* Anal Biochem, 1976. **72**: p. 248-54.
63. Hofmann, M.C., D. Abramian, and J.L. Millan, *A haploid and a diploid cell coexist in an in vitro immortalized spermatogenic cell line.* Dev Genet, 1995. **16**(2): p. 119-27.

64. Katschinski, D.M., et al., *Role of tumor necrosis factor alpha in hyperthermia-induced apoptosis of human leukemia cells.* Cancer Res, 1999. **59**(14): p. 3404-10.
65. Simonin, F., et al., *Detection of poly(ADP ribose) polymerase in crude extracts by activity-blot.* Anal Biochem, 1991. **195**(2): p. 226-31.
66. Hikim, A.P., et al., *Key apoptotic pathways for heat-induced programmed germ cell death in the testis.* Endocrinology, 2003. **144**(7): p. 3167-75.
67. Wang, Y., et al., *Protective effect of Fructus Lycii polysaccharides against time and hyperthermia-induced damage in cultured seminiferous epithelium.* J Ethnopharmacol, 2002. **82**(2-3): p. 169-75.
68. Suominen, J.S., et al., *The effects of mono-2-ethylhexyl phathalate, adriamycin and N-ethyl-N-nitrosourea on stage-specific apoptosis and DNA synthesis in the mouse spermatogenesis.* Toxicol Lett, 2003. **143**(2): p. 163-73.
69. Momparler, R.L., et al., *Effect of adriamycin on DNA, RNA, and protein synthesis in cell-free systems and intact cells.* Cancer Res, 1976. **36**(8): p. 2891-5.
70. Parvinen, M. and T. Vanha-Perttula, *Identification and enzyme quantitation of the stages of the seminiferous epithelial wave in the rat.* Anat Rec, 1972. **174**(4): p. 435-49.
71. Parvinen, M. and N.B. Hecht, *Identification of living spermatogenic cells of the mouse by transillumination-phase contrast microscopic technique for 'in situ' analyses of DNA polymerase activities.* Histochemistry, 1981. **71**(4): p. 567-79.
72. Kato, M.V., et al., *Upregulation of the elongation factor-1alpha gene by p53 in association with death of an erythroleukemic cell line.* Blood, 1997. **90**(4): p. 1373-8.
73. Rawe, V.Y., et al., *WAVE1, an A-kinase anchoring protein, during mammalian spermatogenesis.* Hum Reprod, 2004. **19**(11): p. 2594-604.
74. Vijayaraghavan, S., et al., *Subcellular localization of the regulatory subunits of cyclic adenosine 3',5'-monophosphate-dependent protein kinase in bovine spermatozoa.* Biol Reprod, 1997. **57**(6): p. 1517-23.
75. Vijayaraghavan, S., et al., *Protein kinase A-anchoring inhibitor peptides arrest mammalian sperm motility.* J Biol Chem, 1997. **272**(8): p. 4747-52.
76. Vaulont, S., M. Vasseur-Cognet, and A. Kahn, *Glucose regulation of gene transcription.* J Biol Chem, 2000. **275**(41): p. 31555-8.
77. Hay, C.W. and K. Docherty, *Comparative analysis of insulin gene promoters: implications for diabetes research.* Diabetes, 2006. **55**(12): p. 3201-13.
78. Wicksteed, B., et al., *Glucose-induced translational control of proinsulin biosynthesis is proportional to preproinsulin mRNA levels in islet beta-cells but not regulated via a positive feedback of secreted insulin.* J Biol Chem, 2003. **278**(43): p. 42080-90.
79. Lawrence, M.C., et al., *ERK1/2-dependent activation of transcription factors required for acute and chronic effects of glucose on the insulin gene promoter.* J Biol Chem, 2005. **280**(29): p. 26751-9.
80. Docherty, H.M., et al., *Relative contribution of PDX-1, MafA and E47/beta2 to the regulation of the human insulin promoter.* Biochem J, 2005. **389**(Pt 3): p. 813-20.
81. Francis, J., et al., *Pdx-1 links histone H3-Lys-4 methylation to RNA polymerase II elongation during activation of insulin transcription.* J Biol Chem, 2005. **280**(43): p. 36244-53.
82. Jonsson, J., et al., *Insulin-promoter-factor 1 is required for pancreas development in mice.* Nature, 1994. **371**(6498): p. 606-9.
83. Moede, T., et al., *Identification of a nuclear localization signal, RRMKWKK, in the homeodomain transcription factor PDX-1.* FEBS Lett, 1999. **461**(3): p. 229-34.
84. Macfarlane, W.M., et al., *Glucose stimulates translocation of the homeodomain transcription factor PDX1 from the cytoplasm to the nucleus in pancreatic beta-cells.* J Biol Chem, 1999. **274**(2): p. 1011-6.

85. McKinnon, C.M. and K. Docherty, *Pancreatic duodenal homeobox-1, PDX-1, a major regulator of beta cell identity and function.* Diabetologia, 2001. **44**(10): p. 1203-14.
86. Marshak, S., et al., *Purification of the beta-cell glucose-sensitive factor that transactivates the insulin gene differentially in normal and transformed islet cells.* Proc Natl Acad Sci U S A, 1996. **93**(26): p. 15057-62.
87. Gerrish, K., J.C. Van Velkinburgh, and R. Stein, *Conserved transcriptional regulatory domains of the pdx-1 gene.* Mol Endocrinol, 2004. **18**(3): p. 533-48.
88. Wang, H., et al., *Experimental models of transcription factor-associated maturity-onset diabetes of the young.* Diabetes, 2002. **51 Suppl 3**: p. S333-42.
89. Wenger, R.H. and D.M. Katschinski, *The hypoxic testis and post-meiotic expression of PAS domain proteins.* Semin Cell Dev Biol, 2005. **16**(4-5): p. 547-53.
90. Mohanty, S., et al., *Overexpression of IRS2 in isolated pancreatic islets causes proliferation and protects human β-cells from hyperglycemia-induced apoptosis.* Exp Cell Res, 2005. **303**(1): p. 68-78.
91. Wenger, R.H., et al., *Mouse hypoxia-inducible factor-1α is encoded by two different mRNA isoforms: expression from a tissue-specific and a housekeeping-type promoter.* Blood, 1998. **91**(9): p. 3471-3480.
92. Marti, H.H., et al., *Isoform-specific expression of hypoxia-inducible factor-1α during the late stages of mouse spermiogenesis.* Mol Endocrinol, 2002. **16**(2): p. 234-243.
93. Martin, F., et al., *Copper-dependent activation of hypoxia-inducible factor (HIF)-1: implications for ceruloplasmin regulation.* Blood, 2005. **105**(12): p. 4613-9.
94. Wang, H., G. Kouri, and C.B. Wollheim, *ER stress and SREBP-1 activation are implicated in β-cell glucolipotoxicity.* J Cell Sci, 2005. **118**(Pt 17): p. 3905-15.
95. Lilla, V., et al., *Differential gene expression in well-regulated and dysregulated pancreatic beta-cell (MIN6) sublines.* Endocrinology, 2003. **144**(4): p. 1368-79.
96. Iseli, T.J., et al., *AMP-activated protein kinase beta subunit tethers alpha and gamma subunits via its C-terminal sequence (186-270).* J Biol Chem, 2005. **280**(14): p. 13395-400.
97. Salt, I., et al., *AMP-activated protein kinase: greater AMP dependence, and preferential nuclear localization, of complexes containing the alpha2 isoform.* Biochem J, 1998. **334 (Pt 1)**: p. 177-87.
98. Turnley, A.M., et al., *Cellular distribution and developmental expression of AMP-activated protein kinase isoforms in mouse central nervous system.* J Neurochem, 1999. **72**(4): p. 1707-16.
99. Ai, H., et al., *Effect of fiber type and nutritional state on AICAR- and contraction-stimulated glucose transport in rat muscle.* Am J Physiol Endocrinol Metab, 2002. **282**(6): p. E1291-300.
100. Evans, A.M., et al., *Does AMP-activated protein kinase couple inhibition of mitochondrial oxidative phosphorylation by hypoxia to calcium signaling in O2-sensing cells?* J Biol Chem, 2005. **280**(50): p. 41504-11.
101. Hallows, K.R., et al., *Physiological modulation of CFTR activity by AMP-activated protein kinase in polarized T84 cells.* Am J Physiol Cell Physiol, 2003. **284**(5): p. C1297-308.
102. Hudson, E.R., et al., *A novel domain in AMP-activated protein kinase causes glycogen storage bodies similar to those seen in hereditary cardiac arrhythmias.* Curr Biol, 2003. **13**(10): p. 861-6.
103. Polekhina, G., et al., *Structural basis for glycogen recognition by AMP-activated protein kinase.* Structure, 2005. **13**(10): p. 1453-62.
104. Bateman, A., *The structure of a domain common to archaebacteria and the homocystinuria disease protein.* Trends Biochem Sci, 1997. **22**(1): p. 12-3.

105. Scott, J.W., et al., *CBS domains form energy-sensing modules whose binding of adenosine ligands is disrupted by disease mutations.* J Clin Invest, 2004. **113**(2): p. 274-84.
106. Corton, J.M., et al., *5-aminoimidazole-4-carboxamide ribonucleoside. A specific method for activating AMP-activated protein kinase in intact cells?* Eur J Biochem, 1995. **229**(2): p. 558-65.
107. Hawley, S.A., et al., *5'-AMP activates the AMP-activated protein kinase cascade, and Ca2+/calmodulin activates the calmodulin-dependent protein kinase I cascade, via three independent mechanisms.* J Biol Chem, 1995. **270**(45): p. 27186-91.
108. Hawley, S.A., et al., *Characterization of the AMP-activated protein kinase kinase from rat liver and identification of threonine 172 as the major site at which it phosphorylates AMP-activated protein kinase.* J Biol Chem, 1996. **271**(44): p. 27879-87.
109. Hawley, S.A., et al., *Complexes between the LKB1 tumor suppressor, STRAD alpha/beta and MO25 alpha/beta are upstream kinases in the AMP-activated protein kinase cascade.* J Biol, 2003. **2**(4): p. 28.
110. Woods, A., et al., *LKB1 is the upstream kinase in the AMP-activated protein kinase cascade.* Curr Biol, 2003. **13**(22): p. 2004-8.
111. Hawley, S.A., et al., *Calmodulin-dependent protein kinase kinase-beta is an alternative upstream kinase for AMP-activated protein kinase.* Cell Metab, 2005. **2**(1): p. 9-19.
112. Woods, A., et al., *Ca2+/calmodulin-dependent protein kinase kinase-beta acts upstream of AMP-activated protein kinase in mammalian cells.* Cell Metab, 2005. **2**(1): p. 21-33.
113. Hurley, R.L., et al., *The Ca2+/calmodulin-dependent protein kinase kinases are AMP-activated protein kinase kinases.* J Biol Chem, 2005. **280**(32): p. 29060-6.
114. Stahmann, N., et al., *Thrombin activates AMP-activated protein kinase in endothelial cells via a pathway involving Ca2+/calmodulin-dependent protein kinase kinase beta.* Mol Cell Biol, 2006. **26**(16): p. 5933-45.
115. Tamas, P., et al., *Regulation of the energy sensor AMP-activated protein kinase by antigen receptor and Ca2+ in T lymphocytes.* J Exp Med, 2006. **203**(7): p. 1665-70.
116. Salt, I.P., et al., *AMP-activated protein kinase is activated by low glucose in cell lines derived from pancreatic beta cells, and may regulate insulin release.* Biochem J, 1998. **335 (Pt 3)**: p. 533-9.
117. da Silva Xavier, G., et al., *Role of AMP-activated protein kinase in the regulation by glucose of islet beta cell gene expression.* Proc Natl Acad Sci U S A, 2000. **97**(8): p. 4023-8.
118. Friedman, J.M. and J.L. Halaas, *Leptin and the regulation of body weight in mammals.* Nature, 1998. **395**(6704): p. 763-70.
119. Kamohara, S., et al., *Acute stimulation of glucose metabolism in mice by leptin treatment.* Nature, 1997. **389**(6649): p. 374-7.
120. Muoio, D.M., et al., *Leptin directly alters lipid partitioning in skeletal muscle.* Diabetes, 1997. **46**(8): p. 1360-3.
121. Minokoshi, Y., et al., *Leptin stimulates fatty-acid oxidation by activating AMP-activated protein kinase.* Nature, 2002. **415**(6869): p. 339-43.
122. Minokoshi, Y., et al., *AMP-kinase regulates food intake by responding to hormonal and nutrient signals in the hypothalamus.* Nature, 2004. **428**(6982): p. 569-74.
123. Andersson, U., et al., *AMP-activated protein kinase plays a role in the control of food intake.* J Biol Chem, 2004. **279**(13): p. 12005-8.

124. Kola, B., et al., *Cannabinoids and ghrelin have both central and peripheral metabolic and cardiac effects via AMP-activated protein kinase.* J Biol Chem, 2005. **280**(26): p. 25196-201.
125. Yamauchi, T., et al., *Adiponectin stimulates glucose utilization and fatty-acid oxidation by activating AMP-activated protein kinase.* Nat Med, 2002. **8**(11): p. 1288-95.
126. Tomas, E., et al., *Enhanced muscle fat oxidation and glucose transport by ACRP30 globular domain: acetyl-CoA carboxylase inhibition and AMP-activated protein kinase activation.* Proc Natl Acad Sci U S A, 2002. **99**(25): p. 16309-13.
127. Andreelli, F., et al., *Liver adenosine monophosphate-activated kinase-alpha2 catalytic subunit is a key target for the control of hepatic glucose production by adiponectin and leptin but not insulin.* Endocrinology, 2006. **147**(5): p. 2432-41.
128. Bolster, D.R., et al., *AMP-activated protein kinase suppresses protein synthesis in rat skeletal muscle through down-regulated mammalian target of rapamycin (mTOR) signaling.* J Biol Chem, 2002. **277**(27): p. 23977-80.
129. Kimura, N., et al., *A possible linkage between AMP-activated protein kinase (AMPK) and mammalian target of rapamycin (mTOR) signalling pathway.* Genes Cells, 2003. **8**(1): p. 65-79.
130. Krause, U., L. Bertrand, and L. Hue, *Control of p70 ribosomal protein S6 kinase and acetyl-CoA carboxylase by AMP-activated protein kinase and protein phosphatases in isolated hepatocytes.* Eur J Biochem, 2002. **269**(15): p. 3751-9.
131. Inoki, K., T. Zhu, and K.L. Guan, *TSC2 mediates cellular energy response to control cell growth and survival.* Cell, 2003. **115**(5): p. 577-90.
132. Xiang, X., et al., *AMP-activated protein kinase activators can inhibit the growth of prostate cancer cells by multiple mechanisms.* Biochem Biophys Res Commun, 2004. **321**(1): p. 161-7.
133. Rattan, R., et al., *5-Aminoimidazole-4-carboxamide-1-beta-D-ribofuranoside inhibits cancer cell proliferation in vitro and in vivo via AMP-activated protein kinase.* J Biol Chem, 2005. **280**(47): p. 39582-93.
134. Jones, R.G., et al., *AMP-activated protein kinase induces a p53-dependent metabolic checkpoint.* Mol Cell, 2005. **18**(3): p. 283-93.
135. Imamura, K., et al., *Cell cycle regulation via p53 phosphorylation by a 5'-AMP activated protein kinase activator, 5-aminoimidazole- 4-carboxamide-1-beta-D-ribofuranoside, in a human hepatocellular carcinoma cell line.* Biochem Biophys Res Commun, 2001. **287**(2): p. 562-7.
136. Blazquez, C., et al., *The AMP-activated protein kinase prevents ceramide synthesis de novo and apoptosis in astrocytes.* FEBS Lett, 2001. **489**(2-3): p. 149-53.
137. Shaw, R.J., et al., *The tumor suppressor LKB1 kinase directly activates AMP-activated kinase and regulates apoptosis in response to energy stress.* Proc Natl Acad Sci U S A, 2004. **101**(10): p. 3329-35.
138. Ido, Y., D. Carling, and N. Ruderman, *Hyperglycemia-induced apoptosis in human umbilical vein endothelial cells: inhibition by the AMP-activated protein kinase activation.* Diabetes, 2002. **51**(1): p. 159-67.
139. Kefas, B.A., et al., *AMP-activated protein kinase can induce apoptosis of insulin-producing MIN6 cells through stimulation of c-Jun-N-terminal kinase.* J Mol Endocrinol, 2003. **30**(2): p. 151-61.
140. Kefas, B.A., et al., *AICA-riboside induces apoptosis of pancreatic beta cells through stimulation of AMP-activated protein kinase.* Diabetologia, 2003. **46**(2): p. 250-4.
141. Jung, J.E., et al., *5-Aminoimidazole-4-carboxamide-ribonucleoside enhances oxidative stress-induced apoptosis through activation of nuclear factor-kappaB in mouse Neuro 2a neuroblastoma cells.* Neurosci Lett, 2004. **354**(3): p. 197-200.

142. Saitoh, M., et al., *Adenosine induces apoptosis in the human gastric cancer cells via an intrinsic pathway relevant to activation of AMP-activated protein kinase.* Biochem Pharmacol, 2004. **67**(10): p. 2005-11.
143. Wang, W., et al., *Increased AMP:ATP ratio and AMP-activated protein kinase activity during cellular senescence linked to reduced HuR function.* J Biol Chem, 2003. **278**(29): p. 27016-23.
144. Inoki, K., et al., *TSC2 is phosphorylated and inhibited by Akt and suppresses mTOR signalling.* Nat Cell Biol, 2002. **4**(9): p. 648-57.
145. Gamble, J. and G.D. Lopaschuk, *Insulin inhibition of 5' adenosine monophosphate-activated protein kinase in the heart results in activation of acetyl coenzyme A carboxylase and inhibition of fatty acid oxidation.* Metabolism, 1997. **46**(11): p. 1270-4.
146. Beauloye, C., et al., *Insulin antagonizes AMP-activated protein kinase activation by ischemia or anoxia in rat hearts, without affecting total adenine nucleotides.* FEBS Lett, 2001. **505**(3): p. 348-52.
147. Kovacic, S., et al., *Akt activity negatively regulates phosphorylation of AMP-activated protein kinase in the heart.* J Biol Chem, 2003. **278**(41): p. 39422-7.
148. Horman, S., et al., *Insulin antagonizes ischemia-induced Thr172 phosphorylation of AMP-activated protein kinase alpha-subunits in heart via hierarchical phosphorylation of Ser485/491.* J Biol Chem, 2006. **281**(9): p. 5335-40.
149. Kramer, H.F., et al., *Distinct signals regulate AS160 phosphorylation in response to insulin, AICAR, and contraction in mouse skeletal muscle.* Diabetes, 2006. **55**(7): p. 2067-76.
150. Treebak, J.T., et al., *AMPK-mediated AS160 phosphorylation in skeletal muscle is dependent on AMPK catalytic and regulatory subunits.* Diabetes, 2006. **55**(7): p. 2051-8.
151. Zheng, D., et al., *Regulation of muscle GLUT-4 transcription by AMP-activated protein kinase.* J Appl Physiol, 2001. **91**(3): p. 1073-83.
152. Lochhead, P.A., et al., *5-aminoimidazole-4-carboxamide riboside mimics the effects of insulin on the expression of the 2 key gluconeogenic genes PEPCK and glucose-6-phosphatase.* Diabetes, 2000. **49**(6): p. 896-903.
153. Koo, S.H., et al., *The CREB coactivator TORC2 is a key regulator of fasting glucose metabolism.* Nature, 2005. **437**(7062): p. 1109-11.
154. Shaw, R.J., et al., *The kinase LKB1 mediates glucose homeostasis in liver and therapeutic effects of metformin.* Science, 2005. **310**(5754): p. 1642-6.
155. Sullivan, J.E., et al., *Inhibition of lipolysis and lipogenesis in isolated rat adipocytes with AICAR, a cell-permeable activator of AMP-activated protein kinase.* FEBS Lett, 1994. **353**(1): p. 33-6.
156. Daval, M., et al., *Anti-lipolytic action of AMP-activated protein kinase in rodent adipocytes.* J Biol Chem, 2005. **280**(26): p. 25250-7.
157. Wijkander, J., et al., *Insulin-induced phosphorylation and activation of phosphodiesterase 3B in rat adipocytes: possible role for protein kinase B but not mitogen-activated protein kinase or p70 S6 kinase.* Endocrinology, 1998. **139**(1): p. 219-27.
158. Garton, A.J., et al., *Phosphorylation of bovine hormone-sensitive lipase by the AMP-activated protein kinase. A possible antilipolytic mechanism.* Eur J Biochem, 1989. **179**(1): p. 249-54.
159. Hardie, D.G. and D. Carling, *The AMP-activated protein kinase--fuel gauge of the mammalian cell?* Eur J Biochem, 1997. **246**(2): p. 259-73.
160. Schibler, U. and P. Sassone-Corsi, *A web of circadian pacemakers.* Cell, 2002. **111**(7): p. 919-22.

161. Kahn, B.B., et al., *AMP-activated protein kinase: ancient energy gauge provides clues to modern understanding of metabolism.* Cell Metab, 2005. **1**(1): p. 15-25.
162. Hardie, D.G., *The AMP-activated protein kinase pathway--new players upstream and downstream.* J Cell Sci, 2004. **117**(Pt 23): p. 5479-87.
163. Camenisch, G., et al., *General applicability of chicken egg yolk antibodies: the performance of IgY immunoglobulins raised against the hypoxia-inducible factor 1α.* FASEB J, 1999. **13**(1): p. 81-88.
164. Stiehl, D.P., et al., *Increased prolyl 4-hydroxylase domain proteins compensate for decreased oxygen levels. Evidence for an autoregulatory oxygen-sensing system.* J Biol Chem, 2006. **281**(33): p. 23482-91.
165. Weir, J.B., *New methods for calculating metabolic rate with special reference to protein metabolism.* J Physiol, 1949. **109**(1-2): p. 1-9.
166. Lightfoot, J.T., et al., *Genetic influence on daily wheel running activity level.* Physiol Genomics, 2004. **19**(3): p. 270-6.
167. Kopp, C., et al., *Influence of estrus cycle and ageing on activity patterns in two inbred mouse strains.* Behav Brain Res, 2006. **167**(1): p. 165-74.
168. Surwit, R.S., et al., *Diet-induced type II diabetes in C57BL/6J mice.* Diabetes, 1988. **37**(9): p. 1163-7.
169. Spiegelman, B.M. and J.S. Flier, *Obesity and the regulation of energy balance.* Cell, 2001. **104**(4): p. 531-43.
170. Hsu, C.L. and G.C. Yen, *Effect of gallic acid on high fat diet-induced dyslipidaemia, hepatosteatosis and oxidative stress in rats.* Br J Nutr, 2007: p. 1-9.
171. Yuan, G., K.Z. Al-Shali, and R.A. Hegele, *Hypertriglyceridemia: its etiology, effects and treatment.* Cmaj, 2007. **176**(8): p. 1113-20.
172. Hao, H.X., *PAS kinase regulates energy homeostasis through inhibition of AMPK expression.* 2007(manuscript submitted).
173. Wielinga, P.Y., B. Alder, and T.A. Lutz, *The acute effect of amylin and salmon calcitonin on energy expenditure.* Physiol Behav, 2007.
174. Um, S.H., et al., *Absence of S6K1 protects against age- and diet-induced obesity while enhancing insulin sensitivity.* Nature, 2004. **431**(7005): p. 200-5.
175. Fujii, N., et al., *Role of AMP-activated protein kinase in exercise capacity, whole body glucose homeostasis, and glucose transport in skeletal muscle -Insight from analysis of a transgenic mouse model.* Diabetes Res Clin Pract, 2007.
176. Schrauwen, P., et al., *Improved glucose homeostasis in mice overexpressing human UCP3: a role for AMP-kinase?* Int J Obes Relat Metab Disord, 2004. **28**(6): p. 824-8.
177. Dobrzyn, P., et al., *Stearoyl-CoA desaturase 1 deficiency increases fatty acid oxidation by activating AMP-activated protein kinase in liver.* Proc Natl Acad Sci U S A, 2004. **101**(17): p. 6409-14.
178. Merrill, G.F., et al., *AICA riboside increases AMP-activated protein kinase, fatty acid oxidation, and glucose uptake in rat muscle.* Am J Physiol, 1997. **273**(6 Pt 1): p. E1107-12.
179. Terada, S., et al., *Effects of low-intensity prolonged exercise on PGC-1 mRNA expression in rat epitrochlearis muscle.* Biochem Biophys Res Commun, 2002. **296**(2): p. 350-4.
180. Zong, H., et al., *AMP kinase is required for mitochondrial biogenesis in skeletal muscle in response to chronic energy deprivation.* Proc Natl Acad Sci U S A, 2002. **99**(25): p. 15983-7.
181. Lowell, B.B. and G.I. Shulman, *Mitochondrial dysfunction and type 2 diabetes.* Science, 2005. **307**(5708): p. 384-7.
182. Borradaile, N.M., et al., *Disruption of endoplasmic reticulum structure and integrity in lipotoxic cell death.* J Lipid Res, 2006. **47**(12): p. 2726-37.

183. Kudo, N., et al., *High rates of fatty acid oxidation during reperfusion of ischemic hearts are associated with a decrease in malonyl-CoA levels due to an increase in 5'-AMP-activated protein kinase inhibition of acetyl-CoA carboxylase.* J Biol Chem, 1995. **270**(29): p. 17513-20.
184. Du, X., et al., *Insulin resistance reduces arterial prostacyclin synthase and eNOS activities by increasing endothelial fatty acid oxidation.* J Clin Invest, 2006. **116**(4): p. 1071-80.
185. Tanaka, T., et al., *Central melanocortin signaling restores skeletal muscle AMP-activated protein kinase phosphorylation in mice fed a high-fat diet.* Cell Metab, 2007. **5**(5): p. 395-402.
186. Kitz Kramer, D., et al., *Role of AMP kinase and PPARdelta in the regulation of lipid and glucose metabolism in human skeletal muscle.* J Biol Chem, 2007.
187. Schwartz, M.W., et al., *Leptin increases hypothalamic pro-opiomelanocortin mRNA expression in the rostral arcuate nucleus.* Diabetes, 1997. **46**(12): p. 2119-23.
188. Ando, S. and S. Aquila, *Arguments raised by the recent discovery that insulin and leptin are expressed in and secreted by human ejaculated spermatozoa.* Mol Cell Endocrinol, 2005. **245**(1-2): p. 1-6.